TAMPEREEN TEKNILLINEN YLIOPISTO
TAMPERE UNIVERSITY OF TECHNOLOGY

TIMOFEI ZAICEV
MASTER OF SCIENCE THESIS

Design and analysis of antennas using characteristic mode theory

Examiners: Jari Kangas, Jouko Heikkinen
Examiners and topic approved by the
Faculty Council of the Faculty of Computing and Electrical Engineering
on June 3rd, 2015

ABSTRACT

TIMOFEI ZAICEV: Design and analysis of antennas using characteristic mode theory
Tampere University of technology
Master of Science Thesis, 84 pages, 2 Appendix pages
January 2016
Master's Degree Programme in Electrical Engineering
Major: Radio-frequency electronics
Examiners: Jari Kangas, Jouko Heikkinen

Keywords: characteristic modes, patch antennas, isospectral domains

This master thesis reports usage of characteristic modes in design and analysis of antennas. It provides detailed information about physical meaning of characteristic modes in case of radiators and coaxially fed patch antennas. Theory of characteristic modes [TCM] shows physical insight about radiation processes that are taking place in antennas.

Antenna analysis procedure using TCM is described for several patch antennas. These cases show that TCM can be used to predict and to analyze radiation parameters of antennas. In addition, isospectral domains are introduced in terms of TCM and it is shown that such domains results in similar or even identical TCM results.

A single band rectangular patch antenna for Wi-Fi applications and a dual-band circular patch antenna are designed using TCM. It is discovered that radiation properties predicted by TCM hold for constructed TCM-based models of antennas if construction is very precise. This is especially important for multiband antennas.

As a result, this master thesis can serve as a basis for further researches in the field of characteristic modes related to patch antennas and isospectral domains. Possible directions of future work also mentioned.

PREFACE

Significant help was provided by Jari Kangas by providing small conversations and checking of the master thesis text. Indeed, after small talks with Jari new ideas and possible solutions raised, interest about particular topic increased.

Additional contribution all along master thesis was provided also by Jouko Heikkinen. He helped in construction and measurement stages of the master thesis by providing materials, accesses to Satimo StarLab laboratory and by giving usable advices regarding construction process, in general. As a result, detailed patch antenna construction explanation appeared in the master thesis based on my experience, knowledge and Jouko's advices. Moreover, Jouko provided additional parts for future works related to isospectral antennas.

Background this master thesis is based on previous studies made by different authors in the field of characteristic modes. Moreover, additional help was provided by Ing. Miloslav Capek, Ph.D, from CTU in Prague. Miloslav provided information about backgrounds related to characteristic mode implementation using MATLAB.

Tampere, 15.12.2015

Timofei Zaicev

CONTENTS

LIST OF SYMBOLS AND ABBREVIATIONS

$A(J)$	magnetic vector potential due to surface current *J*
α_n	characteristic angle values of n-th characteristic mode
AR	axial ratio
BW	bandwidth
BW_{frac_n}	fractional bandwidth of n-th characteristic mode
BW_n	bandwidth of n-th characteristic mode
CM	cavity model
D	directivity
E	electric intensity
E^i	incident electric field
EM waves	electro-magnetic waves
E_n	characteristic electric field of n-th characteristic mode
ϵ	permittivity
$f_{gnd_{alone}}$	resonant frequency of characteristic mode, in case of stand-alone the ground plane
$\phi(J)$	scalar potential due to surface current
f_{L_n}	lower border frequency for bandwidth definition of n-th characteristic mode
f_n	eigenfrequencies
$f_{rad_{alone}}$	resonant frequency of characteristic mode, in case of stand-alone radiator
$f_{rad_{gnd}}$	resonant frequency of characteristic mode, when radiator and the ground plane both presented
f_{res_n}	resonant frequency of n-th characteristic mode
f_{U_n}	upper border frequency for bandwidth definition of n-th characteristic mode
G	gain
GPS	global positioning system
γ_n	weighting coefficients of n-th characteristic mode
h	height
I_n	eigencurrents in matrix form of n-th characteristic mode
J	surface current
k	efficiency factor of the antenna
k_n	wavenumber in free space of n-th mode
L	length
λ_n	eigenvalues of n-th characteristic mode
LHCP	left-hand circular polarization
L(J)	electric linear operator, inverse to the electric intensity at any point in space due to surface current
M	weight operator
MIMO	multiple input multiple output
MoM	method of moments
MS	modal significance
MS_n	modal significance coefficients of n-th characteristic mode

$MS_{n_{half-power}}$	modal significance coefficients corresponding to half of the power reduction
μ	permeability
ν	general eigenvalues of characteristic mode
PEC	perfect electric conductor
PMC	perfect magnetic conductor
Q_n	quality factor of n-th characteristic mode
RHCP	right-hand circular polarization
$R(J)$	real part of impedance operator
RL	return loss
S	surface
$S(\theta,\phi)_{\text{av}}$	average power density from pattern in spherical coordinates
$S(\theta,\phi)_{\max}$	maximum power density from pattern in spherical coordinates
TCM	theory of characteristic modes
TE	transverse electric
TM	transverse magnetic
VNA	vector network analyzer
V_n	excitation coefficient of n-th characteristic mode
W	width
WLAN	wireless local area network
$X(J)$	imaginary part of impedance operator
$Z(J)$	generalized impedance operator

1. INTRODUCTION AND OVERVIEW

During last decades wireless communications have been developing significantly. Consequently, there has been great interest towards antenna design and analysis. In wireless communications there is significant interest in small size, compact, low profile, flexible, and light weight antennas. In addition, antenna design criteria become stricter. As a result, very often antennas are expected to work in multiple bands or to have broad bandwidth [BW] to satisfy several wireless communication standards. Patch antennas can satisfy many antenna design criteria and nowadays they are used widely.

However, as requirements increase, design and analysis of antennas becomes more difficult. As a result, numerical methods require more calculation power. In addition, computer-based programs like HFSS and FEKO help designers to test antennas before physical implementation. Nevertheless, the success of the final design is highly dependent on designer's experience and intuition. The design process often includes trial and error to meet the given design criteria. In industry antennas have to be designed within strict period of time and with respect to high standards. So, the above mentioned simulation programs are therefore gaining popularity.

Characteristic modes can be explained as an orthogonal set of currents, which all together describe the total current on the surface of a conducting body. This method was not used often in last decades, because amount of computational steps needed to obtain results is quite high. Even despite the fact that characteristic modes are able to show a lot about antenna's physical behavior. Amount of computational steps is quite big, because all calculations should be repeated for each desired frequency. An eigenvalue equation that involves the generalized impedance matrix Z on each desired frequency should be solved by directly applying method of moments [MoM]. However, nowadays these computational steps can be performed more efficiently due to much more powerful modern computers and optimization algorithms used for matrix calculations, available e.g. in the program MATLAB. Because of using direct MoM for all conducting bodies in some space Ω, all the internal couplings through the radiation are taken into account. This gives flexibility and provides additional possibilities in analysis of antennas using TCM.

By applying direct inversion of the generalized impedance matrix it would be possible to obtain total current distribution on the surface of a conductor body. However, characteristic modes give more understanding about physical behavior. If characteristic modes are used, then the total current is represented as combination of orthogonal current modes. The same holds also for the total radiation pattern and the total radiation

pattern can be represented as a vector sum of characteristic mode radiation patterns. This provides possibilities to observe which modes are involved in the radiation process at a given frequency and how this kind of knowledge is valuable for antenna design and analysis.

Finally, isospectral domain properties for radiators are studied in this thesis. Isospectral domains of the same size always have the same eigenvalue spectrum. Thus, using isospectral properties for different geometrical shapes, it is possible to perform analysis of antennas with different shapes and the same size, but having similar properties. This can be used to enhance flexibility in designing of antennas in the future.

1.1 List of objectives

This thesis focuses on TCM analysis of patch antennas. As a result, the following problems and aims were stated for this thesis:

- Gather and analyze previous studies of TCM in antenna design and analysis
- Describe and analyze theoretical and physical behavior of eigenvalues of characteristic modes
- Relate TCM studies to antennas in general
- Perform rectangular radiator's TCM analysis
- Studies of characteristic mode excitation
- Studies of isospectral properties of radiators using TCM
- Analysis of antennas using TCM
- Design of patch antenna using TCM

1.2 Previous studies

General description of theoretical properties for eigenvalues of characteristic modes and their characteristic radiation patterns was given in the second half of the 20^{th} century by R.F. Harrington and J.R. Mautz. These authors described and proved theoretical properties of characteristic modes [15]. Mathematical expressions and proofs provided in [15] show generalized approach of solving characteristic mode problem.

In [6] is given clear and logical analysis of dipole and wire antennas in terms of TCM. It is shown that TCM provides the same results as other computational methods for these types of antennas. In addition, [6] contains many other applications related to systematic antenna design principles using TCM. This work shows that it is possible to use TCM to study bandwidth properties of an antenna and its input impedance. It also gives examples of antennas, constructed based on TCM analysis.

Theory of characteristic modes has been used also in other antenna design applications. For example, in [3] is given design and analysis procedure of multiple input multiply output [MIMO] triangular antenna. It is shown that appropriate modes can be excited by feeding certain points of an antenna, which are determined based on TCM mode analysis. Theoretical results provided for antennas designed with TCM are in correspondence to practical measurements.

Another way of using TCM is shown in [13, 16]. The characteristic modes are used to design and to predict radiation properties of fractal antenna. This work is useful, because authors of this scientific paper have used characteristic mode current distribution information to excite needed modes at certain frequency band.

Furthermore, different shapes and types of antennas analyzed using TCM are reported in [6]. For example, the effect of the ground plane on bowtie antenna is studied from TCM point of view. In addition, circular polarization as a conclusion from TCM properties is observed in [6].

Another way of using TCM for antenna design is in bandwidth enhancement of an antenna, which is shown in [24]. The use of TCM to enhance bandwidth of multiband MIMO antenna is reported in [24]. The first 5 modes were analyzed separately.

It is important that TCM as a method can be implemented in MATLAB [7]. It could give advantages for antenna designers, such as lower software price and the possibility to follow and understand each computational step in detail.

To conclude, the previous studies show that it is possible to use TCM in wide scope of design cases related to antennas. Theory of characteristic modes allows thorough analysis on feeding placements, BW, notches, slots, ground plane effect, radiation pattern shape in antenna design, and many other properties.

1.3 Structure of the thesis

In chapter 2, required theoretical information about antennas and their properties is gathered. In addition, mathematical model of characteristic modes is described, using rectangular radiator as an example. Rectangular radiator is chosen, because this master thesis focuses on patch antennas.

Chapter 3 is related to the study of radiator properties from TCM point of view. It demonstrates the effect of geometry changes and a ground plane presence on characteristic modes. In addition, radiator scaling and the effect of multiple radiators are described using TCM. In this chapter cavity model is related to characteristic mode theory. Moreover, the effect of isospectral geometries applied for radiators is shown in terms of TCM. Finally, polarization effects are described using TCM. It is shown how

to use TCM to create required polarization and how to predict polarization of an antenna based on TCM analysis.

Chapter 4 demonstrates possibilities of antenna analysis using TCM. Three antenna examples are analyzed in this chapter using TCM. This chapter shows straight relation between measured results of antenna parameters and the results obtained from TCM. In addition, this chapter shows properties of circular patch antennas from TCM point of view.

Chapter 5 describes design of two patch antennas based on TCM approach given in the same chapter. This chapter focuses on explanation how to use TCM approach in antenna design to obtain predictable radiation properties of constructed antennas. In addition, one out of two designed patch antennas is constructed and measured using TUT facilities.

Finally, chapter 6 will provide conclusions of this master thesis. In addition, proposals for future work will be given.

2. THEORETICAL BACKGROUND

This chapter reviews theoretical background of characteristic modes. It describes basic definitions and required derivations of the characteristic mode theory. In addition, theoretical properties of terms used in the theory of characteristic modes are defined. As a result, the solution based on TCM for the total surface current on conducting surface is provided.

Furthermore, this chapter relates TCM to radiators. Conclusions about theoretical backgrounds of TCM are given at the end of this chapter.

2.1 Revision of the required antenna theory

To use the theory of characteristic modes and to understand radiation processes of antennas, it is necessary to keep in mind basic definitions used to describe antenna behavior. All antennas can be characterized by their physical size, gain, polarization, radiation resistance, directivity and radiation pattern. Moreover, in most cases antennas can be considered as reciprocal. It means that the antenna is behaving equally in transmission and receiving cases.

Radiation pattern of the antenna shows power distribution or field strength of EM wave in space around the antenna. Radiation patterns can be represented in spherical polar coordinate system, see Figure 1. Spherical coordinate system and radiation pattern example from FEKO commercial software are shown in Figure 1.

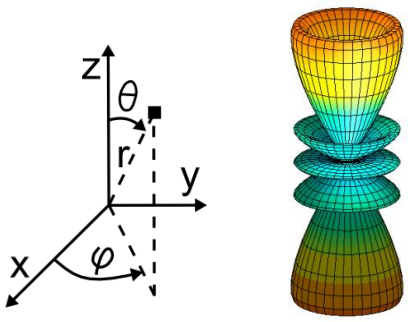

Figure 1. *Spherical coordinate system and radiation pattern example [21]*

This thesis focuses on patch antenna structures. Patch antenna can be defined as an antenna having radiator plane, ground plane, dielectric substrate and a feed line. Example of a co-axial fed rectangular patch antenna is shown in Figure 2.

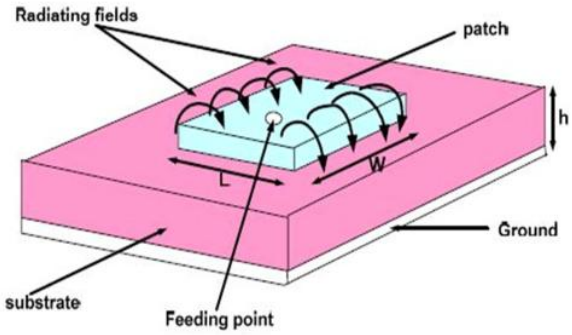

Figure 2.*Coaxially fed patch antenna [22]*

The patch antenna geometry consists of parameters *h*, *L*, and *W*, which are respectively height of a substrate, width and length of radiator plane, as it is shown in Figure 2. Another important parameter is dielectric constant ϵ of the substrate. In addition, placement and type of feed is important as well. All these parameters will be discussed in later chapters in terms TCM.

Usually the overall 3D radiation pattern of an antenna is not required, since antenna designers are interested in such antenna parameters as gain, polarization and axial ratio. It is enough to take a cut-plane from 3D radiation pattern to obtain those. Plane cuts are made by defining specific ranges of the angles ϕ, θ in spherical coordinate system, which was shown in Figure 1. Plane cut radiation example is given in Figure 3.

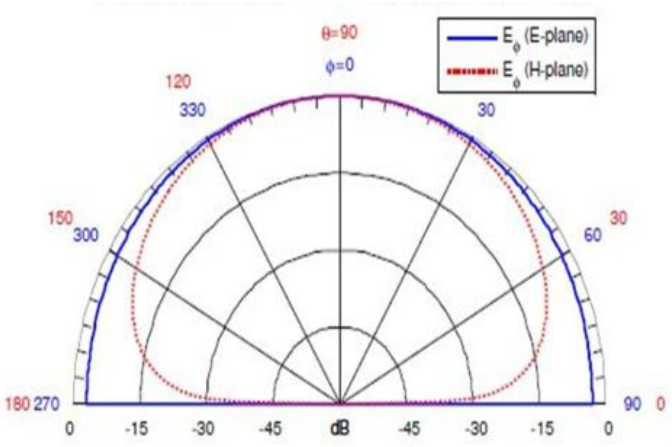

Figure 3. *E-plane and H-plane radiation pattern of the patch antenna shown in Figure 2 [22]*

If radiation plane cut corresponding to the strongest EM emission of the antenna is obtained, it is possible to define directivity of the antenna *D*. This term can be interpreted as the maximum directive gain found among all solid angles of the radiation

pattern. For patch antennas directivity is usually in the range of 5-9 dBi [19]. There are different possibilities for directivity calculation, for example:

$$D = \frac{S(\theta,\phi)_{\max}}{S(\theta,\phi)_{\text{av}}} \quad (1)$$

where $S(\theta,\phi)_{\max}$ and $S(\theta,\phi)_{\text{av}}$ refer respectively to maximum and average to power density in spherical coordinate system. Gain G of the antenna, is taking into account both directivity and efficiency factor $k \in [0;1)$ of the antenna, can be obtained from:

$$G = kD \quad (2)$$

As a result, gain is always less than directivity, due to losses in the antenna.

Polarization of the antenna describes time-varying properties of the radiated EM wave along the direction of propagation. There are three types of polarizations: linear, circular and elliptical [4]. In linear case, electric field will have two equal components in Cartesian system with phase difference of 0^0. In circular case, the field will have two components with phase difference of 90^0. In elliptical case, phase difference differs from 90^0 value. Axial ratio [AR] describes relation between two components of the radiated EM wave [4]. These two field components are orthogonal to the direction of propagation. Linear, elliptical and circular polarization examples are provided together with their corresponding axial ratio values in Figure 4.

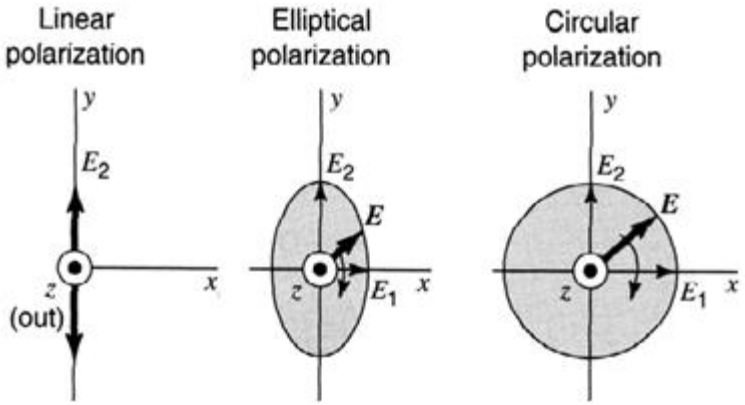

Figure 4. *Field components and AR of linear, elliptical and circular polarizations [19]*

Axial ratio for linear polarization is infinite, for circular it is 1, but for elliptical it can have any other value different from 1 and infinite, see Figure 4. Usually designers are aiming to have least possible return loss and highest possible gain value which would satisfy design criterias on the resonant frequency of the antenna. Bandwidth of the antenna is a figure of merit of a frequency range within which antenna behaves according to given specifications [4].

2.2 Theory of characteristic modes for antenna problems

The theory of characteristic modes provides the solution for a weighted set of orthogonal current modes, which can exist on a conducting surface [15]. Theory was proposed in 1970's first by R.J. Garbacz and R.H. Turpin, and then refined by R.F. Harrington and J.R. Mautz [15]. Characteristic modes can be obtained from MoM impedance matrix by solving eigenvalue equations, as proved in [14, 15]. Based on the method of electric-field-integral-equation formulation, initial operator equation should be stated as shown in equation (3) [17]. This operator relates the current *J* on the surface *S* of a conducting body to the tangential incident electric field E^i

$$\left[L(J) - E^i\right]_{\tan} = 0 \tag{3}$$

where 'tan' denotes to the tangential components on some surface *S*. In equation (3) the following terms are defined as:

$$L(J) = \mathrm{j}\omega A(J) + \nabla\phi(J) \tag{4}$$

$$A(J) = \mu \oiint_S J(r')\Psi(r,r')\mathrm{d}s' \tag{5}$$

$$\phi(J) = -\frac{1}{\mathrm{j}\omega\epsilon} \oiint_S \nabla' \cdot J(r')\Psi(r,r')\mathrm{d}s' \tag{6}$$

$$\psi(r,r') = \frac{\exp(-jk|r-r'|)}{4\pi|r-r'|} \tag{7}$$

in these equations *r* denotes a field point, r' to a source point. Moreover, ϵ, μ, k are respectively permittivity, permeability and a wavenumber in free space. The term $A(J)$is magnetic vector potential and the term $\phi(J)$ is scalar potential [13]. The standard situation for characteristic mode calculation is shown together with the coordinates in Figure 5.

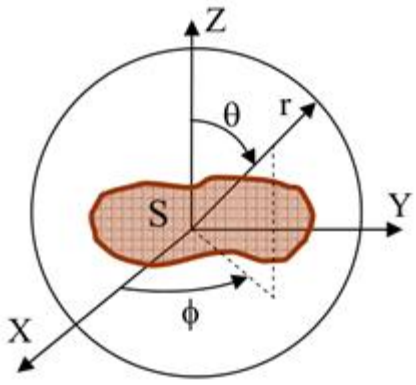

Figure 5. *The system for characteristic mode calculations of a conducting body in free space [6]*

The term $-L(J)$ shown in equation (4) is an electrical linear operator, which physically gives the electric intensity *E* at any point in space due to the current on the surface of a conducting body [15]. It is possible to distinguish dimensions of a tangential component of *L* operator. By definition, tangential component is obtained by performing inner

product operation with a unit normal vector to a surface *S*. Yet, it is possible to conclude that tangential part of $L(J)$, which is a linear operator, has the dimension units of impedance. Furthermore, tangential part of the L operator can be complex. It means that impedance operator $Z(J)$ can be obtained as:

$$Z(J) = [L(J)]_{\tan} = R(J) + jX(J) \tag{8}$$

where $R(J)$ and $X(J)$ are defined as

$$R(J) = \frac{1}{2}(Z(J) + Z(J)^*) \tag{9}$$

$$X(J) = \frac{1}{2\mathrm{j}}(\mathrm{Z}(J) - \mathrm{Z}(J)^*). \tag{10}$$

In addition, $R(J)$ and $X(J)$ operator parts of matrix $Z(J)$ are real and symmetric, because $Z(J)$ operator is symmetric. Here and further in the text the term "real" will refer to the real set of numbers. In addition, for simplicity reason, argument (J) will be omitted from expressions and, for example, R, X, Z will be used. Moreover, *R* operator is positive, since the power radiated by current *J* on a surface *S* is always equal or larger than zero. Implementation of the characteristic mode method over conducting surface is carried out using Rao-Wilton-Glisson [RWG] edge elements [23]. Simulations and practical calculations are commonly composed by MoM using RWG edge elements.

If the whole conducting surface is divided into RWG elements, the total surface current can be expressed by a sum of the contributions given by basis functions over all edge elements with unknown coefficients. Use of the RWG elements guarantees that the surface current is continuous across element boundaries. However, meshing quality which affect the RWG element quality, has the effect on final results [7]. This is discussed in more details in chapter 5.

Theory given in [11] should be used further to find out impedance operator discussed earlier. The weighted eigenvalue equation has to be used to find out impedance operator *Z*. Eigenvalue equation is shown in equation (12):

$$ZJ = \nu MJ \tag{12}$$

where *M* is the weight operator and ν are general eigenvalues. The weight operator *M* should be chosen such that radiation patterns would be orthogonal to satisfy eigencurrent definition mentioned earlier. Such conditions can be fulfilled if and only if the weight operator *M* will be equal to the real part of impedance matrix shown in equation (8). Hence, *M* = *R*. Finally, by letting $\nu = 1 + \mathrm{j}\lambda$ [15] and replacing the weight operator, and by using equations (8, 10), results in:

$$(R + \mathrm{j}X)J = RJ + \mathrm{j}XJ = (1 + \mathrm{j}\lambda)RJ = RJ + \mathrm{j}\lambda RJ \rightarrow XJ = \lambda RJ \tag{13}$$

By solving equation (13) using approach described in [16], it will result in the solution set of eigencurrents J_n and eigenvalues λ_n of n-th characteristic mode. As it was proved, operators *R* and *X* of impedance matrix are symmetric and belong to the real set of numbers, and thus, eigenvalues λ_n and eigencurrents J_n also will be real. This statement is true also in the opposite way. To obtain real values of eigenvalues and

eigencurrents it is required to have impedance operator to be symmetrical. In real computation tasks Galerkin's method [10] is used to represent equation (13) as:

$$[X][I]_n = \lambda_n[R][I]_n \tag{14}$$

where matrix I_n refers to eigencurrents, λ_n to eigenvalues. From equation (14) it is possible to conclude that eigencurrents I_n and corresponding to them eigenvalues λ_n are dependent on the shape, size and material parameters of a conducting surface *S*. The term characteristic current, which is widely used in literature, can be interpreted as the solution set of eigencurrents of equation (14). Physically characteristic currents show various currents, which can be supported by a conducting structure [15]. Consequently, eigenvalues obtained from equation (14) will have their magnitudes proportional to reactive radiated power. It means that modes are resonating when eigenvalues are equal to zero. So, when the reactive component at a certain frequency is zero, corresponding characteristic mode will resonate. In general, from [6] and from equation (14) it comes out that the following conditions hold:

1. If $\lambda_n > 0$, the mode is storing magnetic energy
2. If $\lambda_n = 0$, the mode is resonating
3. If $\lambda_n < 0$, the mode is storing electric energy

These conditions are such, because in polar reactive power vector representation, capacitive reactive power always has a negative sign, but reactive inductive power always has a positive sign. As a result, it follows that eigenvalues should have the same sign as a vector reactive power to satisfy equality conditions of equation (14).

Furthermore, since eigencurrents satisfy orthogonality conditions, it follows that also characteristic far-fields produced by these eigencurrents will be orthogonal [16]. It means that characteristic modes radiate power independently from one another. By assuming normalized eigencurrents, and by using orthogonality properties discussed above, the following property comes out:

$$\langle \overrightarrow{J_m^*}, Z(\overrightarrow{J_n}) \rangle = (1 + \mathrm{j}\lambda_n)\delta_{mn} \tag{15}$$

where Kronecker delta-function $\delta_{mn} = 0 \text{ if } m \neq n,$ and $\delta_{mn} = 1, \text{if } m = n$. It means that the total current on the surface of a conducting body can be expressed as:

$$J = \sum_n \gamma_n J_n \tag{16}$$

where γ_n is an unknown weighting coefficient, which have to be found. By substituting equation (16) into equation (3) and by taking into account equation (15), the following results will take place:

$$\left[\gamma_n \mathrm{L}(J_n) - E^i\right]_{\tan} = \sum_{\mathrm{n}} \gamma_n \langle J_m, ZJ_n \rangle - \langle J_m, E^i \rangle = 0 \rightarrow$$

$$\rightarrow \gamma_n(1 + \mathrm{j}\lambda_n) = \langle J_n, E^i \rangle \rightarrow \gamma_n = \frac{\langle J_n, E^i \rangle}{(1+\mathrm{j}\lambda_n)} \tag{17}$$

where $\langle J_n, E^i \rangle$ is an excitation coefficient [16]. Excitation coefficient can be expressed as:

$$V_n^i = \langle J_n, E^i \rangle = \oint_{\mathrm{n}} J_n \cdot E^i \mathrm{d}s. \quad (18)$$

By substituting the coefficient γ_n obtained from equation (17) into equation (16) and by taking into account equation (18), it is possible to find out that the total surface current on a conducting body in case of the presence of excitation source is:

$$J = \sum \frac{V_n^i J_n}{1+\mathrm{j}\lambda_n} \quad (19)$$

The solution shown in equation (19) takes into account the effect of excitation's position, eigencurrents, eigenvalues, magnitude and phase of excitation source. The product $V_n^i J_n$ in equation (19) shows how well excitation voltage source is coupled to the *n*-th eigencurrent mode. So, $V_n^i J_n$ together with weighting coefficient γ_n define if the characteristic mode will be excited on the conducting surface or not. Eigenvalues, as it is now proved, are of significant importance, because they show information about characteristic modes.

2.3 Characteristic mode theory related to radiators

The general solution for eigencurrents, eigenvalues and total current shown in chapter 2.2 can be used for antenna structures. In the simplest case, antenna can be considered as radiator in free space. So, it is possible to apply known rules and conclusions made in chapter 2.2 to describe such radiators and their physical properties based on TCM.

Example of eigenvalue magnitudes over frequency range for radiator of the size 40x60 mm^2 in free space is shown in Figure 6. Perfect electric conductor [PEC] condition is assumed. From equations (4, 6, 8) it follows that eigenvalues have the value range of $\lambda_n \in [-\infty; +\infty]$. The characteristic mode is resonating at a given frequency if eigenvalue is zero, as it was mentioned in chapter 2.2. Nevertheless, if there are many graphs of eigenvalues on one plot, it is difficult to distinguish zero-crossing condition. As a result, different representations of eigenvalues are often used.

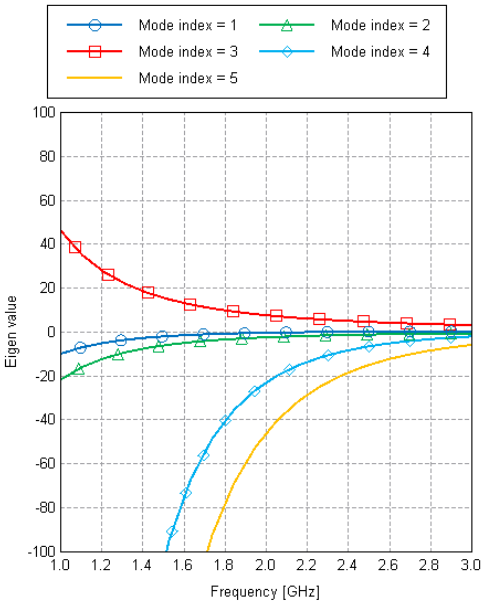

Figure 6. *Eigenvalues of 40x60 mm rectangular patch antenna radiating surface in free space*

If eigenvalues of a certain radiating surface in free space are shown in magnitude form as in Figure 6, then it is possible to state two things – what kind of energy was stored in certain characteristic mode at desired frequency and which characteristic mode is radiating. Radiation of the characteristic mode is found by checking zero-crossing condition, as it was shown before. Based on theory from chapter 2.2, the third characteristic mode is storing magnetic energy, but characteristic modes 2, 4 and 5 are contributing to electric energy, see Figure 6. The first characteristic mode is resonating at 2.4 GHz frequency, when eigenvalue is zero. Till zero value of the first characteristic mode is storing electric energy, but after 2.4 GHz value the first characteristic mode is storing magnetic energy.

Nevertheless, magnitude-only representation of eigenvalues is not showing all properties of a given conducting surface. Bandwidth and quality factor are not defined and cannot be estimated from characteristic mode representation form shown in Figure 6. As a result, another representation of eigenvalues can be used, called modal significance of *n*-th characteristic mode MS_n [6]. The general equation of modal significance is:

$$MS_n = \left|\frac{1}{1+j\lambda_n}\right|. \tag{20}$$

The term MS_n physically represents normalized magnitudes of characteristic mode currents. The magnitude of modal significance is dependent only on the shape and size of a conducting object, as it comes from equation (20). The characteristic mode is resonating if and only if eigenvalue is approaching to zero. So, in terms of MS it means

that equation's (20) right side should approach to 1. This can be proved by letting eigenvalue, shown in equation (20), to approach to zero:

$$\lim_{\lambda_n \to 0} \left| \frac{1}{1+j\lambda_n} \right| = 1. \quad (21)$$

Thus, it is proved that the characteristic mode is resonating if MS is "1". All in all, modal significance is another mathematical representation of eigenvalue magnitudes. This representation form provides additional analyzing options for conducting surfaces.

In Figure 7 MS coefficients, corresponding to eigenvalues found in Figure 6, are shown. Results are presented in terms of MS_n coefficients for characteristic modes. Characteristic modes are represented in terms of different parabolic curves, some of them have extrema points. Now it is easier to distinguish between maxima points of given characteristic mode MS curves. Thus, it is easier to observe resonating characteristic modes.

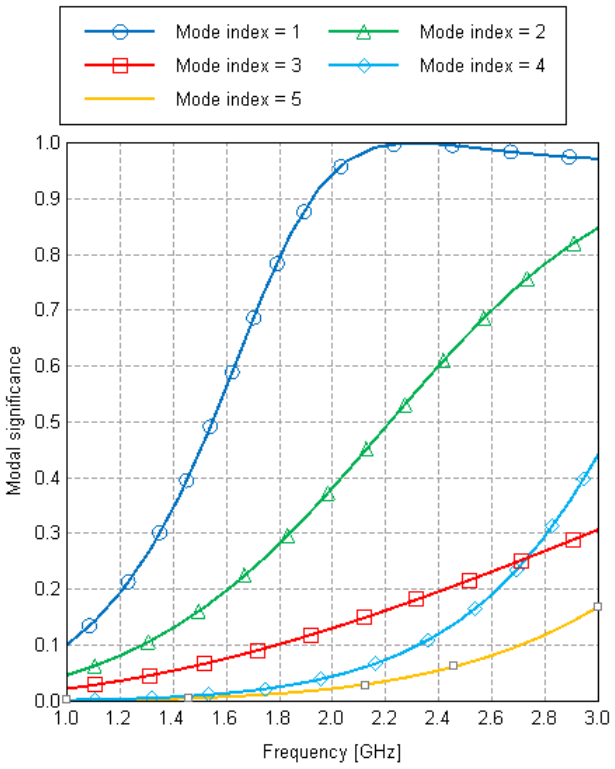

Figure 7. *Modal significance of 40x60 mm rectangular patch antenna radiating surface in free space*

It is possible to define bandwidth of a radiating characteristic mode, since characteristic modes are represented in terms of parabolic and normalized curves. By definition, bandwidth is defined within the frequency range where power is changing not more than by half from maximum [4]. For current representation it would mean reduction by a factor of $\sqrt{2}$. This rule can be applied in equation (20). It results in the following border conditions for bandwidth:

$$MS_{n_{half-power}} = \left|\frac{1}{1+\mathrm{j}\lambda_n}\right| = \frac{1}{\sqrt{2}} \approx 0.707. \quad (22)$$

As a result, it is possible to calculate eigenvalue λ_n for which equation (22) satisfies equality conditions:

$$\left|\frac{1}{1+j\lambda_n}\right| = \frac{1}{|1+j\lambda_n|} = \frac{1}{\sqrt{2}} \rightarrow \sqrt{1+\lambda_n^2} = \sqrt{2} \rightarrow \lambda_n = \pm 1\ . \quad (23)$$

It means that by checking 0.707 magnitude level in Figure 7 it is possible to obtain upper f_{U_n} and lower f_{L_n} border frequency set for any characteristic mode. However, this is done only for resonating characteristic modes. It means the characteristic mode has to have maxima point equal to 1 in MS representation. So, the frequency range $[f_{L_n}; f_{U_n}]$ defines BW_n. Moreover, based on equation (23) it follows that BW_n for eigenvalue representation of a resonating characteristic mode is found by checking ± 1 levels. Nevertheless, it was found that eigenvalues may have infinite magnitudes, and hence, precise evaluation of ± 1 levels can be problematic. Bandwidth is often expressed as a fraction of the frequency difference with respect to resonating frequency. It is called fractional bandwidth of n-th characteristic mode BW_{frac_n}, it can be defined as:

$$BW_{frac_n} = \frac{|f_{L_n} - f_{U_n}|}{f_{res_n}} \quad (24)$$

where f_{res_n} is resonating frequency of n-th characteristic mode. In addition, based on equation (24) it is possible to derive quality factor Q_n measure of n-th characteristic mode. Quality factor is expressed as:

$$Q_n = \frac{1}{BW_{frac}} \quad (25)$$

where Q_n is quality factor of a given mode. Since $\mathrm{BW_{frac}} << 1$, it should be noted that quality factor Q_n should be bigger than 1. Quality factor of a given characteristic mode describes the same as in general radio-frequency applications. Quality factor describes sharpness of MS_n curves. So, higher Q_n value is, sharper MS_n curves will be and vice versa.

Using MS representation form in Figure 7, it is possible to state that the first characteristic mode is resonating at 2.4 GHz in given frequency range. This was also discovered above using eigenvalue representation form in Figure 6. To discover BW of the first characteristic mode, 0.707 level should be checked in Figure 7 . So, the lower border frequency of the first mode is 1.7 GHz, but the upper is not seen, because the frequency range is not large enough. It should be taken into account that there can be also no upper border frequency at all within reasonable increase of the frequency range.

Sometimes both eigenvalue magnitude and MS representation forms are not providing clear enough results. Thus, another representation form is considered - by using characteristic angles α_n [6], which are defined as:

$$\alpha_n = \pi - \text{atan}(\lambda_n) \text{ or } \alpha_n = 180^{\text{o}} - \text{atan}(\lambda_n) \quad (26)$$

where both radial and degree representations are shown. This is mathematical derivation from magnitude eigenvalue representation form. Characteristic angle representation form gives different possibilities to analyze conducting structures. From physical point of view, characteristic angles of characteristic modes describe the phase angle between characteristic current J_n and characteristic electric field E_n [6]. Example of characteristic angle representation, corresponding to eigenvalue magnitude form representation from Figure 6, is shown in Figure 8.

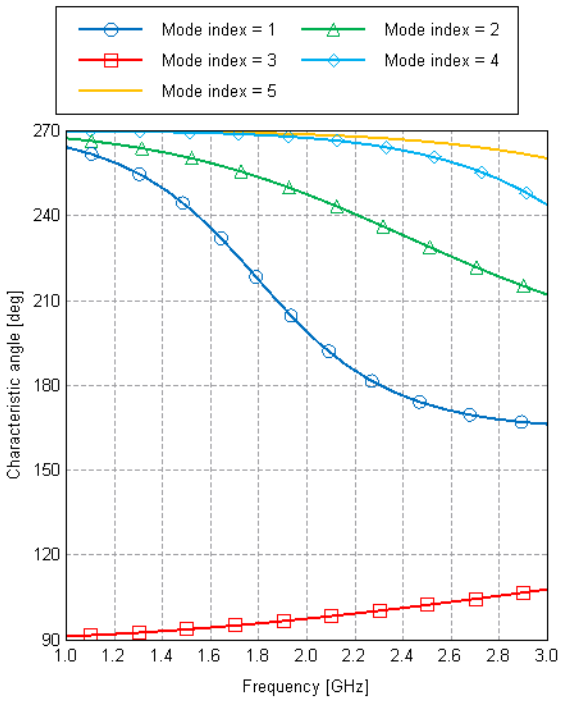

Figure 8. *Characteristic angle of 40x60 mm rectangular patch antenna radiating surface in free space*

In characteristic angle representation form the characteristic mode is resonating when it is equal to π rad or 180^{o} degree level. This is because equation (24) will have such values, if 0 value of the eigenvalue will be substituted into it. So, it is required to check 180^{o} degree level in Figure 8 to see at which frequency the mode is resonating. To describe how to obtain BW of the characteristic mode in characteristic angle form, the results obtained in equation (22) can be substituted into equation (26). By doing so, it is possible to calculate upper and lower degree levels to obtain bandwidth of the resonating characteristic mode. It follows that these border-degree levels of characteristic mode BW are at 135^{o} and 225^{o} respectively for upper and lower border frequencies. Based on arctangent function's nature, it is possible to state that the value range of characteris-

tic angle coefficients is $\alpha_n \in [90^o; 270^o]$. Indeed, there are no values outside of the obtained characteristic angle range, see Figure 8 . Finally, quality factor of resonating mode can be calculated by using formula (23), once BW is known.

From Figure 8 it can be observed that the first mode is the only mode which is resonating within given frequency range. The first mode is resonating at 2.3 GHz frequency, because at that frequency characteristic angle is equal to 180^o. It proves that characteristic angle representation form gives the same results as were discovered earlier. To obtain BW, the lower border frequency of the first mode is obtained by checking 225 degree level. Lower border of BW is 1.7 GHz, just like it was observed in MS and eigenvalue magnitude representation cases. However, the upper border frequency of BW cannot be defined, because there is no crossing point at 135^o level for the first characteristic mode. Thus, precise values for quality and *BW* are not calculated. The first mode is resonating in quite large BW, since upper border limit is outside of given frequency range. It means that quality factor of the first resonating mode is very low.

2.4 Summary of the theory of characteristic modes

Big advantage of TCM is that matrix operators R, X and eigenvalues together with eigencurrents are real. For TCM implementation on conducting bodies, RWG edge elements are used. Galerkin's method is used to solve eigenvalue equation. As a result, the solution set of eigencurrents and eigenvalues can be obtained. For each desired frequency, new calculations for all characteristic modes have to be performed. Both feed and characteristic mode excitation are taken into account by introducing excitation and weighting coefficients. From physical point of view, coefficient $V_n^i J_n$ shows how well excitation voltage source is coupled to n-th characteristic mode current.

It was discovered that eigenvalues have positive values if corresponding characteristic modes are storing magnetic energy. If eigenvalues have negative values, then characteristic modes are storing electric energy. Eigenvalues can be represented in magnitude, MS or characteristic angle forms.

Physically characteristic mode currents show various currents or fields, which can be supported by radiators. In addition, characteristic angles of characteristic modes describe phase angle between characteristic current J_n and characteristic field E_n. Moreover, modal significance coefficients show normalized magnitudes of characteristic mode currents.

Characteristic modes are resonating in the following cases: if eigenvalue magnitude is zero; if MS is approaching to 1; if characteristic angle is equal to 180^o. In addition, bandwidth of the characteristic mode can be obtained by checking the following levels in different representation forms: ± 1 level in eigenvalue magnitude representation; 0.707 level in MS representation; 135^o and 225^o degree levels in characteristic angle

representation. Eigenvalue range is infinite as given in chapter 2.3. The value range of MS is from 0 to 1, but the value range of characteristic angles is from 90^o to 270^o degrees, including border values for both MS and characteristic angle. Quality factor of any resonating characteristic mode can be calculated from BW_n.

Material permittivity and permeability parameters are affecting the values of eigencurrents and eigenvalues. All in all, eigencurrents and eigenvalues are dependent on frequency, on material parameters and shape of the conducting surface. Eigencurrents are orthogonal. As a result, corresponding characteristic radiation patterns are orthogonal as well. The overall radiating energy is calculated by summing up energies from all characteristic modes at desired frequency. So, more precise results can be obtained if more characteristic modes are taken into account.

3. CHARACTERISTIC MODE STUDIES OF RADIATORS

This chapter provides information how changes in radiator's geometry affect characteristic modes. Moreover, the effect of the ground plane presence is shown in this chapter. In addition, multiple rectangular radiator configurations are described. Excitation of different modes on different radiators is reported. Also, rectangular radiators are scaled in accordance with the scale theory. The process is described from TCM point of view. All calculations are performed using characteristic mode solver in the commercial program FEKO [12]. In study cases, characteristic mode calculations are performed in free space, using PEC condition for conducting surfaces.

This thesis focuses on patch antennas. Patch antennas always consist of both radiator(s) and a ground plane. In general, radiating elements and a ground plane of the antenna can be considered as radiators. Thus, in this chapter both radiator and the ground plane are analysed separately and together to emphasize their effect on characteristic modes.

Furthermore, isospectral conducting surfaces are studied and their properties are described using TCM. At the end of this chapter conclusions are provided.

3.1 Characteristic mode properties of rectangular radiator in free space

Rectangular radiator shape is one of the most typical shapes for radiating element and for ground planes of patch antennas. Thus, it is important to know properties of this shape in terms of TCM to explain physical insight of antennas. Meshed structure of rectangular radiator made in FEKO is shown in Figure 9. Geometrical shape of radiator shown in Figure 9 is described by parameters width W and length L. The size of this radiator is W = 30 mm, L = 40 mm.

Characteristic angle values versus frequency of the first 5 characteristic modes for chosen rectangular radiator are shown in Figure 10. It was discovered earlier that the characteristic mode is resonating if characteristic angle at chosen frequency is 180^{o}. Hence, from Figure 10 it follows that the first characteristic mode is resonating at 3.56 GHz, the second mode at 6.76 GHz and the fourth mode at 5.6 GHz. Both the third and the fifth modes are not resonating in the given frequency range.

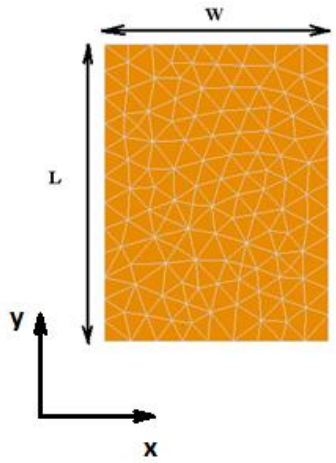

Figure 9. *Rectangular conducting surface in free space, 30x40 mm*

Above mentioned statements are correct for this particular radiator and for chosen frequency range, which is from 3 GHz to 7 GHz. If another frequency range would be chosen, the third and the fifth modes could have resonating frequencies. From Figure 10 it comes out that the third and the fifth characteristic modes may resonate at larger frequency than 7 GHz. It is because their characteristic angle curves are closing to 180^{o} degrees by increasing frequency. All in all, it means that the given rectangular radiator can radiate only using characteristic modes 1, 2 and 4 over the given frequency range. If antenna designers are interested in a given frequency range for a particular rectangular radiator, they should consider above mentioned modes to be excited. If needed, the same analysis approach of characteristic modes can be done also for any other frequency range and radiator shape.

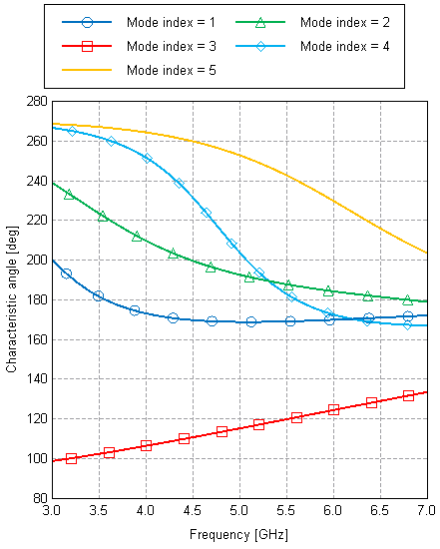

Figure 10. *Characteristic angle values for the first 5 modes of 30x40 mm rectangular plate*

Characteristic surface current distributions of the first 5 characteristic modes at 3.6 GHz frequency for rectangular radiator are shown in Figure 11. Characteristic surface current

flows in generalized form are given in Figure 12. It will be observed in more details in chapter 4 that the generalized characteristic surface current flow for rectangular radiator is not changing with frequency. Thus, it is possible to use obtained generalized characteristic surface current flows as normalized current distribution patterns for rectangular radiators of any size.

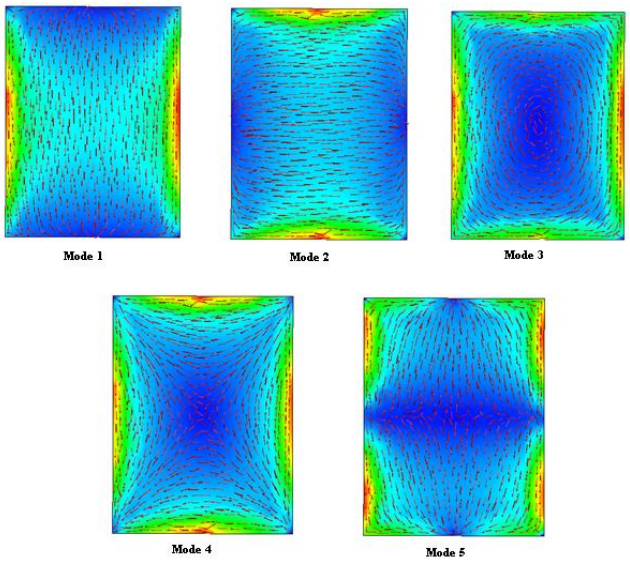

Figure 11.*Characteristic surface current distributions of the first 5 characteristic modes of rectangular radiator in free space at 3.6 GHz*

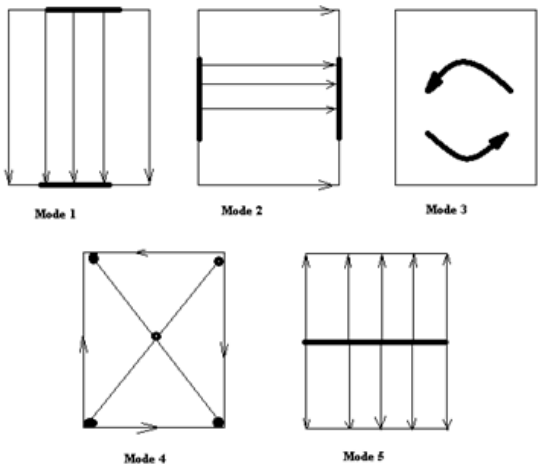

Figure 12. *Generalized characteristic surface current flows of the first 5 characteristic modes of rectangular radiator in free space at 3.6 GHz*

Information about characteristic surface current distributions shown in Figure 11 can be used to excite required modes. Excitation of the mode is dependent on weighting coefficients as it was discovered in chapter 2. Moreover, since all characteristic modes are orthogonal, characteristic surface current distributions can be used to study polarization. Excitation of characteristic modes is discussed in more details chapter 3.1.3.

From Figure 11 it is possible to state the physical nature of characteristic surface currents. It is observable that characteristic modes 3 and 4 contain of closed loop current flows. It means that these characteristic modes have inductive nature [5]. Characteristic modes 1, 2 and 5 consist of parallel characteristic surface current flows. Consequently, these modes have capacitive nature.

Each characteristic mode produces its own characteristic radiation pattern. Since generalized characteristic surface current flows are constant, characteristic radiation patterns in XY plane in normalized form will also remain constant. Such characteristic radiation patterns can be used for design and analysis of antennas. Characteristic radiation patterns in XY plane in normalized and decibel format for the first 5 characteristic modes are given in Figure 13.

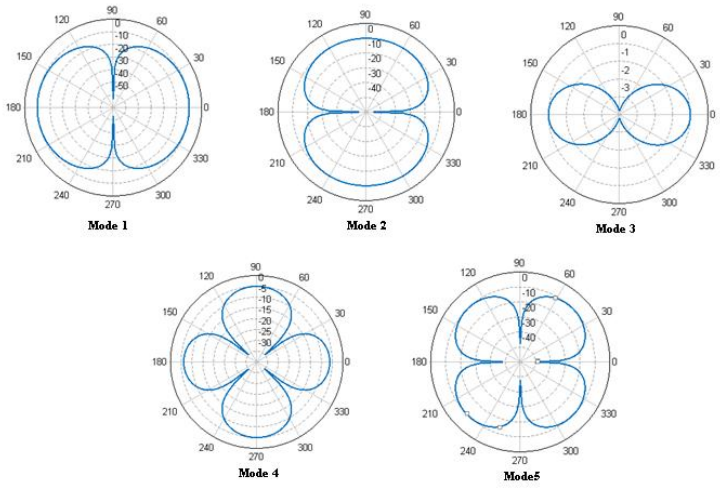

Figure 13. *Characteristic radiation patterns in XY plane for the first 5 characteristic modes of rectangular radiator in free space at 3.6 GHz*

Finally, information provided in [5] proves that obtained results of this chapter are in correspondence with previous studies in this field. From [7, 13] it can be noted that the first 3 characteristic modes are mainly exploited by antenna designers. As a result, in general, these modes are the most important to study for practical antenna designs.

3.1.1 The effect of geometrical changes on characteristic modes

In this section geometrical parameters of rectangular radiator, shown in Figure 9, are changed and the effect on characteristic modes is observed. If the effect of geometrical changes in rectangular radiator on characteristic modes is known, it can give possibilities to predict behaviour of characteristic modes. It means that the effect on resonant frequency, BW, quality factor and on other parameters of characteristic modes

will be predicted. In this thesis focus is on resonant frequency changes of characteristic modes.

The effect of changes of a rectangular radiator width on characteristic mode resonant frequency is shown in Table 1. Characteristic modes 1, 2 and 4 were chosen to emphasize the effect of the above mentioned changes on fundamental characteristic modes 1, 2 and to show the effect on higher characteristic mode - 4. Rectangular radiator from Figure 9 is used, where width parameter changed from 25 mm to 38 mm. Length is constant and equal to 40 mm during this study case.

Table 1. *The effect of width changes of rectangular radiator on characteristic mode resonant frequency*

Width [mm]	Mode 1 [GHz]	Mode 2 [GHz]	Mode 4 [GHz]
25	3.40	7.84	6.66
30	3.56	6.76	5.60
35	3.80	5.51	5.04
38	4.00	4.65	4.82

Graphical representation of the results shown in Table 1 provides wider possibilities for conclusions, see Figure 14. From Figure 14 it follows that by increasing width of radiator, different effects on characteristic mode resonant frequencies can be observed. So, resonant frequency of the first mode is directly proportional to changes of width, while resonant frequencies of the second and the fourth characteristic modes are inversely proportion to the same changes. As a result, resonant frequencies of these characteristic modes converge if width increases and diverge if width decreases. The mode 1 is varying, because geometrical parameters of the radiator are changing.

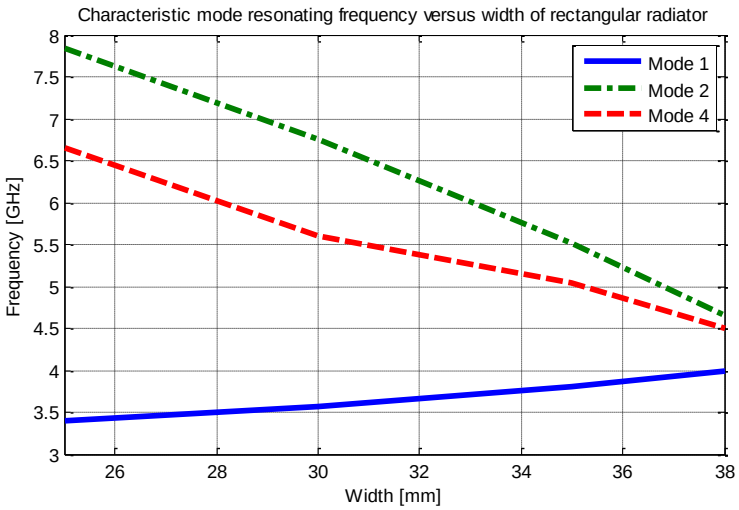

Figure 14. *The effect of width changes on characteristic mode resonant frequency*

Next, the effect of length changes on characteristic mode resonant frequency is studied. Rectangular radiator from Figure 9 is used in this study case. Length of rectangular

radiator is changed from 35 mm to 50 mm. Width of the rectangular radiator is constant and equal to 30 mm in this study case. The results of this study case are shown in Table 2 It is observable from Table 2 that resonant frequencies of all presented modes are directly proportional to changes of length parameter.

Table 2. *The effect of length changes of rectangular radiator on characteristic mode resonant frequency*

Length [mm]	Mode 1 [GHz]	Mode 2 [GHz]	Mode 4 [GHz]
35	4.30	6.92	5.83
40	3.56	6.76	5.60
45	3.08	6.58	5.50
50	2.71	6.34	5.41

The results shown in Table 2 are graphically represented in Figure 15. Resonant frequencies of characteristic modes diverge if length increases and converge if length decreases, as it follows from Figure 15,

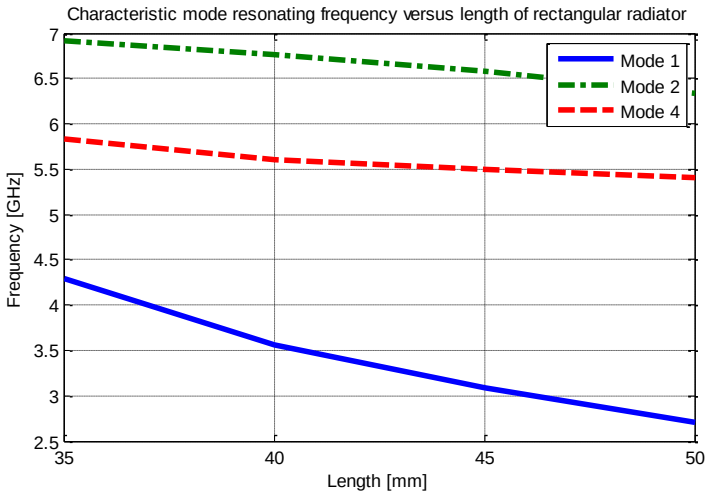

Figure 15. *The effect of length changes on characteristic mode resonant frequency*

In order to relate the results obtained in this chapter to patch antennas, it is required to know the effect of the ground plane and substrate on resonant frequencies of characteristic modes. In [5] it is reported that the ground plane and substrate have significant effect on resonant frequencies of characteristic modes. The ground plane and substrate decrease resonant frequencies of characteristic modes. However, discovered divergence and convergence properties of characteristic mode resonant frequencies can be applied for the antenna design and analysis.

In addition, from Figure 14 and Figure 15 it is possible to make conclusion about regularity of radiator. In both study cases one side of radiator is kept constant, while another is changing. So, it can be concluded that resonant frequencies of the first and the second modes are converging into a single point, once L and W become more equal.

Consequently, by taking previous statements into account and based on Figure 11, it follows that in case of regular radiator's geometry, the first and the second characteristic modes will have the same resonant frequency. That is because of the specific characteristic surface current distributions of the first 2 characteristic modes of a rectangular radiator shown in Figure 11.

Indeed, when condition $W = L = 30$ mm holds, it is discovered that the first and the second characteristic modes both resonate at 4.77 GHz frequency. This proves earlier mentioned statements. Similar results will appear also in chapter 3.1.2. However, the same resonant frequency of the first 2 modes does not mean that both of them will be excited equally if one of them is excited. That is because the first and the second characteristic modes have different surface current distributions, see Figure 11.

3.1.2 The effect of the ground plane presence on characteristic modes

To study the effect of the ground plane, radiator shown in Figure 9 is used together with the second rectangular radiator placed in parallel to it. The second radiator, which is placed in parallel, serves as the ground plane. In this chapter it is assumed that the ground plane is equal to or bigger than the radiator.

All in all, two study cases are observed in this chapter. The first study case relates changes of the ground plane size on characteristic modes, while height between radiator and the ground plane is constant and equal to 5 mm. Four different sizes of the ground plane are taken: 30x40 mm^2, 50x50 mm^2, 55x55 mm^2, 60x60 mm^2. In the first case the ratio of the side lengths is different from the other three cases, this was done to show the case when radiator's and ground's sizes are equal.

The second study case of this chapter relates changes of height on characteristic modes, while the ground plane size is constant and equal to 40x50 mm. In this study case radiator is as in Figure 9. The effect on the first characteristic mode is only observed due to very big computational time in this study case. Problems in calculation of characteristic mode values are described in more details in chapter 5. The generalized view for both study cases is shown in Figure 16, where it is possible to see radiator and the ground plane parallel to it.

When separate radiator and ground plane – having certain characteristic surface current distribution – are brought together to form a parallel plate structure, their characteristic surface current distributions remain the same. It is discovered that this holds for all modes. As a result, this can be used in design and analysis of antennas using TCM.

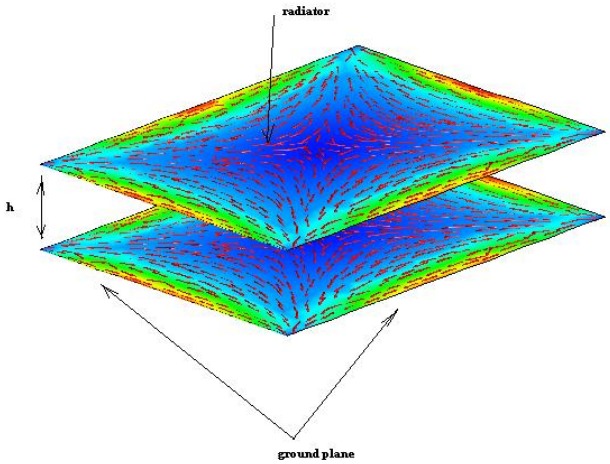

Figure 16. *Surface current distribution of the fifth characteristic mode for parallel rectangular plate situation at 3.6 GHz*

The results of the first study case of this chapter are summarized in Table 3 and Table 4. Resonant frequencies of characteristic modes for stand-alone radiator and the ground plane are shown in Table 3. Resonant frequencies of characteristic modes decrease if size of the stand-alone ground plane increases, as it comes from the results shown in Table 3. Indeed, this is basic antenna property [4], which states, in general, that resonant frequency of the antenna decreases if overall antenna's size increases and vice versa. Nevertheless, at this point it is proved that this concept holds also for radiators in terms of TCM analysis.

Table 3. *Resonant frequencies of characteristic modes of radiator and the ground plane of different size in stand-alone case*

Mode	Radiator 30x40 (GHz)	Ground 30x40 (GHz)	Ground 50x50 (GHz)	Ground 55x55 (GHz)	Ground 60x60 (GHz)
1	3.56	3.56	3.34	3.05	2.85
2	6.87	6.87	3.34	3.05	2.85
4	5.6	5.6	3.74	3.40	3.16

Table 4. *The effect of the ground plane size changes on characteristic mode resonant frequency*

Mode	Radiator/ground: 30x40/30x40 (GHz)	Radiator/ground 30x40/50x50 (GHz)	Radiator/ground: 30x40/55x55 (GHz)	Radiator/ground: 30x40/60x60 (GHz)
1	3.41	3.38	3.30	3.14
2	6.21	5.83	5.70	5.51
4	3.36	3.30	3.27	3.23

Furthermore, the effect of the ground plane presence together with radiator is shown in Table 4. The ground plane presence of all sizes decreases resonant frequencies of characteristic modes in comparison to stand-alone cases shown in Table 3. In addition,

when the ground plane size increases, resonant frequencies of characteristic modes are decreasing even more, similar to discovered earlier stand-alone ground plane case. All these results are in correspondence with notations about the ground plane presence reported in [6].

This study case proves that there is impact effect between the ground plane and radiator in terms of characteristic modes. Two terms should be introduced at this point: (1) characteristic mode resonant frequency of the ground plane and radiator in stand-alone case, $f_{gnd_{alone}}$ and $f_{rad_{alone}}$, respectively, and (2) characteristic mode resonant frequency in case when both radiator and the ground plane are present, $f_{rad+gnd}$. Consequently, it follows that $f_{rad+gnd} \in [f_{gnd_{alone}}; f_{rad_{alone}}]$, which comes from comparison of the results from Table 3 and Table 4. The only exception is when the ground plane and radiator have the same size. In that case resonant frequency of the characteristic mode is out of $f_{rad+gnd}$ value range. In most antenna cases, the ground plane is considered bigger in size than radiating element. Finally, the results of characteristic mode resonant frequencies obtained for regular ground plane sizes prove the statement about equality of the first and the second characteristic modes. It was stated in chapter 3.1.1.

The results of the second study case are shown in Table 5. From these results it is possible to conclude that by increasing height, resonant frequency of the characteristic mode is increasing and vice versa. So, resonant frequency changes proportionally to changes of height. This again shows impact effect between radiator and the ground plane in terms of TCM. When radiator is placed closer to the ground plane, impact has stronger effect. If height is increased, impact has less effect, because then the resonant frequency of the characteristic mode is closer to radiator stand-alone case, as it comes from comparison of Table 5 and Table 3

Table 5. *The effect of height between radiator and the ground plane on resonant frequencies of characteristic modes*

Height (mm)	Resonant frequency (GHz)
5	3.41
4	3.39
3	3.37
2	3.34

3.1.3 Excitation of characteristic modes on radiators

The aim of this chapter is to show how to excite characteristic modes using TCM. In particular, rectangular radiator is used. However, it is possible to use the same analysis method, as it is shown in this chapter, to excite characteristic modes on radiators of different geometries. In this paragraph, the excitation voltage source of 1 V is used.

To study how well the characteristic mode is excited, it is required to observe modal excitation and weighting coefficients as it was mentioned in chapter 2. The idea of characteristic mode excitation is based on choosing proper radiator feed placement. Feed is placed based on characteristic surface current distribution. It should be done so that weighting coefficients for desired characteristic mode at needed frequency will have high values relatively to all other characteristic modes.

The study case of this chapter is based on observing the effect on weighting coefficients of characteristic modes using different feed placements. Weighting coefficients are real, as it was proved in chapter 2. So, analysis process due to this fact becomes much easier. In this chapter it is assumed that the first characteristic mode of rectangular radiator shown in Figure 9 should be excited. The first characteristic mode of chosen radiator is resonating at 3.56 GHz, as it was discovered in chapter 3.1.

All in all, it is possible to define 5 special points for feed placement on rectangular radiator based on characteristic surface current distribution of the first characteristic mode given in Figure 11. These special points are shown in Figure 17. The red bold point represents feed. The first 5 results of normalized weighting coefficients for the first five characteristic modes are shown in Figure 18. It follows that if the radiator is symmetrical in some axis, then feed symmetrical placement will lead to equal results for weighting coefficients of characteristic modes. In addition, the first characteristic mode is excited quite well at 3.56 GHz, when feed is placed in the middle of a rectangular radiator and close to the top or bottom edges of given rectangular radiator, see Figure 18. The term „quite well" means that weighting coefficient of the first characteristic mode at 3.56 GHz is higher than for other characteristic modes.

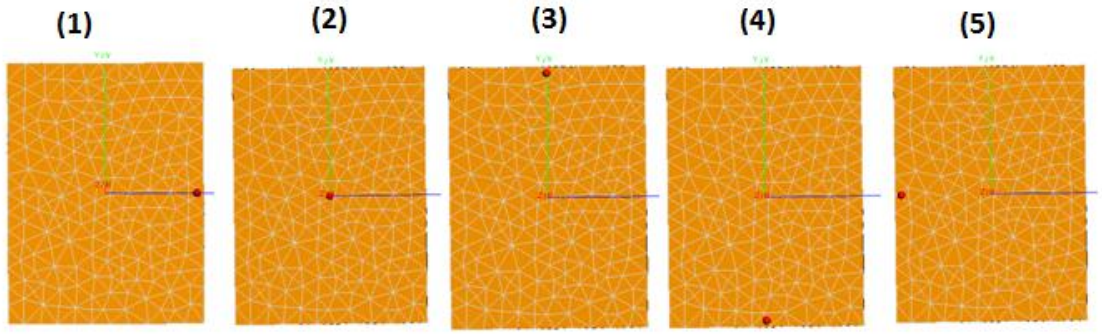

Figure 17. *Feed placement on rectangular radiator*

However, the results obtained by placing feed in the middle of bottom or top edges of rectangular radiator did not provide the best possible results. It means that other characteristic modes are still significantly excited. Excitation of other characteristic modes is unwanted, because then energy is wasted on unneeded characteristic modes. It is required to excite only the first characteristic mode, as assumed for example purposes. So, feed placement should be modified to improve excitation of the first characteristic mode.

Feed position can be changed with respect to characteristic surface distribution of the first characteristic mode. Based on previously found feed placement it is possible to conclude that the area of rectangular radiator, which would provide better excitation results for the first characteristic mode, should have a bit higher surface current distribution values. So, feed should be placed close to bottom or top edge of rectangular radiator, see Figure 11 and Figure 18. On the same time, feed has to be moved closer to the center of rectangular radiator. Modified feed placement and corresponding excitation and weighting coefficients for the first 5 characteristic modes are given in Figure 19. Indeed, using modified feed position, which was obtained by empirical trials based on characteristic current distribution of the first characteristic mode, weighting coefficients for the first characteristic mode are much higher than for all other modes over given frequency range. So, it is possible to conclude that different feed placements have significant impact on characteristic mode excitation.

The modal excitation coefficient, studied in chapter 2, is also related to characteristic mode excitation. This is shown using the results of modal and weighting excitation coefficients, see Figure 19. Modal excitation coefficient, in general, describes how well certain characteristic mode is coupled to the source. Whereas weighting coefficients show the real effect of characteristic modes on characteristic surface currents at desired frequency.

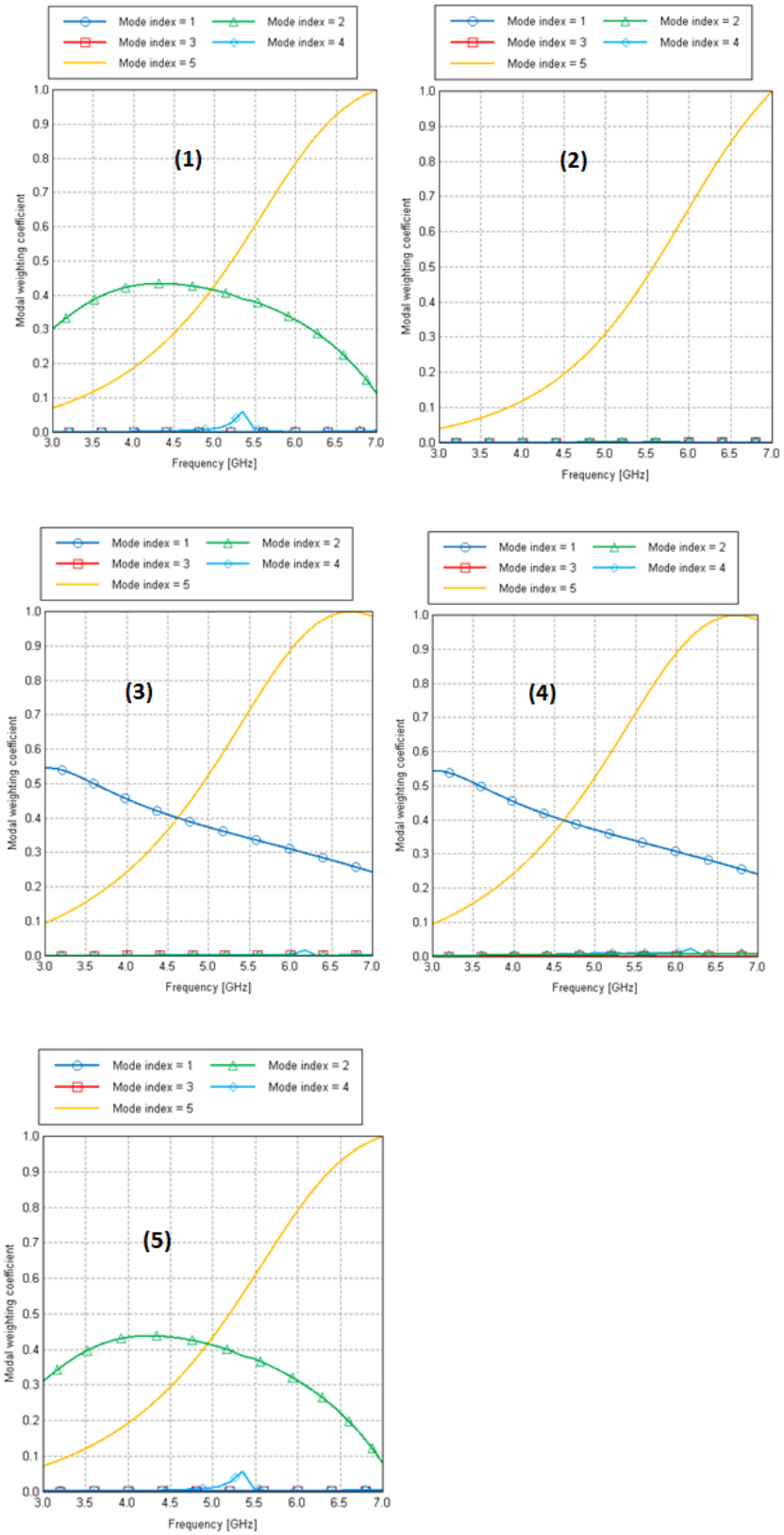

Figure 18. *Normalized weighting coefficients for 5 different feeder placements on rectangular radiator*

However, if only modal excitation coefficients are studied, this may lead to wrong understanding of characteristic mode excitation. Example of modal excitation coefficients is provided in Figure 19. Modal excitation coefficients are showing that the fifth characteristic mode is excited well. However, weighting coefficients are proving that the fifth characteristic mode has almost no impact on characteristic currents over given frequency range, especially at desired resonant frequency of 3.56 GHz. Thus, in order to study excitation of characteristic modes, it is required to observe weighting coefficients.

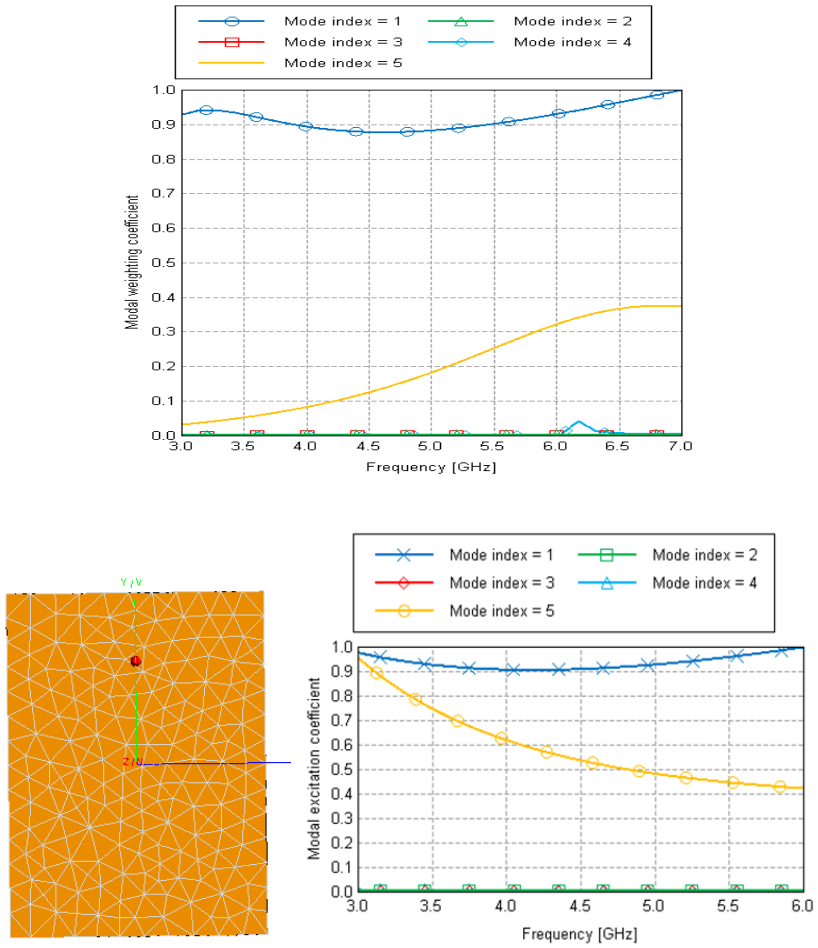

Figure 19. *Modified feeder placement for the first characteristic mode excitation*

3.1.4 The effect of multiple rectangular planar radiators in free space

In this chapter 4-plate and 2-plate configurations of rectangular radiators in free space are observed. Each single rectangular radiator is assumed to have the same size as in Figure 9. The aim is to show the effect of multi-plate configurations on characteristic surface current distribution. As a result, this can help, for example, in design and analysis of antenna arrays and dual patch antennas.

Characteristic surface current distributions of the first five characteristic modes are shown in Figure 20. It is observable that all rectangular radiators are interacting with each other in 4-plate configuration. This holds for all five characteristic modes. Furthermore, all five characteristic modes recall surface current distribution of the first and the second characteristic modes in stand-alone case of a single rectangular radiator, see Figure 11. So, properties of a single rectangular radiator, from TCM point of view, are useful also for multi-plate configurations.

In addition, during simulations in FEKO, it is observed that distance between plates in multi-plate configuration has an effect on the characteristic surface current distribution. When the distance between the plates was increased, each plate began to act having less impact from other plates. As a result, characteristic surface current distribution on *each separate* plate became more similar to stand-alone rectangular radiator case.

Another effect was observed when distance between plates decreased. Each plate had more impact from other plates. As a result, the overall characteristic surface current distribution in multi-plate configuration *all-together* became more similar to stand-alone rectangular radiator case.

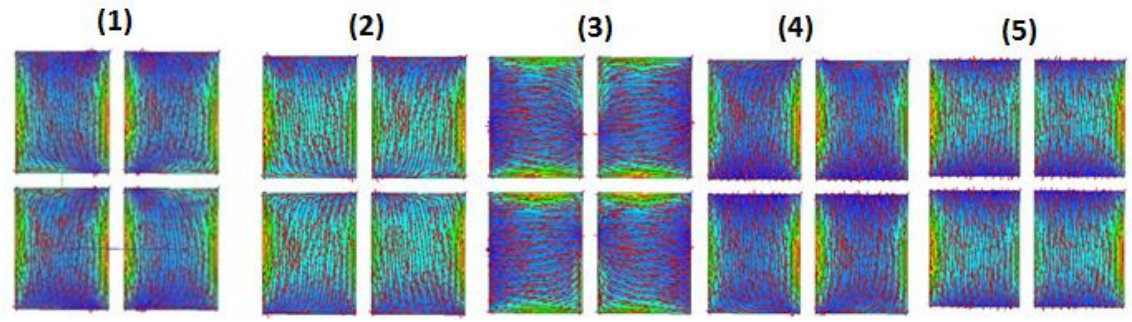

Figure 20. *Characteristic surface current distribution of the first 5 modes at 3.6 GHz for 4-plate configuration*

Characteristic surface current distributions of the first 5 characteristic modes for 2-plate configuration in free space are shown in Figure 21. Several conclusions can be done based on Figure 21. It is worth to notice that the third and the fourth characteristic modes have closed loops in characteristic surface current flows. It means that these characteristic modes have inductive nature. Characteristic modes 1, 2 and 5 have parallel current flows. It means that these characteristic modes have capacitive nature. All in all, given characteristic modes are acting in correspondence to single rectangular radiator case explored in chapter 3.1.1.

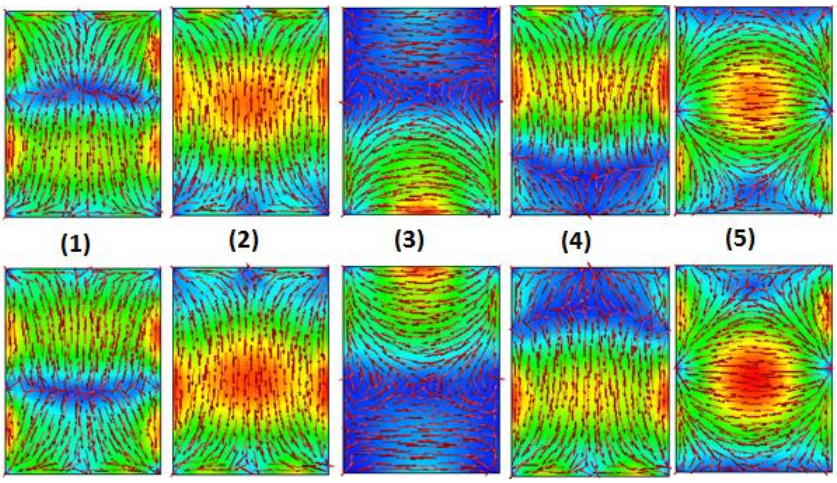

Figure 21. *Characteristic surface current distribution of the first 5 modes at 3.6 GHz for 2-plate configuration*

Dual-radiator configurations can be used to implement, for example, dual-patch antennas to work in several frequency bands. Radiator for the dual-patch antenna, implemented and meshed in free space, is shown in Figure 22, ground plane was omitted from this analysis. Based on given radiator shape, dual patch antenna was produced during "Antenna Project" course in Tampere University of Technology. In this project, two rectangular radiators were connected together using feeding line and further connected to co-axial feed at the middle point of it.

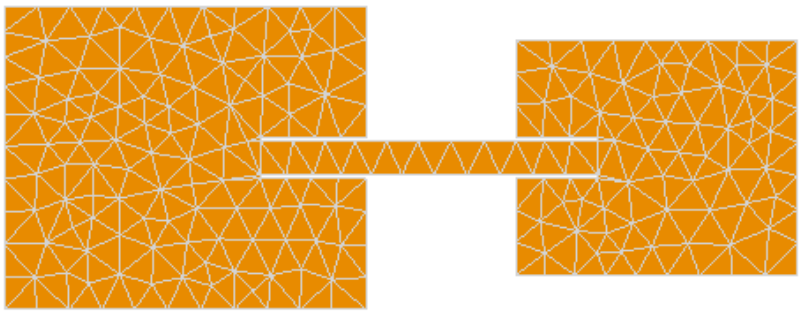

Figure 22. *Radiator of dual-patch antenna*

The overall surface area of dual-patch radiator shown in Figure 22 has overall length 195 mm and width is 95 mm. Thus, computational time in FEKO is long. As a result, only the first 3 characteristic modes were considered in this study case. Characteristic surface current distributions of the first 3 characteristic modes for dual-radiator geometry are shown in Figure 23. It follows that the best placement of feed, to excite characteristic modes 1, 2 and 3, is in the middle of feeding line in both vertical and horizontal direction, as it comes from information of chapter 3.1.3. Indeed, the same placement of feed was discovered also during "Antenna Project" course in TUT. However, it was found using trial and error approach. Nevertheless, this proves that TCM can be applied to find proper feed placement.

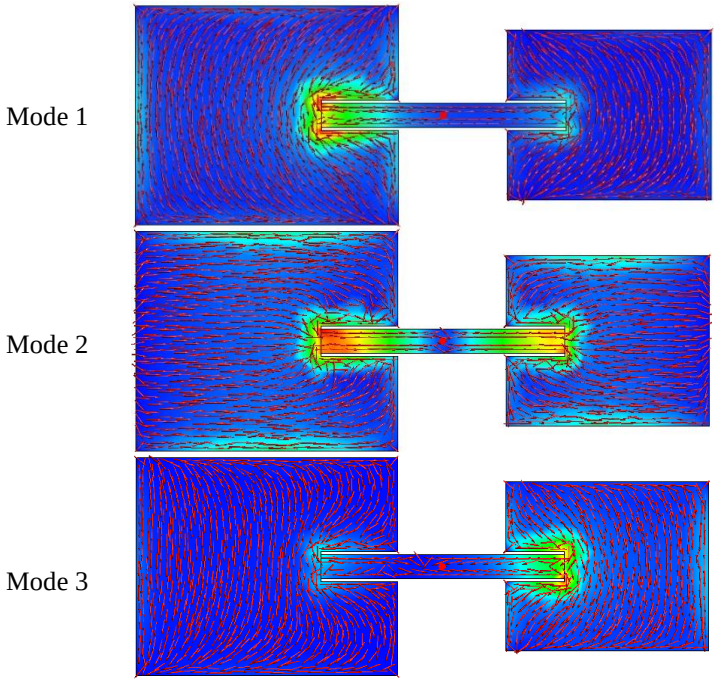

Figure 23. *Characteristic surface distributions of the first 3 characteristic modes for dual-radiator at resonant frequencies of characteristic modes*

It is possible to describe working principles of dual-radiator from TCM point of view. The main aim is to explore dual frequency band nature of such structure. To explain this is in details, it is required to study characteristic angles and weighting coefficients of dual-radiator shown in Figure 23. Characteristic angles and weighting coefficients for the first 3 characteristic modes are given in Figure 24 .

Based on characteristic angle values, it is possible to conclude that over given frequency range characteristic modes 1, 2 and 3 are resonating respectively at 1.22 GHz, 1.43GHz and 1.71 GHz. For the third characteristic mode interpolation is used. Furthermore, weighting coefficients are showing that the first characteristic mode is not excited over given frequency range with such feed placement. Thus, the second and the third characteristic modes should be considered to explain possible dual frequency band nature of given radiator. Given radiator should work at 1.43 GHz and 1.71 GHz. As a result, at 1.43 GHz frequency the second characteristic mode is excited, while all the rest characteristic modes are not, see Figure 24. Furthermore, at 1.71 GHz the third characteristic mode best excited. So, at this point dual-band nature of dual-radiator is explained. Similar approach, as described in this chapter, can be used for any other geometrical shape of radiators.

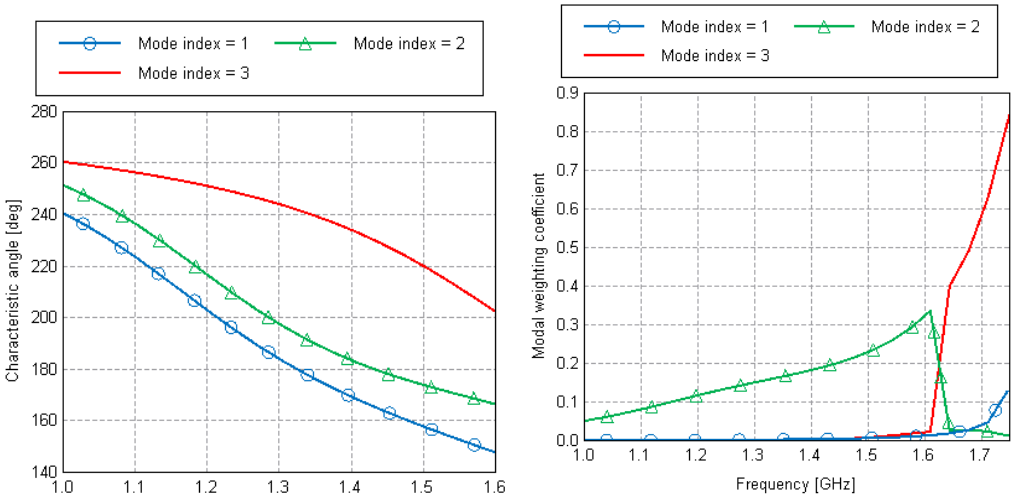

Figure 24. *Characteristic angle and weighting coefficients for the first 3 characteristic modes of dual-radiator*

In addition, normalized characteristic radiation patterns in XY plane of the first 3 characteristic modes are shown in Figure 25. So, dual-radiators are acting as a single radiator in terms of characteristic radiation patterns, as follows from comparison of Figure 13 and Figure 25. To conclude, direct correlation between characteristic radiation patterns of a single and dual radiator is observable.

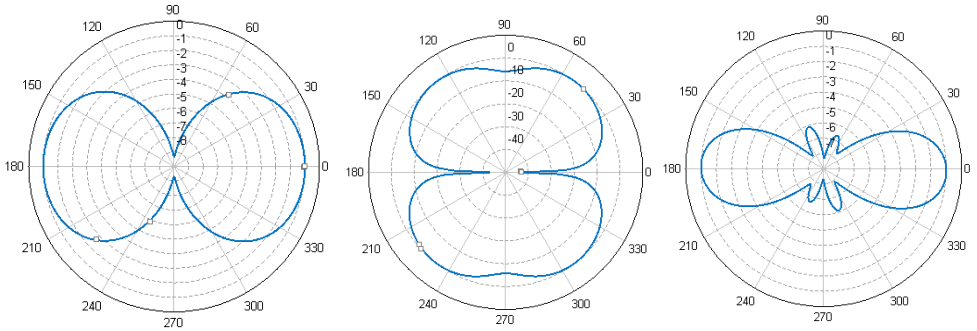

Figure 25. *Normalized characteristic radiation patterns in XY plane of the first 3 characteristic modes for dual-radiator geometry at resonant frequencies*

3.1.5 The effect of radiator scaling on characteristic modes

The basic idea of this chapter is to show scaling theory of antennas [4] in case of TCM, using rectangular radiators, as an example. Study cases of lossy and PEC conditions are observed in this chapter.

To scale the antenna, it is required to fulfil scaling conditions described in Table 6, where *n* is scaling factor. Nevertheless, in the real life it is not always possible to scale conductance of conducting surface, because finite set of metals is available in practice. Copper is chosen as lossy metal example for this chapter. For both lossy and PEC study

cases 20x30 mm^2 and 40x60 mm^2 rectangular radiators are used, see Figure 26. Thus, it is assumed to aim on scaling coefficient of 2.

Table 6. *Scaling parameters for the antenna [4]*

Parameter	Equation	Parameter	Equation
Length	$l' = l/n$	Permittivity	$\epsilon' = \epsilon$
Time	$t' = t/n$	Permeability	$\mu' = \mu$
Wavelength	$\lambda' = \lambda/n$	Velocity	$v' = v/n$
Capacitance	$C' = C/n$	Impedance	$Z' = Z$
Echo area	$L' = L/n$	Antenna gain	$G_0' = G_0$
Frequency	$f' = nf$	Conductivity	$\sigma' = n\sigma$

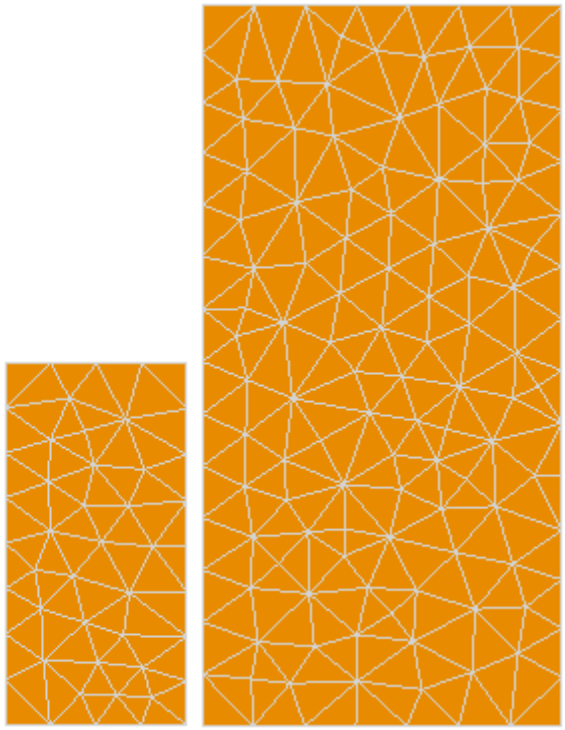

Figure 26. *Pair of scaled rectangular radiators in 1:1 scale*

In the first study case, PEC condition is applied to radiators shown in Figure 26. Characteristic angle coefficients of this study case are shown in Figure 27. As an example, the first characteristic mode can be observed. In case of smaller radiator, the first characteristic mode is resonating at 6.444 GHz, whereas, scaled by factor of 2, bigger radiator has the resonant frequency of the first characteristic mode at 3.222 GHz. Thus, this shows that scaling theory of antennas can be applied also for TCM using PEC condition.

In the second study case, cuprum material is applied to radiators shown in Figure 26. As a result, it is discovered that the first characteristic mode of smaller radiator is resonating at 6.6371 GHz, whereas bigger scaled radiator has resonating frequency of the first characteristic mode at 3.3265 GHz. So, as predicted before, difference in

resonant frequencies is less than double, because conductivity of metal was not changed during scaling. Scaling factor in this case is 1.9952. To conclude, it means that in practical applications, scaling theory can be applied also for lossy metals using TCM.

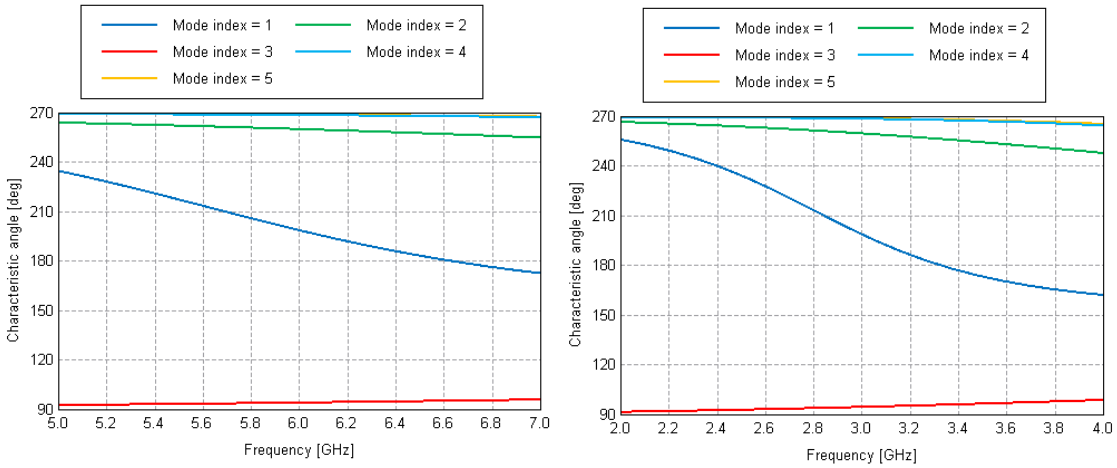

Figure 27. *Characteristic angles for the first 5 characteristic modes for a pair of scaled rectangular radiators with PEC condition*

3.2 Relation of cavity model to characteristic mode theory

Patch antennas can be analysed using cavity model [4]. Cavity model [CM] introduces possibilities to obtain required parameters of the antenna, including resonant frequency. Since this method is used widely, e.g. for patch antenna analysis and design, it is required to understand how it correlates with TCM results. Eigenvalues and eigencurrents are not dependent on any excitation source, as it was discovered in chapter 2. Thus, it is required to examine CM when the antenna has no feed.

Cavity model can be applied if it is assumed that height of the patch above the ground plane is small and thus only E_z component is dominant. In addition, CM can be applied if and only if there is no fringing field at the boundary of the patch. As a result, Neumann boundary condition for electric field $\frac{\delta E_z}{\delta n} = 0$ can be introduced, where n is the outer normal to the patch's boundary. Finally, CM is introduced when there is no internal coupling. In the case when feed is not connected to the antenna, the Helmholtz wave equation and the Neumann boundary condition will be written as:

$$\Delta_{xy} E_z + k^2 E_z = 0. \tag{27}$$

Thus, by solving equation (27) for eigenfields and eigenfrequencies [13], it results in:

$$f_n = \frac{c_0 k_n}{2\pi\sqrt{\epsilon_{eff}}} \tag{28}$$

where $k_n^2 = \lambda_n$ [13], λ_n is the eigenvalue, c_0 is the speed of light, and ϵ_{eff} is effective dielectric constant. Using equation (28) it is possible to relate cut-off frequency obtained from CM to TCM. However, since full-wave MoM is taken into account during TCM, it takes all the internal coupling through the radiation in contrary to CM [13]. This is an advantage of TCM over CM.

To compare cut-off frequencies of transverse electric [TE] modes obtained from CM with resonant frequencies of characteristic modes obtained from TCM, single rectangular radiator in free space is chosen. The expression for cut-off frequency of TE modes in rectangular waveguide is [9]:

$$f_{mn} = \frac{c}{2}\sqrt{\left(\frac{m}{a}\right)^2 + \left(\frac{n}{b}\right)^2} \tag{29}$$

where *m* and *n* are indexes for corresponding TE mode, whereas *a* and *b* are respectively the length *L* and the width *W* shown in Figure 9. Using dimensions in Figure 9 equation (29) gives $f_{cutoff_{TE_{10}}}$ = 3.75 GHz, $f_{cutoff_{TE_{01}}}$ = 5 GHz, and $f_{cutoff_{TE_{11}}}$ = 6.25 GHz. These results correspond respectively to resonant frequencies of the modes given in Figure 10, which are $f_{res_{Mode1}}$= 3.56 GHz, $f_{res_{Mode4}}$= 5.6 GHz, $f_{res_{Mode2}}$= 6.76 GHz. So, it is possible to conclude that the results of TE mode resonant frequencies are close to resonant frequencies of characteristic modes. There is difference in the results, but within such difference given characteristic modes can be still considered as resonating. For example, the difference between $f_{cutoff_{TE_{10}}}$ and $f_{res_{Mode1}}$ is 0.19 GHz. Based on Figure 10, it is possible to see that at 3.75 GHz frequency the first characteristic mode has characteristic angle value 177^o. So, it proves that within given frequency difference characteristic modes are close to perfect resonating conditions, which would be at characteristic angle value of 180^o. All in all, it means that CM can be related to TCM.

Resonant frequency f_{mn} of transverse magnetic [TM] mode of rectangular patch antenna can be obtained as:

$$f_{mn} = \frac{c}{2\sqrt{\epsilon_{eff}}}\sqrt{\left[\frac{m}{L+2\Delta L}\right]^2 + \left[\frac{n}{W+2\Delta W}\right]^2} \tag{30}$$

where and are the equivalent length ΔL and width ΔW account for the fringing fields at the open ends along the patch length and width [9]. If radiator, ground plane and a substrate are introduced into TCM calculation, equation (30) can be used to compare resonant frequencies from TCM and CM.

3.3 Polarization analysis using theory of characteristic modes

In this section characteristic field polarization types are described from TCM point of view. Characteristic fields are generated by characteristic surface currents. Characteristic fields are orthogonal to each other, because characteristic surface currents are orthogonal to each other. It means that the total field around radiator can be expressed as a vector sum of characteristic field components of excited characteristic modes.

All in all, there are only three different polarization types, as it was described in chapter 2. This section focuses on linear and circular polarization types.

3.3.1 Linear polarization of characteristic fields

Linear polarization holds if radiated time-harmonic wave has two orthogonal linear components that are in time phase or in $180^{o}n$, where $n \in \mathrm{Z}$, out-of-phase [4]. So, components axial ratio should be much greater than 1, infinite value in pure linear polarization case.

From definition of linear polarization it follows that characteristc field will be linearly polarized, if generalized characteristic surface current flows of characteristic modes will have capacitive nature, see Figure 12. It results in parallel surface current flows.

Excitation of any characteristic mode can be described using excitation or weighting coefficients, as it was described in previous sections. It means that weighting coefficients will have directly proportional effect on AR. In another words, higher values of weighting coefficients will lead to higher values of AR at certain frequency and vice versa. The same statement holds also for excitation coefficients, since they are dependent on eigencurrents. Nevertheless, excitation coefficients are not taking into account eigenvalues, thus, they are indirectly related to AR of characteristic fields.

Based on the above statements and on theory from chapter 2 it is possible to conclude that for *linear polarization* the following statements are true from TCM point of view:

1. it is required to excite at least one characteristic mode resulting in parallel characteristic surface current flows
2. characteristic angle of a characteristic mode at required frequency has to be $\alpha_{chosen\ mode} = 180^{o}$
3. weighting and excitation coefficients at required frequency for a characteristic mode: $v_{chosen\ mode} \gg v_{any\ other\ mode}$; $V^{i}_{chosen\ mode} \gg V^{i}_{any\ other\ mode}$.

The above mentioned statemens can be proved. For example, simple rectangular patch antenna for Wi-Fi application can be designed using generalized TCM antenna design

appoach, which is described in chapter 5. Linear polarization at 2.4 GHz resonant frequency is assumed.

As a result, total surface current of the antenna and characteristic surface current of the first characteristic mode both are shown in Figure 28. It is possible to see that the total surface current, indeed, corresponds to characteristic surface current of the first characteristic mode. So, it means that characteristic modes with capacitive nature will prodoce similar total surface current on the radiator's surface.

Axial ratio of the antenna is shown in Figure 29. It is possible to see that AR at a resonant frequency for all θ angles is > 38 dB, which corresponds to linear polarization case.

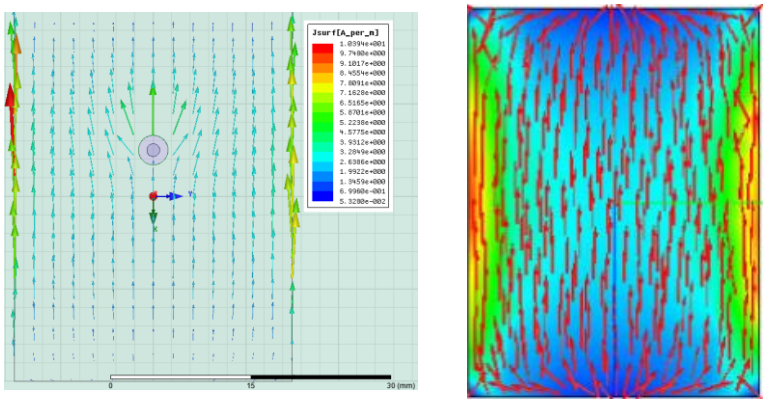

Figure 28. *Total surface current of the patch antenna for Wi-Fi application (left) and characteristic surface current of the first characteristic mode (right), both at 2.4 GHz*

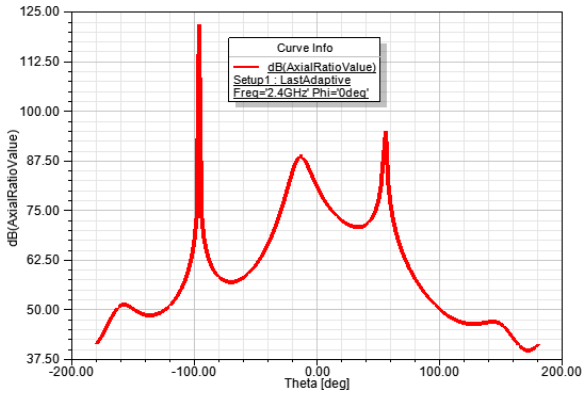

Figure 29. *AR of the patch antenna for Wi-Fi application at 2.4 GHz*

All in all, given example proves all the above mentioned statements about linear polarization from TCM point of view. So, it is possible to analyse and to generate linear polarization using theory of characteristic modes.

3.3.2 Circular polarization of characteristic fields

Circular polarization holds if time-harmonic field has two orthogonal linear components with the same magnitude and a time-phase difference of odd multiples of 90^o [4]. Circular polarization can be achieved by both special geometries and different feed in antennas [4]. However, total surface current flows of the antenna in all cases will form closed loops. So, from TCM point of view, the main aim is to excite at least two characteristic modes, such that the total surface current produced by them would have closed loop current distribution, it corresponds to inductive nature case, see Figure 12.

In the definition of a circular polarization it is stated that magnitudes of the field components should have the same magnitude. In chapter 2 it was mentioned that from physical point of view, modal significance represents normalized characteristic surface currents of characteristic modes. Thus, it means that for a circular polarization, at required frequency, modal significance values of two excited characteristic modes have to be the same. So, in circular polarization case at required frequency weighting coefficients have to be equal.

In addition, from the same definition of a circular polarization, it is mentioned that field components are orthogonal. From physical point of view, characteristic angle represents phase angle between characteristic surface current and corresponding characteristic field. Thus, it means that characteristic angle difference between two excited characteristic modes have to be 90^o. So, it is possible to define conditions for a circular polarization from TCM point of view [6]:

1. it is required to excite at least two characteristic modes *n* and *m* resulting in closed loop total surface current flow
2. at required frequency: $MS_n = MS_m$ or $\nu_n = \nu_m$
3. $|\alpha_n - \alpha_m| = 90^o$.

As an example, triangular radiator is chosen to show how to generate circular polarization using only one feed. Based on characteristic surface currents of a triangular radiator it is assumed that characteristic modes 2 and 4 have to be excited, because their vector sum will result in closed loop surface current flow, see Figure 30.

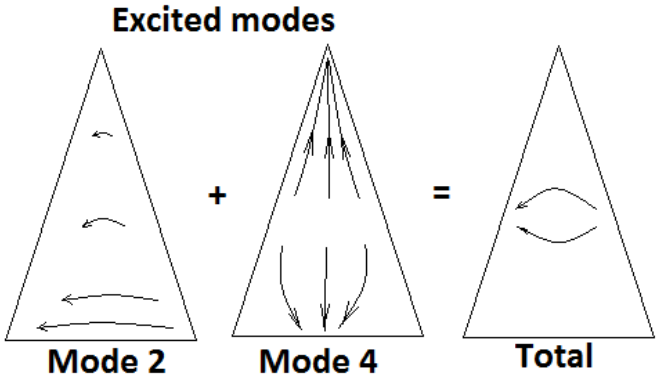

Figure 30. *Generalized total surface current flow made from characteristic modes 2 and 4 on a triangular radiator*

Best feed position for the second and the fourth modes excitation can be found using trial and error method. So, feed position is determined such that two characteristic modes 2 and 4 are excited best. Triangular radiator's characteristic angle, weighting coefficient and modal significance values are shown in Figure 31.

It is possible to see that characteristic weighting coefficients of the second and the fourth modes have much higher values than for all other characteristic modes. Thus, it means that these two characteristic modes are excited best in the frequency range from 2 GHz to 4 GHz. Modal significance value equality for characteristic modes 2 and 4 holds at 2.77 GHz. However, MS coefficients are not dependent on excitation, thus, it is more important at which frequency weighting coefficients are equal. Weighting coefficients of characteristic modes 2 and 4 are equal at 2.1 GHz and 3.3 GHz. Characteristic angle differences of characteristic modes 2 and 4 at frequencies 2.1 GHz and 3.3 GHz are respectively $\Delta_{2.1GHz} = 100^o, \Delta_{3.3GHz} = 20^o$. So, it means that at 3.3 GHz frequency circular polarization cannot hold, because characteristic angle difference of the modes is much smaller than 90^o. Nevertheless, at 2.1 GHz elliptic (close to circular) polarization will appear, because characteristic angle difference is close to 90^o. For ideal circular polarization, feed location should be changed such that weighting coefficients for the modes would be equal at 2.77 GHz frequency by trial and error based on characteristic current distribution.

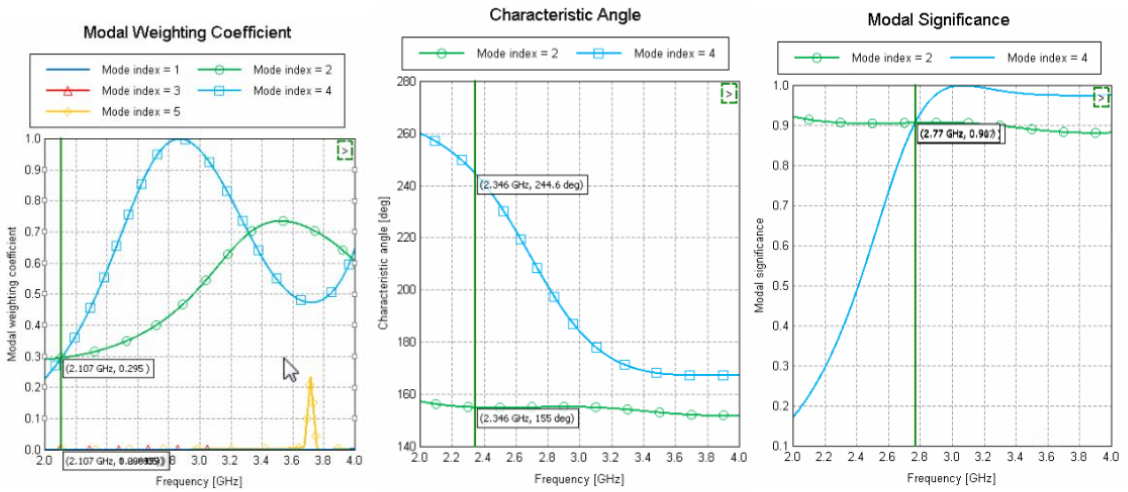

Figure 31. *Weighting coefficients, characteristic angles and modal significance coefficients of a triangular radiator for frequency range 2-4 GHz*

All in all, it follows that it is non-trivial task to generate circular polarization at given frequency using radiator of arbitrary geometrical shape. The most problematic is to excite several characteristic modes equally on a given radiator. This task may become even more difficult if some part of a radiator has been cut away, because in that case characteristic surface currents will be frequency-dependent. Nevertheless, previously shown example of a triangular radiator proves that circular polarization of the antenna can be studied and generated using TCM.

3.4 Radiators of isospectral geometries

In 1956 the question stated by Mark Kac became as a starting point in the research field of isospectral domains. The question was – "Can one hear the shape of a drum?" [8]. From mathematical point of view, it means whether there exist at least two non-isometric domains on the plane such that the spectra of the Laplacian of them coincide [20]. Such domains are called isospectral. This chapter is showing isospectral properties of radiators, having isospectral geometries, in terms of TCM. Two study cases are considered in this chapter: study of isospectral pairs and study of isospectral couples. It means that in the first case only two isospectral domains are studied at one time. In the second case, several isospectral domains are studied at one time. In both study cases the overall area of isospectral domains should be the same [20]. So, in theory, it means that TCM properties of such domains should be similar.

From theory, all isospectral domain pairs and couples have the same frequency spectrum [20]. Isospectral domains can provide flexibility for antenna designers in choosing different geometrical shapes with similar radiation properties. By the default, isospectral domains can be made using the set of triangles [20]. However, triangles can be replaced by any other geometrical shape, which would fit into them. As a result,

different isospectral domain geometries can be obtained. This process is shown in Figure 32.

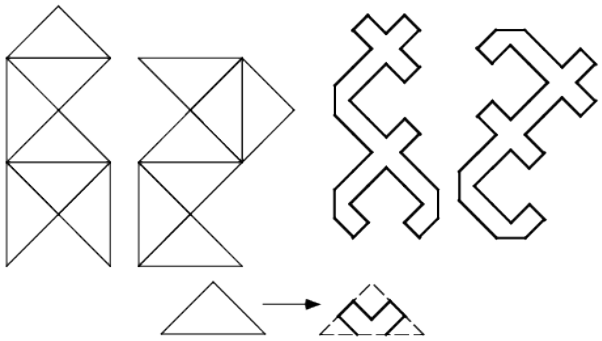

Figure 32. *Creation of different geometrical shapes, having isospectral properties [8]*

Pair of radiators, having geometrical properties of isospectral domains, based on Figure 32, were created and implemented in FEKO, see Figure 33. Characteristic angle coefficients for the first 5 characteristic modes are shown in Figure 34. It is possible to see there only one plot of characteristic angle results. It is because characteristic angles for both isospectral geometries are the same. Thus, it proves that isospectral properties can be applied also for radiators. Hence, a pair of radiators with isospectral properties can be called as *isospectral radiators*. In general, the term isospectral radiators can be used for radiators whose characteristic mode values are the same and whose geometries are isospectral. Furthermore, the above mentioned definition can be rephrased in terms of chapter 3.1.1. So, a pair of radiators having the same characteristic mode values, but whose geometries are not isospectral, can be called as *semi-isospectral radiators*.

To relate isospectral properties of characteristic modes to real antennas it is required to study characteristic surface current distributions and characteristic radiation patterns in XY plane shown in Figure 35. Characteristic surface current distributions and characteristic radiation patterns in XY plane for the first 5 characteristic modes for isospectral radiator pair shown in Figure 33, are given in Figure 35.

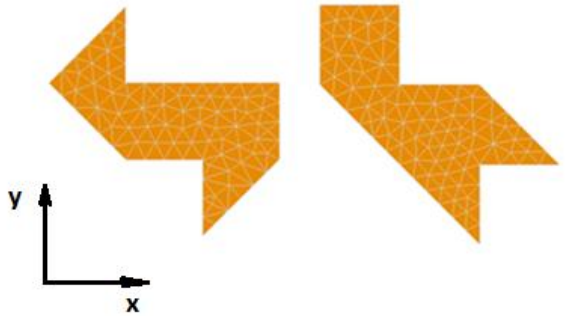

Figure 33. *Pair of radiators of isospectral geometry*

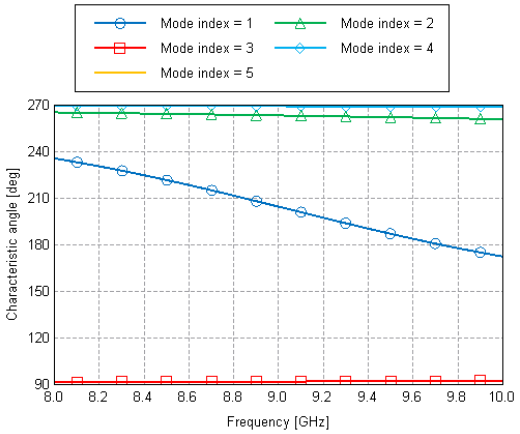

Figure 34. *Characteristic angle coefficients of the first 5 characteristic modes of isospectral radiator pair*

Based on comparison between Figure 35 and Figure 11 it is possible to conclude that characteristic surface current distributions of the first 5 characteristic modes recall the same physical nature as in case of a single rectangular radiator observed in chapter 2. It means that characteristic modes 1, 2 and 5 have capacitive nature, but characteristic modes 3 and 4 have inductive nature.

Characteristic radiation patterns of isospectral radiators are a bit different. Nevertheless, similarity between them is high. Characteristic radiation patterns are only shifted a bit with respect to each other and have slightly different values. This is unexpected exploration, because both isospectral radiators have absolutely different geometrical shapes.

To conclude, a pair of isospectral radiators provides the same characteristic mode values and has similar characteristic radiation patterns in XY plane. This can be used in antenna design and analysis. All in all, also from TCM point of view, the answer to Mark Kac's question would be - "No, the one cannot hear the shape of drums".

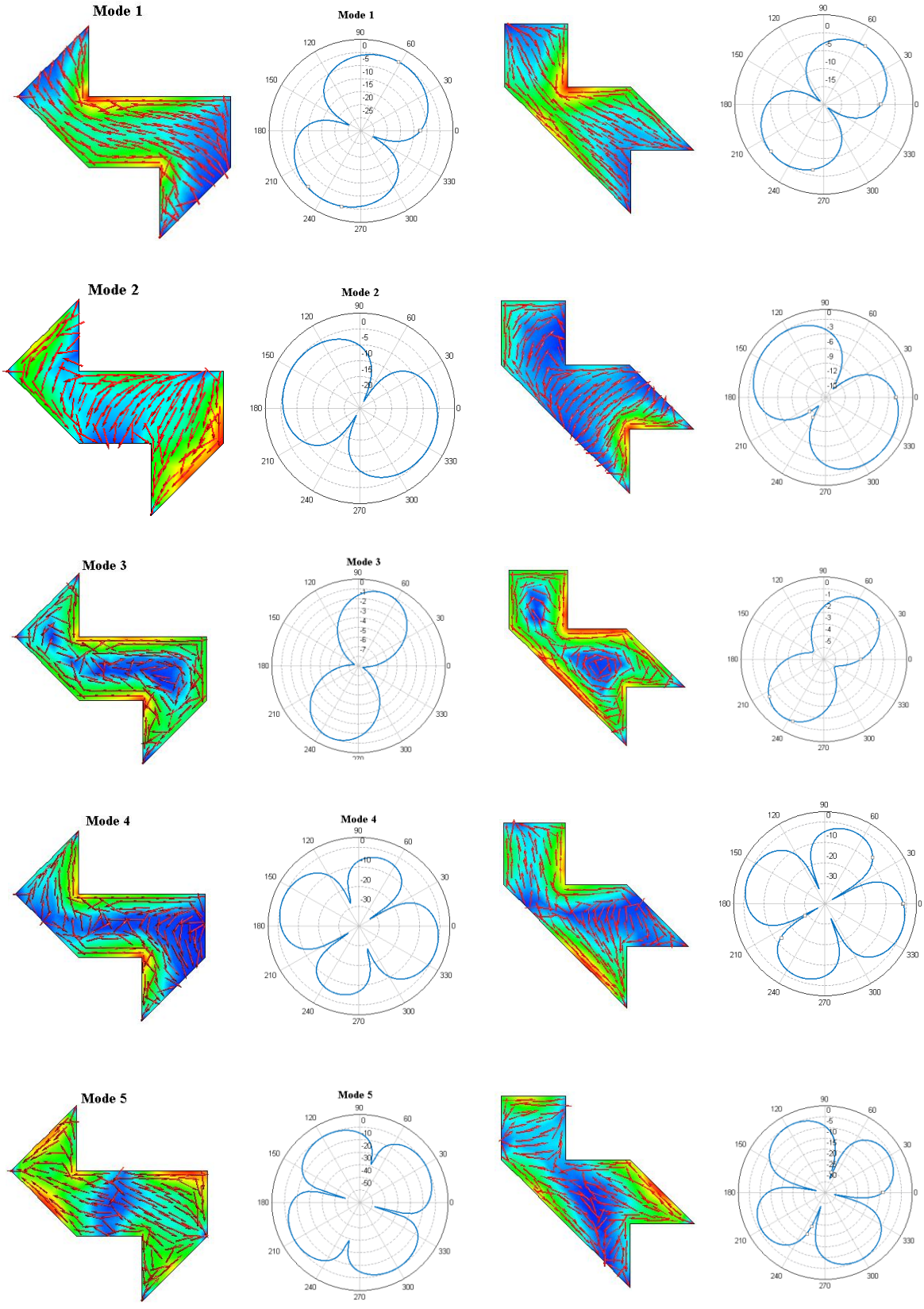

Figure 35. *Characteristic surface currents distributions and characteristic radiation patterns in XY plane of the first 5 characteristic modes of isospectral radiators*

In the second study case of this section, couples of isospectral domains are studied. Example of such couples, together with their FEKO software implementation, is shown in Figure 36.

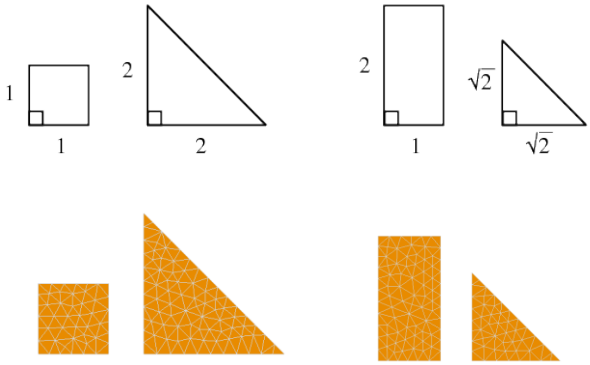

Figure 36. *Isospectral couples*

Characteristic angle coefficients for isospectral couples, shown in Figure 36, are given in Figure 37. Arbitrary frequency range is chosen, and it is from 9 GHz to 11 GHz. Only one plot is represented in Figure 37, because characteristic angle coefficients for both isospectral couples are the same. Thus, it is proved that if couples of radiators, having isospectral geometry property, are used, the same characteristic modes are appearing in both structures. In terms of antenna design this can be interpreted as combinations of antenna arrays with different shapes, but having similar properties.

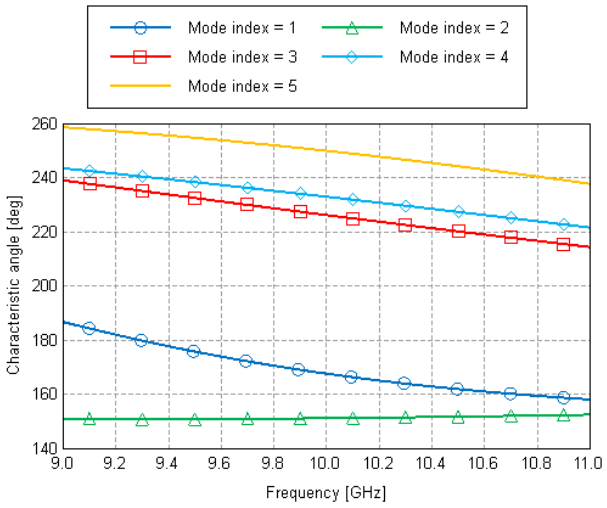

Figure 37. *Characteristic angle coefficients of the first 5 characteristic mode for isospectral couples*

3.5 Summary of the characteristic mode properties of radiators

Based on TCM it follows that to obtain radiation properties of a conducting it is enough to observe the first 5 characteristic modes. Normalized characteristic radiation patterns

and normalized characteristic surface distributions of characteristic modes obtained from single rectangular radiator can be used as a pattern for rectangular radiators of different sizes. It holds also for other geometries, such as triangular and circular. Obtained patterns in single radiator case are useful also in analysing of multi-plate and isospectral plate configurations.

Geometrical changes of rectangular radiator lead to changes in characteristic modes. Changes of width lead to directly proportional changes of the first characteristic mode resonant frequency and to inversely proportional changes of resonant frequency for all the rest characteristic modes. Changes of length are proportional to changes of resonant frequency for all the characteristic modes. If length or width of a rectangular radiator is decreased or increased, resonant frequencies of characteristic modes respectively diverge or converge. Regularity in radiator's geometry leads to the equality of the first and the second characteristic modes. It happens, because of radiator's symmetry and specific characteristic current distribution of these modes.

The presence of the ground plane, in general, decreases resonant frequencies of all characteristic modes. Furthermore, if the area of the ground plane increases, resonant frequency of characteristic modes decreases even more. In case of the ground presence, the resonant frequency of characteristic mode can be found in the frequency interval between resonant frequencies of radiator and the ground plane obtained in stand-alone cases. It is shown that changes in distance between radiator and a ground plane are directly proportional to changes in resonant frequencies of characteristic modes. In addition, it was discovered that CM has correlation with TCM. Resonant frequencies obtained through CM can be checked using eigenvalues obtained from TCM and vice versa. Nevertheless, CM has disadvantage in comparison to TCM, because TCM is taking into account all the internal coupling through the radiation in contrary to CM.

Excitation of the characteristic mode is dependent on feed placement with respect to characteristic surface current distribution. In addition, weighting coefficients should be studied. The characteristic mode can be considered as excited at desired frequency, if weighting coefficient value of this characteristic mode is big, in comparison to other characteristic modes. It is worth to have low-value weighting coefficients of unwanted characteristic modes.

Radiators can be scaled using scaling theory. If PEC condition holds, scaling can be performed ideally with respect to theory. Nevertheless, if lossy metal is applied for both scaled and non-scaled radiators, the results will be different from ideal case. This difference, as discovered, is small. Thus, it is possible to conclude that scaling is applicable for TCM analysis of radiators.

It is shown that polarization is dependent on two main things: excited characteristic mode and characteristic surface current distribution. If characteristic surface current

distribution of excited characteristic mode has capacitive effects then it will result in linear polarization. For both linear and circular polarizations mathematical definitions from TCM point of view were provided. Circular polarization can be created, in general, if at least two characteristic modes would be excited such that total surface current distribution will be closed loop.

It is proved that couples and pairs of radiators, having isospectral geometry properties, can be considered as isospectral radiators. Since such pairs and couples of radiators have equal characteristic mode values. Nevertheless, characteristic radiation patterns differ a bit.

4. ANALYSIS OF ANTENNAS USING CHARACTERISTIC MODES

In this chapter the results from chapters 2 and 3 are used to analyse patch antennas. The aim is to show physical insight of radiating process of patch antennas using TCM. In particular, feed placement, geometrical parameters, radiation pattern, surface current distribution and resonant frequency of patch antennas are explained. Measured results of patch antennas from the following scientific papers are compared with TCM results:

- coaxially fed rectangular patch antenna for 2.4 GHz Wi-Fi application [25]
- coaxially fed rectangular patch antenna for 5.24 GHz WLAN application [18]
- coaxially fed dual-band circular patch antenna for WLAN application [1].

Microstrip antenna [MSA] for Wi-Fi application has a styrofoam ($\epsilon_r = 1.03$) as a substrate. Thus, computation and analysis process can be simplified and the overall results will be close to the case if air ($\epsilon_r = 1$) would be used as a substrate. MSA for 5.24 GHz WLAN application is chosen to show feed placement positioning using TCM. Dual-band patch antenna for WLAN was chosen to emphasize properties discovered in chapter 3 and to describe properties of circular radiators from TCM point of view.

MSAs can be fed using different feed types [4]. This thesis focuses on co-axial feeding. Nevertheless, analysis process for different feed types, in general, is the same as described in chapter 3. If MSAs are fed using microstrip line, it should be considered as a part of radiating element in TCM analysis. During experiments it was discovered that if microstrip line is omitted during TCM analysis process, the overall TCM results will not correspond to the real patch antenna case.

4.1 General analysis procedure using theory of characteristic modes

Based on chapters 2 and 3 the following four-stage TCM analysis procedure for patch antennas is suggested:

1. TCM analysis of stand-alone radiator and stand-alone ground plane in vacuum
    a. Analysis of eigenvalues in case of stand-alone radiator
    b. Analysis of eigenvalues in case of stand-alone ground plane
    c. Analysis of eigenfields in case of stand-alone radiator
    d. Analysis of eigencurrents in case of stand-alone radiator

    e. Analysis of eigencurrents in case of stand-alone ground plane
2. TCM analysis of radiator and a ground plane together in vacuum
    a. Analysis of eigencurrents
    b. Analysis of eigenvalues
    c. Analysis of eigenfields
    d. Analysis of characteristic mode excitation
3. TCM analysis of radiator, ground plane and a substrate together
    a. Analysis of eigenvalues
    b. Analysis of eigencurrents
    c. Analysis of eigenfields.
4. Comparison of measured and TCM results

In the first stage, stand-alone radiator and stand-alone ground plane are analysed using TCM. This stage is important, because it can provide significant information about general radiation properties of the antenna, as it was described in chapters 2 and 3. Moreover, it was observed that this stage is not time-consuming in terms of computational time.

In the second analysis stage, radiator and a ground plane are analysed together. So, properties of the ground plane described in chapter 3 can be used. It was observed that in this analysis stage computational time increases when compared to the first stage. It is so, because both radiator and a ground plane are analysed together simultaneously.

In the third analysis stage, substrate should be added in between of radiator and a ground plane. Substrate can be lossless or lossy. In any case, this stage is the most time-consuming. Thus, maximum possible information and conclusions have to be done from analysis stages 1 and 2 before starting calculations in the third stage.

Finally, in the fourth stage measured results of the patch antenna are compared with TCM results. This should be done, because of two main reasons. First of all, this stage allows to explore relation between characteristic modes and measured results. Thus, physical explanation of the processes in the antenna will be described using TCM. Secondly, comparison of measured and TCM results is needed, because it provides additional self-checking of the results. Measured and TCM results should be in correspondence with each other.

Specific TCM computational problems may appear in analysis stages 1-3. This will be described in more details in chapter 5. By default it is better to use PEC condition for all analysis stages. It was discovered that use of lossy metal parameters may lead to errors in the TCM results, which is described in chapter 5.

However, it is not required to perform such detailed analysis for each antenna. Required steps should be chosen with respect to physical parameters of patch antenna, which have to be analysed using TCM. For example, if it is required to obtain physical explanation

for BW from TCM point of view, it is suggested to perform TCM analysis based on stages: 1.(a,b); 2.(b); 3.(a). It is important to understand required amount of analysis stages, because it affects overall computational time significantly.

4.2 Coaxially fed rectangular patch antenna for 5.24 GHz application

Coaxially fed rectangular patch antenna for WLAN application is analysed in this section using TCM analysis procedure described in chapter 4.1. This patch antenna has design parameters as given in Table 7 [18]. All parameters shown in Table 7 are taken into account during TCM analysis.

Table 7. *Design parameters of patch antenna for 5.24 GHz application*

Parameter	Value
Resonant frequency	5.24 GHz
Ground size	27x31 mm^2
Radiator size	16x21 mm^2
Feed coordinates	{-4.25 mm, 0}
Feed type	co-axial
Dielectric constant of a substrate	2.5
Dielectric loss tangent	0.0009
Height between radiator and a ground plane	1.5748 mm

Geometry of the patch antenna is shown in Figure 38. It is important to define required parameters for TCM analysis, as it was explained in chapter 4.1. TCM is used to analyse *resonant frequency*, *radiation patterns* and *total surface current distribution*. Thus, it follows that to perform analysis, stages 1.(a,c,d); 2.(a,b,d); 3.(a) and 4 from chapter 4.1 have to be performed to explain the above mentioned parameters. Measured results of this antenna are in [18]. Comparison of the results will be performed in parallel during analysis stages 1-3.

Nevertheless, before starting the analysis process, it is possible to predict TCM properties of the antenna based on overall structure of the antenna shown in Figure 38. Based on feed placement, it is possible to guess that the second characteristic mode is excited in the antenna. This prediction will be checked during analysis stages 1-3.

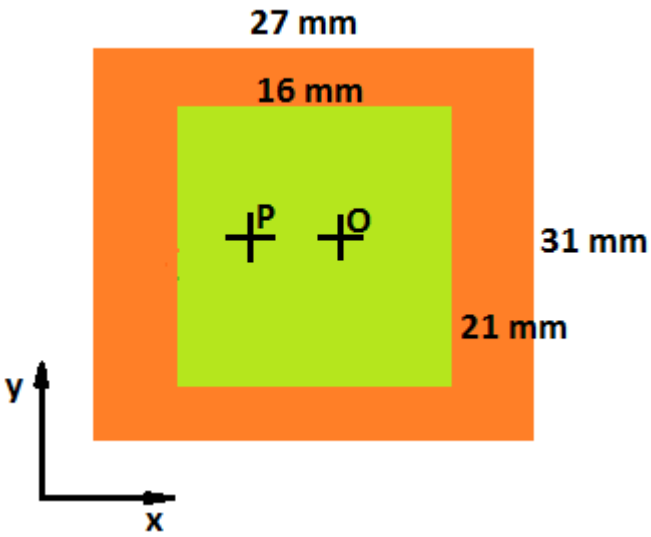

Figure 38. *Geometrical parameters of the coaxially fed rectangular patch antenna for 5.24 GHz application, P={-4.25; 0}, O={0; 0}*

In *the first analysis stage* only stand-alone radiator is used, as explained above. It is possible to observe characteristic angle results of the first 5 characteristic modes of a stand-alone radiator in Figure 39. Frequency range from 4 GHz to 6 GHz was chosen, because resonant frequency of the antenna is 5.24 GHz. It comes out that none of presented characteristic modes are resonating in given frequency range. So, their resonant frequencies are much higher than 6 GHz at this stage. This is because effects of a ground plane and a substrate are not observed in this analysis stage. However, from the results of chapter 3, it is possible to conclude that resonant frequencies of all characteristic modes will reduce significantly once a ground plane will be added. Thus, the first characteristic mode will have resonant frequency lower than 5.24 GHz. At this analysis stage this is only prediction based on properties explored in chapter 3. This prediction will be checked in the second analysis stage.

In addition, characteristic surface current distributions of the first 5 characteristic modes of a stand-alone radiator are shown in Figure 40. It follows that conclusions about characteristic current patterns made in chapter 3 are correct, because characteristic currents in Figure 40are in correspondence with the results of the characteristic currents in Figure 11. Moreover, measured total surface current distribution of the antenna, shown in Figure 41, is in correspondence to characteristic current distribution of the second characteristic mode shown in Figure 40. It proves previously mentioned prediction about excitation of the second characteristic mode in the antenna.

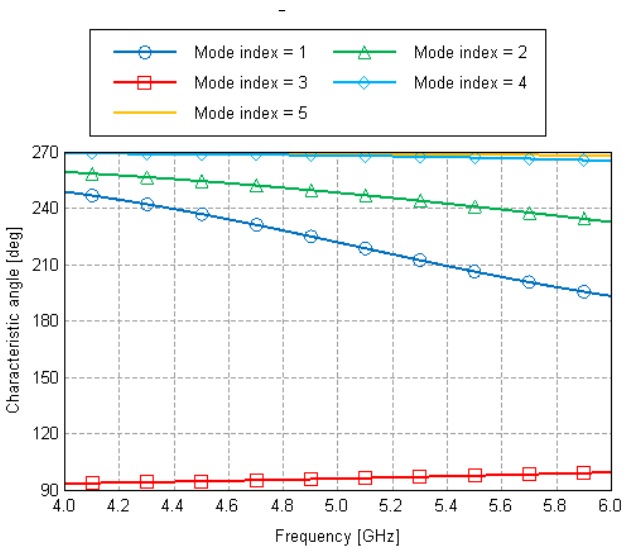

Figure 39. *Characteristic angle results of stand-alone radiator of the patch antenna for 5.24 GHz application*

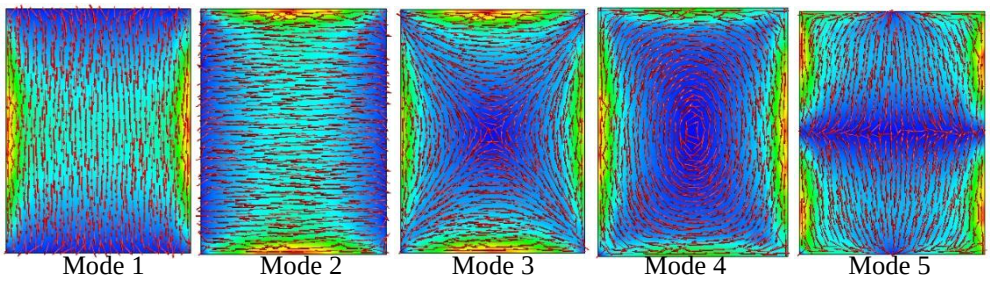

Figure 40. *Characteristic surface current distribution of the first 5 characteristic modes of a radiator element of the patch antenna for 5.24 GHz application. Characteristic modes ordered from left to right in ascending order.*

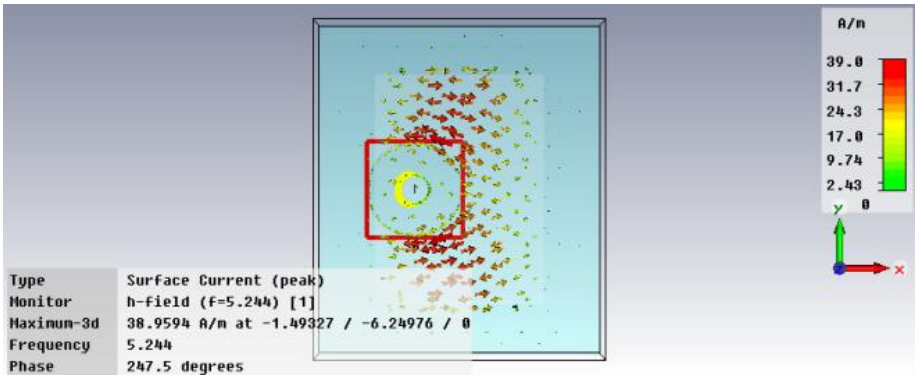

Figure 41. *Total surface current distribution of the patch antenna for 5.24 GHz application [18]*

Finally, characteristic radiation patterns of the second characteristic mode in E-plane (ϕ = 90º, θ = varying) and H-plane (θ = 90º, ϕ = varying) of a stand-alone radiator together with measured results of the antenna are shown in Figure 42. It is possible to see that radiation patterns of a stand-alone radiator of the second characteristic mode are in correspondence with radiation patterns of the antenna. Difference appears, because a ground plane and a substrate are not added and because the effect of other characteristic

modes is not taken into account. The effect of other characteristic modes is possible, and it will be explained in the second analysis stage. Nevertheless, given radiation pattern results show that radiation fields of the antenna are produced mainly by the second characteristic mode. Thus, all radiation parameters of the antenna will be defined mainly by the second characteristic mode. To conclude the first analysis stage, it was discovered that the antenna is functioning as the second characteristic mode for a stand-alone radiator.

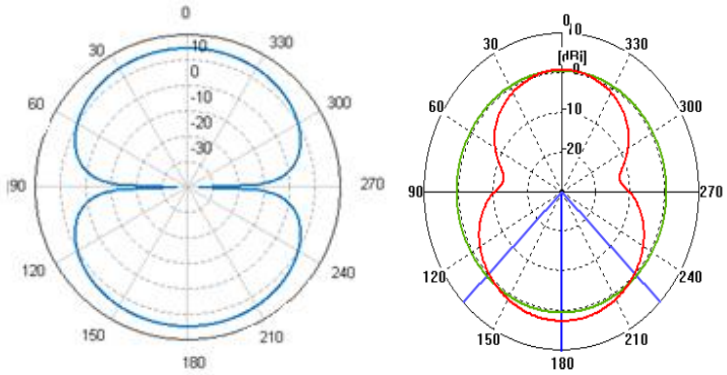

(a) H-plane radiation pattern of stand-alone radiator (left) and the antenna (right) at 5.24 GHz

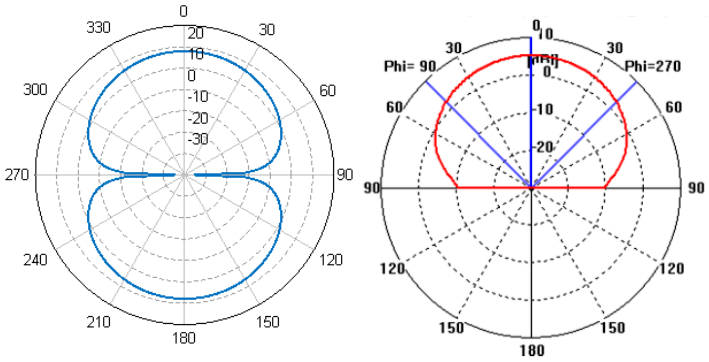

(b) E-plane radiation pattern of stand-alone radiator (left) and the antenna (right) at 5.24 GHz

Figure 42. *Radiation patterns of stand-alone radiator and the antenna for 5.24 GHz application, figures on the right are taken from [18]*

In *the second analysis stage*, ground plane and radiator together are analysed using TCM analysis of eigenvalues, characteristic currents and mode excitation. First of all, excitation of characteristic modes in particular antenna will be analysed. Feed is placed at the coordinates mentioned in [18] which are shown in Table 7 . It is possible to see weighting coefficients of the first 5 characteristic modes in 4-6 GHz frequency range in Figure 43 . It follows that at 5.24 GHz frequency the second characteristic mode has the highest weighting coefficient value with respect to all other modes. It proves that the second characteristic mode is excited in given antenna. However, at 5.24 GHz

frequency also the fifth characteristic mode is partially excited. It means that the fifth characteristic mode will have its effect on antenna's radiation parameters.

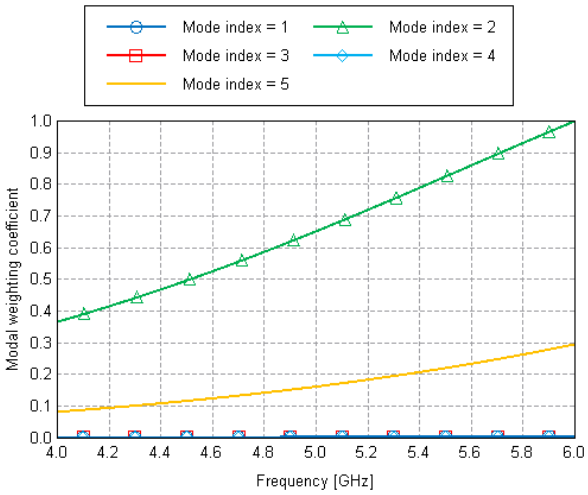

Figure 43. *Weighting coefficients of the first 5 characteristic modes for radiator and a ground plane of the antenna for 5.24 GHz application*

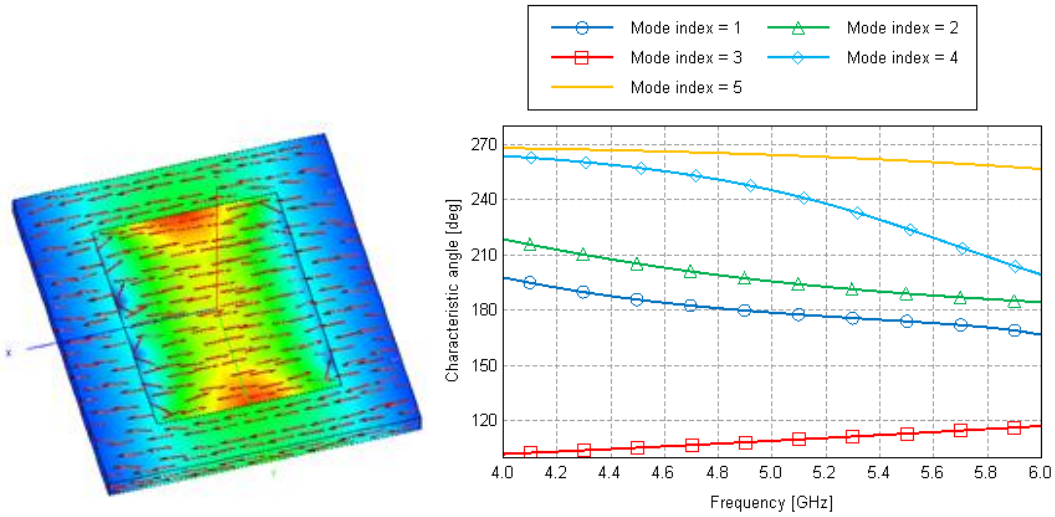

Figure 44. *Characteristic angle results of the first 5 characteristic modes of radiator and a ground plane (right) of the antenna for 5.24 GHz application and characteristic surface distribution of the second characteristic mode at 5.24 GHz (left)*

Characteristic angle results of a radiator and a ground plane together for the first 5 characteristic modes, and also characteristic surface current distribution of the second characteristic mode at 5.24 GHz, are given in Figure 44. Frequency range is the same as in the first analysis stage for particular antenna. It is possible to observe that the first characteristic mode in such configuration is resonating at 4.8 GHz. It proves prediction from the first analysis stage that the first characteristic mode will have resonant frequency lower than 5.24 GHz in case of a ground plane presence. The second characteristic mode is resonating at higher frequency than 6 GHz. Resonant frequency

of the second characteristic mode is not even close to designed value, because substrate is not added in this analysis stage.

In *the third analysis stage,* dielectric substrate is introduced in addition to radiator and a ground plane. Eigenvalues of such configurations for the second characteristic mode are analysed. The second characteristic mode was chosen based on analysis results from the second analysis stage. It was observed and proved that with respect to given feed placement, the second characteristic mode is excited. Characteristic angle results for radiator, a ground plane and substrate together with measured S-parameters of the antenna are given in Figure 45. Frequency range from 4.8 GHz to 5.6 GHz was chosen to enhance resolution in characteristic angle results, because it was expected to have resonant frequency of the second characteristic mode at about 5.24 GHz frequency. It is possible to see that the second characteristic mode is resonating at 5.250 GHz frequency, whereas measured S11 parameters of the antenna are showing that the antenna is resonating at 5.244 GHz. Thus, it proves that TCM results are in correspondence with measured results of the antenna.

It follows that the second characteristic mode is excited in the antenna. In addition, it is proved that for a given antenna, total surface current distribution, radiation patterns and resonant frequency are in correspondence with the second characteristic mode. There is small difference between TCM and measured results in observed radiation parameters, because the fifth characteristic mode is partially excited with respect to given feed placement. However, all physical processes, which are taking place in particular antenna, can be described based on the second characteristic mode.

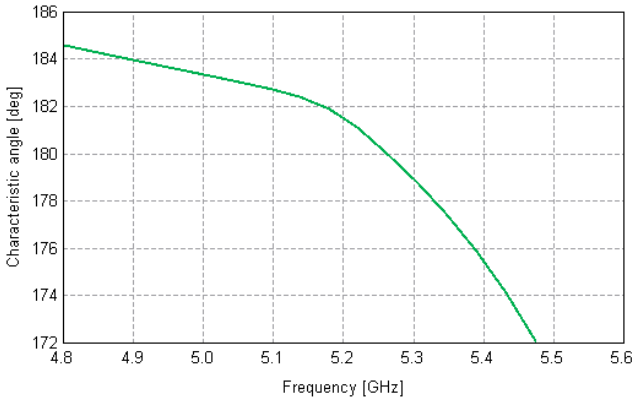

(a) Characteristic angle results of the second characteristic mode

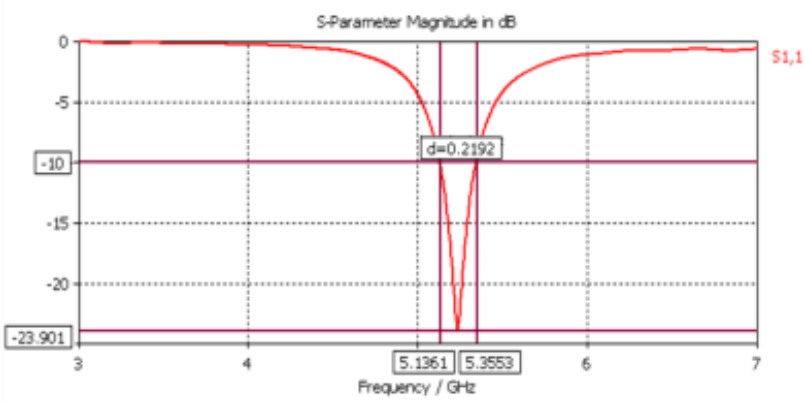

(b) Measured S11 parameters of the antenna

Figure 45. *Characteristic angle results of the second characteristic mode (a) and measured results of the antenna for 5.24 GHz application (b) [18]*

4.3 Coaxially fed rectangular patch antenna for Wi-Fi application

In this section TCM analysis is performed using MSA for Wi-Fi application [25]. This patch antenna has substrate dielectric constant close to air value, because styrofoam is used. Design parameters of the antenna are given in Table 8 . Analysis procedure will be based on information provided in section 4.1.

Steps 1.(a, b), 2.(b), 3.(a) and 4. Of the four-stage procedure be performed. Stage 4 will be done in parallel to stages 1-3. Given antenna's geometry is shown in Figure 46. So, based on feed placement and on characteristic surface currents of a rectangular radiator it is possible to predict that the first characteristic mode is excited in given antenna. This prediction will be checked during analysis stages.

Table 8. *Design parameters of patch antenna for Wi-Fi application*

Parameter	Value
Dielectric constant of a substrate	1.03
Resonant frequency	2.4 GHz
Height between radiator and a ground plane	12 mm
Radiator size	46.23x62.04 mm^2
Ground plane size	118.23x134.04 mm^2
Feed coordinates	[11 mm; 20 mm]

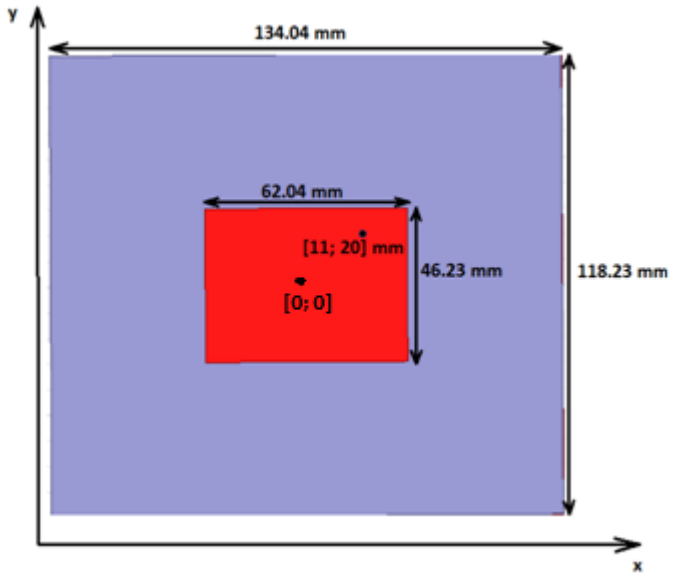

Figure 46. *Coaxially fed rectangular patch antenna for Wi-Fi application [25]*

In *the first analysis stage*, a stand-alone radiator is analysed using TCM. Characteristic angle results of the first 5 characteristic modes for a stand-alone radiator are shown in Figure 47. Frequency range from 1.5 GHz to 3 GHz is chosen, because designed antenna has resonant frequency at 2.4 GHz. It is possible to see that the first characteristic mode is resonating at 2.3 GHz frequency. Characteristic surface current distributions of the first 5 characteristic modes, for given stand-alone radiator, are shown in Figure 48. Indeed, surface current distribution of the first characteristic mode, when compared to feed placement shown in Figure 46, proves prediction about excitation of the first characteristic mode. However, excitation of the first characteristic mode will be discussed in more details in the second analysis stage.

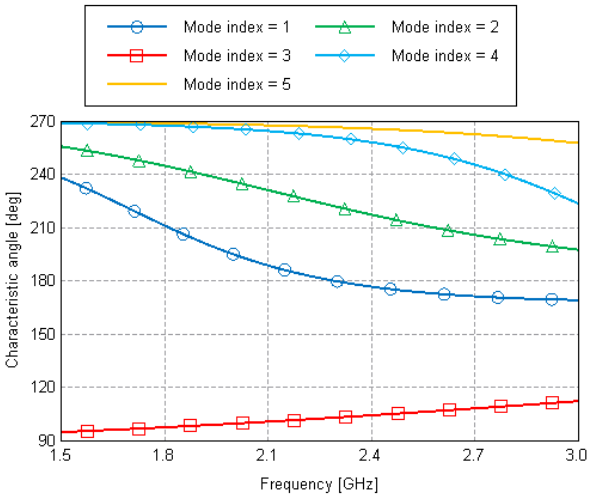

Figure 47. *Characteristic angle results of the first 5 characteristic modes of stand-alone radiator of the antenna for Wi-Fi application*

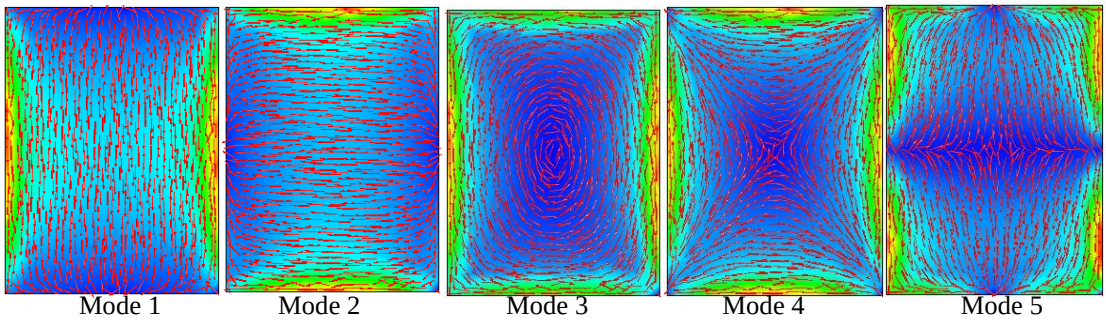

Figure 48. *Characteristic surface distributions of the first 5 characteristic modes of a stand-alone radiator for the given antenna at 2.4 GHz*

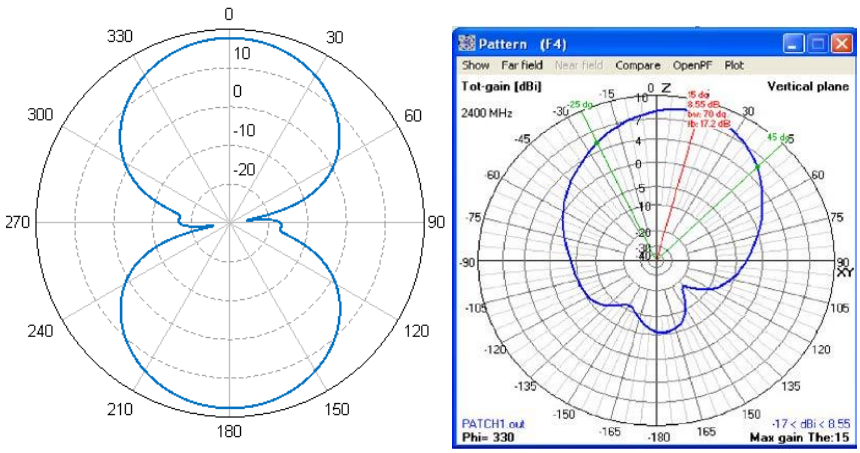

Figure 49. *H-plane radiation patterns of the first characteristic mode of a stand-alone radiator (left) and the given antenna at 2.4 GHz (right) [25]*

H-plane (θ = 90º, ϕ = varying) radiation patterns of the first characteristic mode of a stand-alone radiator and of the complete antenna at 2.4 GHz are given in Figure 49. It is possible to see that radiation patterns are similar. However, difference appears, because a ground plane and substrate are not introduced in this analysis stage.

In *the second analysis stage*, a ground plane together with the radiator is introduced in TCM model. In addition, feed is placed with respect to given coordinates. Weighting coefficients of the first 5 characteristic modes for this configuration are given in Figure 50 . It is possible to observe that at 2.4 GHz frequency, the first and the second characteristic modes are mostly excited with respect to given feed placement. Nevertheless, the first characteristic mode is more excited than the second characteristic mode. It means that the total surface current distribution of the antenna will be produced by vector sum of characteristic surface currents of the first and the second characteristic modes. Furthermore, significant excitation of the second characteristic mode is the reason why radiation pattern of the antenna is different from radiation pattern of the first characteristic mode. In general, all radiation parameters of the antenna can be described by the first characteristic mode, but for more precise values, the effect of the second characteristic mode should be taken into account.

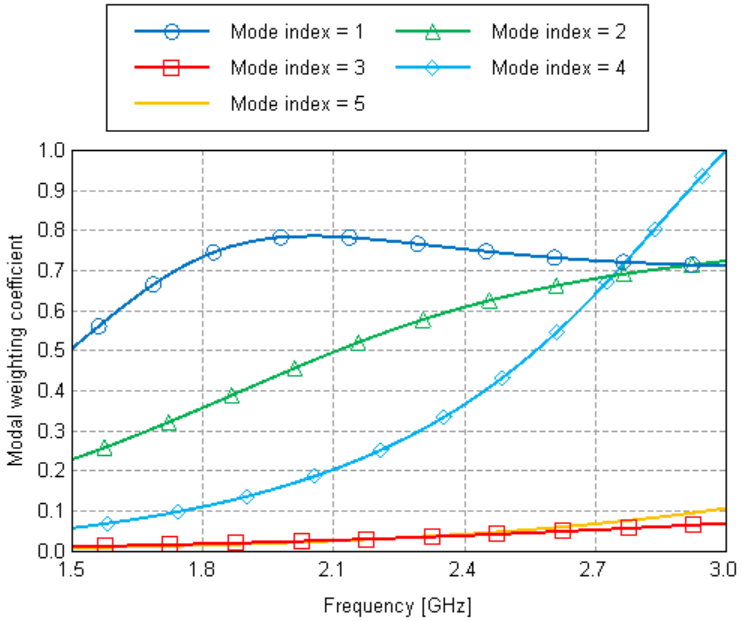

Figure 50. *Weighting coefficients of the first 5 characteristic modes of radiator and a ground plane together of the antenna for Wi-Fi application*

Characteristic angle results of the first characteristic mode in given configuration are shown in Figure 51. It is possible to observe that the first characteristic mode is resonating at 2.54 GHz frequency. Such close result of the resonant frequency to designed value was predicted in the very beginning of the analysis. Difference appears, because dielectric substrate is not added in between of a radiator and a ground plane at this analysis stage. Furthermore, it is known that dielectric substrate, which is going to be added in the third analysis stage, has dielectric constant of 1.03. So, it means that even small difference in dielectric constant value leads to a significant change in resonant frequency. Furthermore, it follows that changes in dielectric constant value are inversely proportional to changes in resonant frequencies of characteristic modes. This prediction will be checked in the third analysis stage.

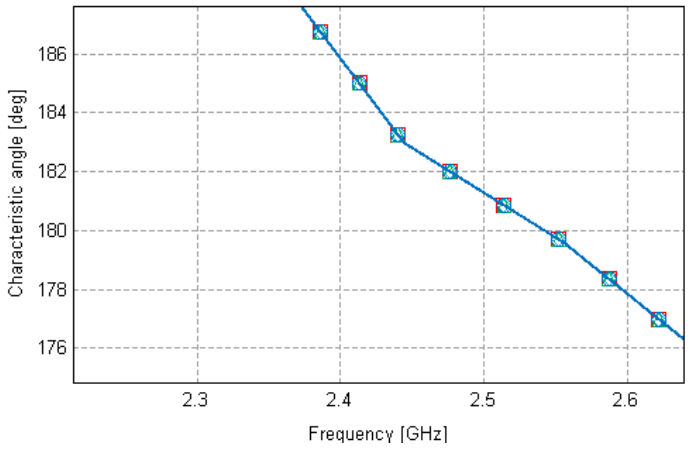

Figure 51. *Characteristic angle values of the first characteristic mode of radiator and a ground plane together of the antenna for Wi-Fi application*

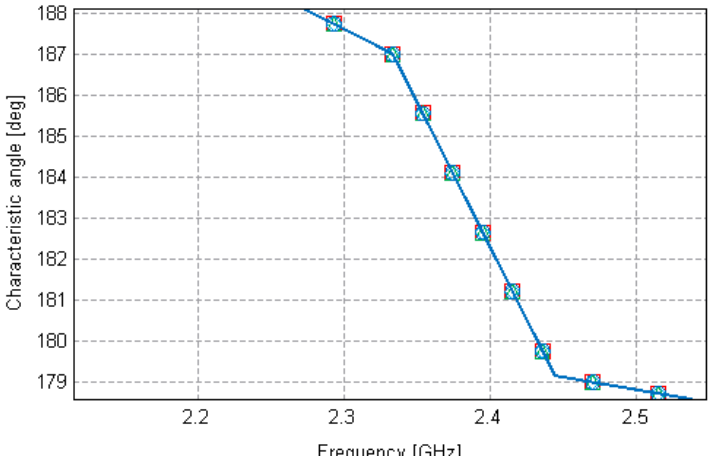

Figure 52. *Characteristic angle results of the first characteristic mode of radiator, a ground plane and substrate of the antenna for Wi-Fi application*

In *the third analysis stage* dielectric substrate is introduced between radiator and a ground plane. Characteristic angle results and characteristic surface current distribution of the first characteristic mode in this configuration is shown in Figure 52. It is possible to observe that the first characteristic mode is resonating at 2.42 GHz, which is very close to designed value of the antenna. Difference appears, because PEC condition was used in all analysis stages for conducting bodies as well as lossless styrofoam substrate was assumed in the third analysis stage. Nevertheless, it is proved now that resonant frequency of the antenna is defined from the first characteristic mode.

4.4 Coaxially fed dual-band circular patch antenna

In this section a dual-band circular patch antenna is analysed using TCM. The main idea is to show how and why dual-band nature appears if slots are introduced. So, analysis procedure is different in this section from the procedure described in section 4.1.

Important design parameters of the antenna [1] are given in Table 9. The overall procedure for analysis:

1. TCM analysis of a stand-alone radiator in free space
2. TCM analysis of a stand-alone radiator with slots in free space
3. TCM analysis of characteristic modes excitation in case of a stand-alone radiator with slots in free space.

For simplicity reasons, lossless substrate is assumed, because no precise information about losses is given in [1]. The above mentioned analysis approach is useful in this case, because it is not required to introduce substrate and a ground plane to study dual-band nature. In general, not introducing substrate and a ground plane, reduce required time for analysis significantly.

Table 9. *Design specifications of a dual-band circular patch antenna for WLAN application*

Parameter	**Value**
Relative permittivity	2.32
Radius of the circular disk	15 mm
Length of the slot	20 mm
Width of the slot	1 mm
Feed location	{-0.325mm; -8.625}
The first resonant frequency	2.9 GHz
The second resonant frequency	3.56 GHz

In *the first analysis stage*, stand-alone radiator is analysed using TCM. Characteristic surface current distributions of the first 5 characteristic modes and corresponding radiation patterns of H-plane (XY plane) are given in Figure 53. It is possible to see that the results of radiation patterns and surface currents are similar to rectangular radiator observed in details in chapter 3. Thus, all radiator properties, in terms of TCM, discovered in chapter 3 can be applied also for circular radiator. In addition, it should be noted that if the radius of a circular radiator increases, generalized characteristic current flows and corresponding characteristic radiation patterns shift clock-wise and vice versa.

The effect of slots in patch antennas from CM point of view can be explored in [1, 4]. Two parallel rectangular slots are introduced in particular antenna. Length and width of slots, as well as substrate's height all together define frequency ratio of two resonant frequencies [1]. Antenna's geometry is shown in Figure 54 [1]. First, feed is introduced for a stand-alone radiator without slots at the location mentioned in Table 9.

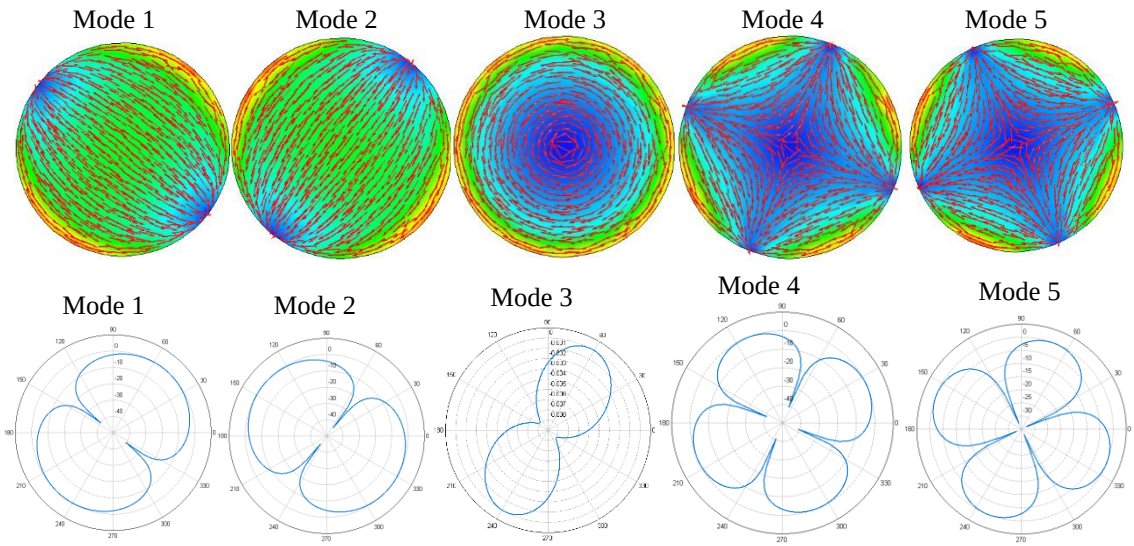

Figure 53. *Characteristic surface current distributions of the first 5 characteristic modes and corresponding radiation patterns in XY plane for stand-alone circular radiator in free space at 2.9 GHz*

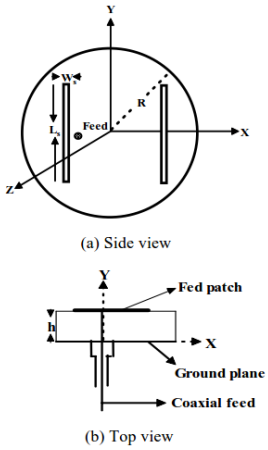

Figure 54. *General view of circular dual-band patch antenna [1]*

The results of characteristic angles for the first 5 characteristic modes and corresponding characteristic *excitation* coefficients, for a stand-alone radiator without slots, are given in Figure 55. It is explored during experiments that it is more important first to observe excitation coefficients instead of weighting coefficients in case of dual-band structures. This is used to decide which two modes to use to implement dual-band antenna. Frequency range from 4 GHz to 6 GHz is chosen, because stand-alone radiator's resonant frequencies of characteristic modes are close to this frequency range. Only 3 curves are given in both plots in Figure 55, because given structure has axial symmetry. As a result, characteristic modes 2 and 4, 1 and 5 are overlapping. In chapter 3 it was mentioned that antenna designers are mainly using fundamental characteristic modes 1, 2 and 3 to implement single-band antenna designs. Thus, from the above it follows that mode couples 2 and 4 or 1 and 5 have to be used to implement dual-band antenna. In addition, it means that one of two characteristic mode couples have to be neglected. To do this, slots can be used.

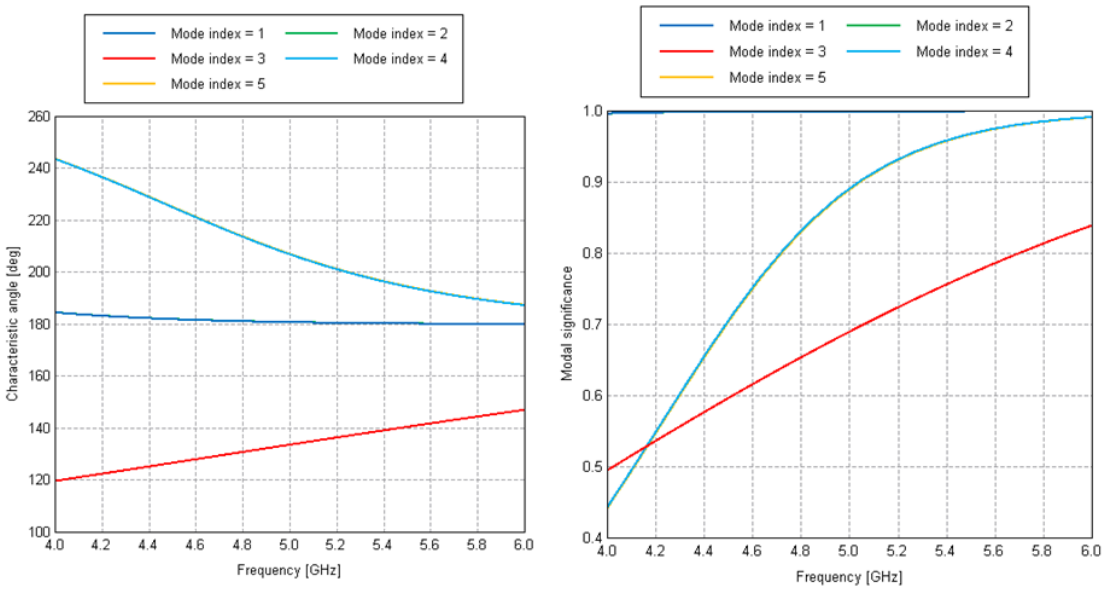

Figure 55. *Characteristic angles (left) and excitation coefficients (right) of the first 5 characteristic modes for a circular radiator without slots in free space*

Next, slots are introduced in a stand-alone radiator in free space with respect to geometrical parameters given in Table 9. Characteristic surface current distributions of the first 5 characteristic modes and corresponding characteristic radiation patterns of a stand-alone radiator with slots in free space are given in Figure 56. It is important that characteristic surface distributions now are *dependent on frequency*, because slots are introduced. It is possible to see that all characteristic surface current distributions are similar to those for a rectangular radiator, scaling was the same in all cases. It is possible to see that the first and the fifth characteristic modes now have much lower characteristic surface current values. Characteristic angle results and excitation coefficients of the first five characteristic modes are given in Figure 57. Frequency range from 5 GHz to 7 GHz was chosen to emphasize characteristic mode resonant properties and their effect on excitation of different dual-modes on a circular radiator. Indeed, it is possible to observe that characteristic modes 1 and 5 have very low excitation coefficients, but characteristic modes 2 and 4 have two peak values at 5.8 GHz and 5.4 GHz respectively. Thus, this proves several things, such as: characteristic surface current distribution is dependent on frequency in case of having slots in its geometry. Slots are reducing excitation possibilities for several characteristic modes. Nevertheless, both earlier mentioned frequencies at peak values of characteristic modes 2 and 4 are not equal to designed value of the antenna. It is because a ground plane and a substrate are not introduced into the model, since the main idea is to show and explain dual-band antenna implementation from TCM point of view, if slots are introduced.

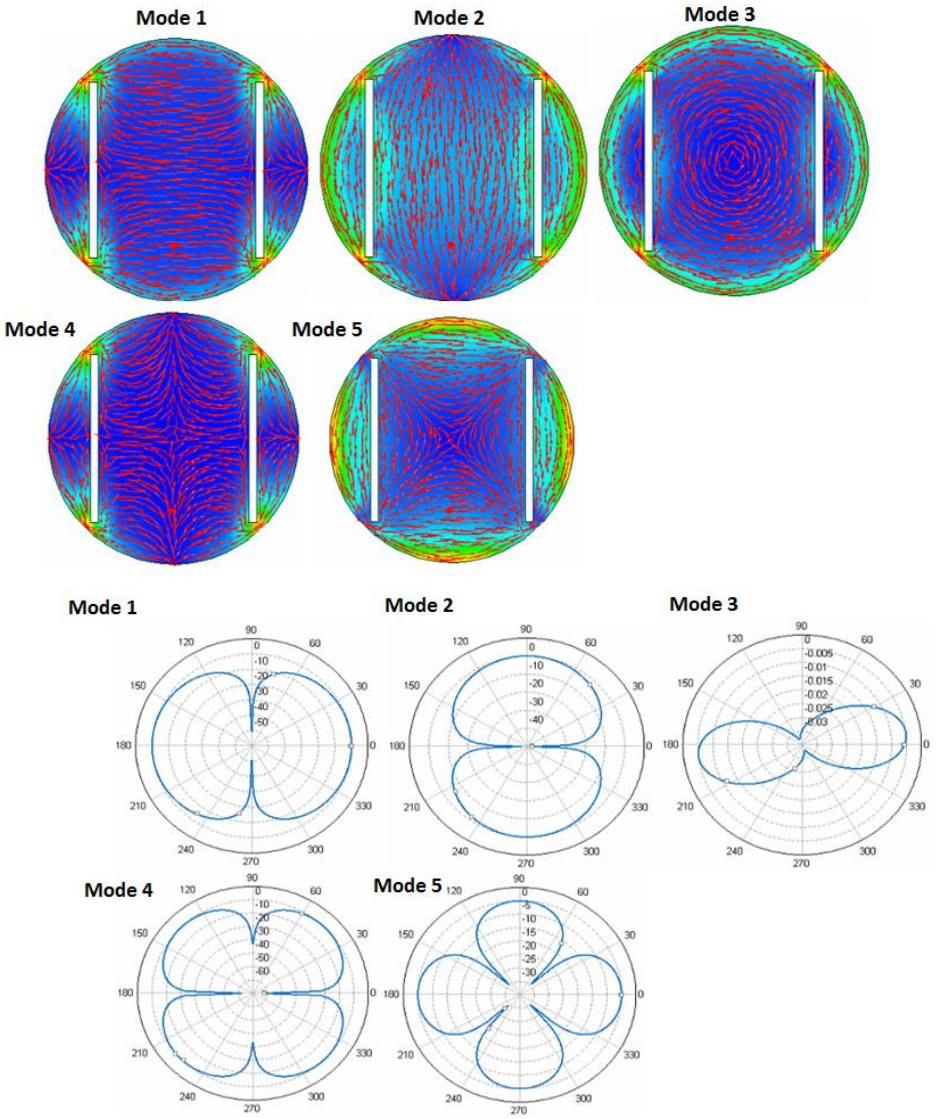

Figure 56. *Characteristic surface current distributions of the first 5 characteristic modes and corresponding characteristic radiation patterns in XY plane at 5 GHz*

Characteristic surface current distribution corresponding to peak values of characteristic modes 2 and 4 are given in Figure 58. In addition, the total surface current distribution of the designed antenna from [1] is given on the same figure. It is possible to see that total surface current distribution is in correspondence with characteristic surface current distributions of the modes 2 and 4. It means that above mentioned conclusions about excitation of the characteristic modes 2 and 4 in the given antenna are correct.

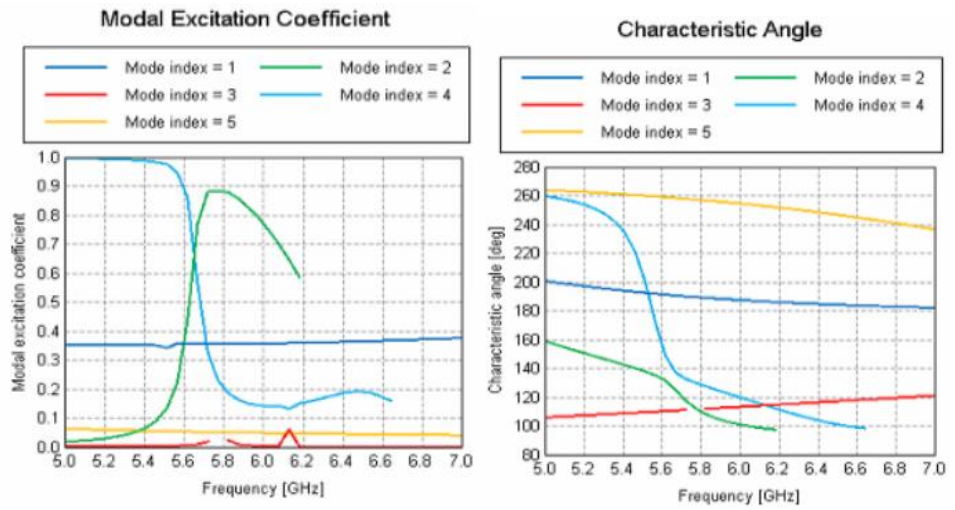

Figure 57. *Excitation and characteristic angle coefficients of a circular patch radiator with slots in free air*

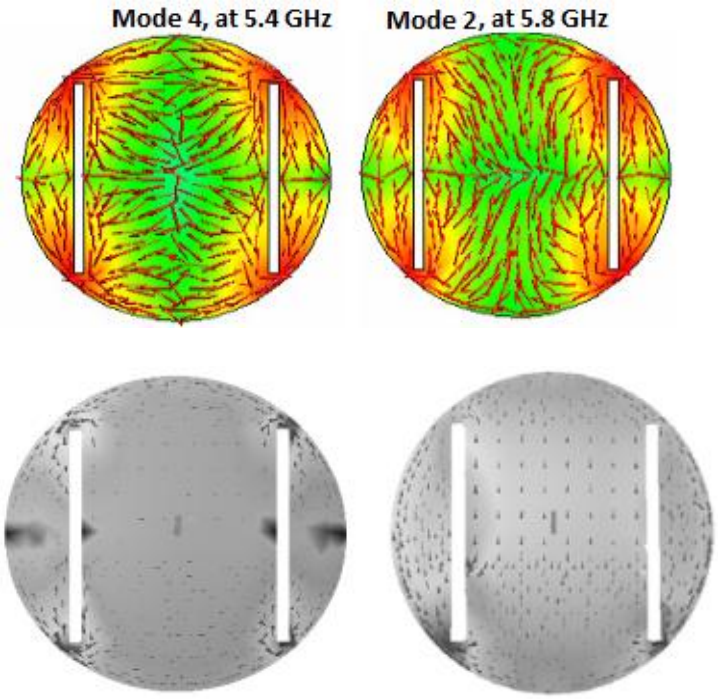

Figure 58. *Top: characteristic surface current distributions of the modes 2 and 4on a radiator at 5.8 GHz and 5.4 GHz*
Bottom: total surface current distribution of the antenna at frequencies 2.9 GHz and 3.56 GHz [1]

4.5 Summary of the analysis of antennas using characteristic modes

General TCM analysis procedure for antennas is introduced and explained in chapter 4. It is proved that antennas can be analysed using approaches and properties described in chapters 2 and 3. Furthermore, it is shown that TCM results of excited characteristic modes of antennas are in correspondence to measured results. Radiation patterns, total

surface current distribution and all other parameters of the antenna can be obtained from excited characteristic mode eigenvalues and eigencurrents. The most precise and close to reality values from TCM can be obtained if the following parameters of the antennas are presented in TCM model: radiator, a ground plane, substrate and feed.

During calculations of weighting coefficients of characteristic modes, it is observed that normalized values of those are frequency independent for stand-alone radiator and for any other configuration, except the case of having slots or other cuts in the radiator.

The effect of the substrate on resonant frequencies of characteristic modes also is explored. It is found that even small change in dielectric constant of the substrate leads to significant change in resonant frequency of characteristic modes. In addition, it is observed that changes of dielectric constant are directly proportional to changes of resonant frequencies of characteristic modes.

For circular patch antennas, normalized characteristic surface currents and corresponding radiation patterns are frequency independent, but overall shape of those is moving clockwise if radius is increasing and vice versa. In general, slots are introducing frequency dependent properties of characteristic surface currents. In addition, slots are neglecting several characteristic modes. By this, excitation of only required characteristic modes is achieved.

5. DESIGN AND CONSTRUCTION OF ANTENNAS USING CHARACTERISTIC MODE THEORY

In this chapter design and construction procedure of antennas from TCM point of view is described. Step-by-step instructions of TCM-based antenna design are provided.

Two patch antennas are designed using TCM design method. The first antenna is a circular dual-band patch antenna for GPS L1 and L2 frequencies. The second antenna is rectangular patch antenna for Wi-Fi resonant frequency. Both antennas are simulated in HFSS commercial software. In addition, the second antenna is also constructed and measured using facilities of Tampere University of Technology.

5.1 Design of antennas using theory of characteristic modes

This chapter describes general procedure of patch antenna design using characteristic mode theory and conclusions from chapters 2, 3 and 4. In addition, suggested procedure of patch antenna design is applied for two antenna design –two-band circular patch antenna for GPS L1 and L2 bands and for a rectangular single-band patch for Wi-Fi frequency.

5.1.1 A procedure for antenna design

The following procedure is suggested for a circular/rectangular patch antenna design using TCM assuming as a substrate Rogers RT\duroid 5880 (tm) with height 3.2 mm:

1. Define resonant frequencies of the antenna, radiation patterns, substrate width and geometrical shape of its radiator and ground parts. Calculate corresponding wavelength of resonant frequencies. For the first trial model can be assumed that radiator's length (or diameter, in case of a circular geometrical shape) is $\sim 0.3536\lambda_{\text{resonant}}$ of lowest resonant frequency. Coefficient 0.3536 was found empirically by trial and error method. In addition, assume that ground part's width and length is approximately 15% bigger;
2. Implement corresponding first trial model with assumed from step 1 parameters in FEKO and calculate eigenvalues of the first 5 characteristic modes. Observe obtained radiation patterns of obtained characteristic modes and their surface characteristic currents;

3. Make a conclusion about characteristic modes, which should be excited at the chosen resonant frequencies of the antenna;
4. Place feed based on characteristic surface current information for required characteristic modes using trial and error method;
5. Tune geometrical parameters step-by-step in order to maximize weighting coefficients of required characteristic modes at resonant frequencies of the antenna;
6. Create antenna's model in HFSS software [2], based on already obtained FEKO model of the antenna. In addition, precise geometrical parameters of feed connectors should be taken into account when creating HFSS model. Perform simulations and check whether results of HFSS are providing required results;
7. If requirements are not fulfilled at the step 6, repeat steps 5-6 again for several times until requirements will be fulfilled.

5.1.2 Design of a dual-band circular patch antenna using theory of characteristic modes

This chapter describes how to apply patch antenna design procedure, which is given in chapter 5.2.1 to design a circular patch antenna for GPS L1 and L2 resonant frequencies. At this point it is not so much important which values of gain will be at required frequencies, the main aim is to show that the previously mentioned generalized procedure is working.

1. It is assumed that system impedance will be 50 Ω, substrate height is chosen to be 3.175 mm. Furthermore, since it is assumed to use L1 and L2 resonant frequencies, it results in $f_{res_1} = 1227.6$ MHz, and $f_{res_2} = 1575.42$ MHz [4]. So, since $f_{res_1} < f_{res_2}, D = 0.3536\lambda_{res_1} = 86.4$ mm – such diameter should be applied for the first trial model, which will be implemented in FEKO software, ground size should be bigger by 36.7 mm. In order to implement dual-nature antenna, it was decided to use symmetrical slots of the length $0.3536\lambda_{res_2} =$ 67.3 mm and 1 mm width in the first trial version. Slot solution was chosen based on a circular patch antenna with slots example described in chapter 4, since many practical aspects then could be compared with information from [1].
2. Radiator-only model with slots was implemented in FEKO and obtained characteristic surface current distributions are given in Figure 60. So, based on trial and error method, it was assumed that feed can be placed on the position, which is coloured red in Figure 60. On the next step, ground plane with trial geometrical parameters was added and weighting coefficients of the whole model were obtained, see Figure 59. So, indeed, it is possible to see that both characteristic modes 2 and 4 can be excited within given frequency range. However, it means also that characteristic mode 4 will be excited less than characteristic mode 2, since weighting coefficients of the fourth mode are

smaller than weighting coefficients of the second characteristic mode. So, it is expected to see in the final measurement results poorer results for L1 band, since characteristic mode 4 will correspond to that band, but characteristic mode 2 will correspond to the results of L2 band.

3. As a result, characteristic modes 2 and 4 can be used for dual-band implementation of a circular patch antenna with slots.
4. Both feed and geometrical parameters of the antenna after this were tuned in FEKO software to maximize weighting coefficients of characteristic modes 2 and 4 at frequency bands L1 and L2, it resulted in geometrical parameters of the antenna given in Table 10.
5. Corresponding HFSS model was based on final tuned version of FEKO model. It is possible to observe HFSS model in Figure 61. Corresponding S11 parameters and radiation pattern at L2 band of the antenna can be found in Figure 62.

Table 10. *Final geometrical parameters of a circular patch antenna after FEKO tuning*

Geometrical parameter	**Value [mm]**
Feed position	[0; -10.9]
Radius	46.85
Length/width of a ground plane	140
Height between ground plane and radiator	3.175
Slot's width and length	1, 51.34
Distance between centers of the slots	72.4

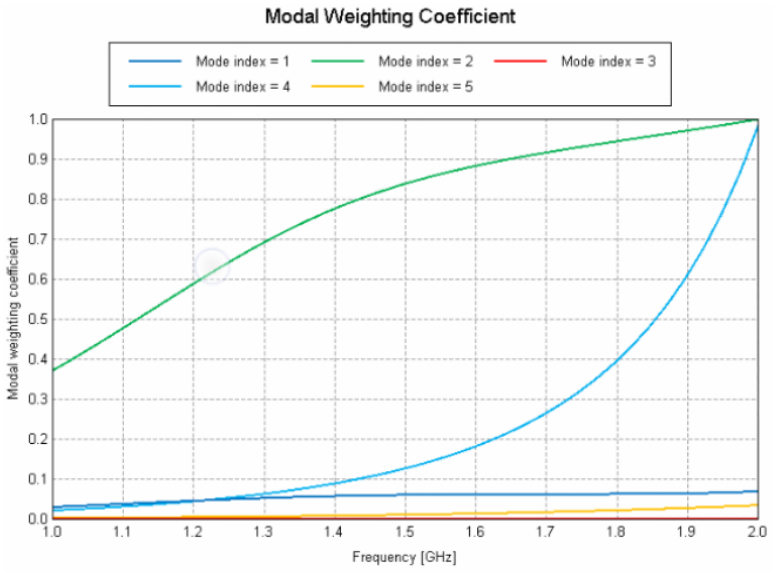

Figure 59. *Weighting coefficients of the first 5 characteristic modes of a circular patch antenna for L1 and L2 bands, 1 GHz – 2 GHz*

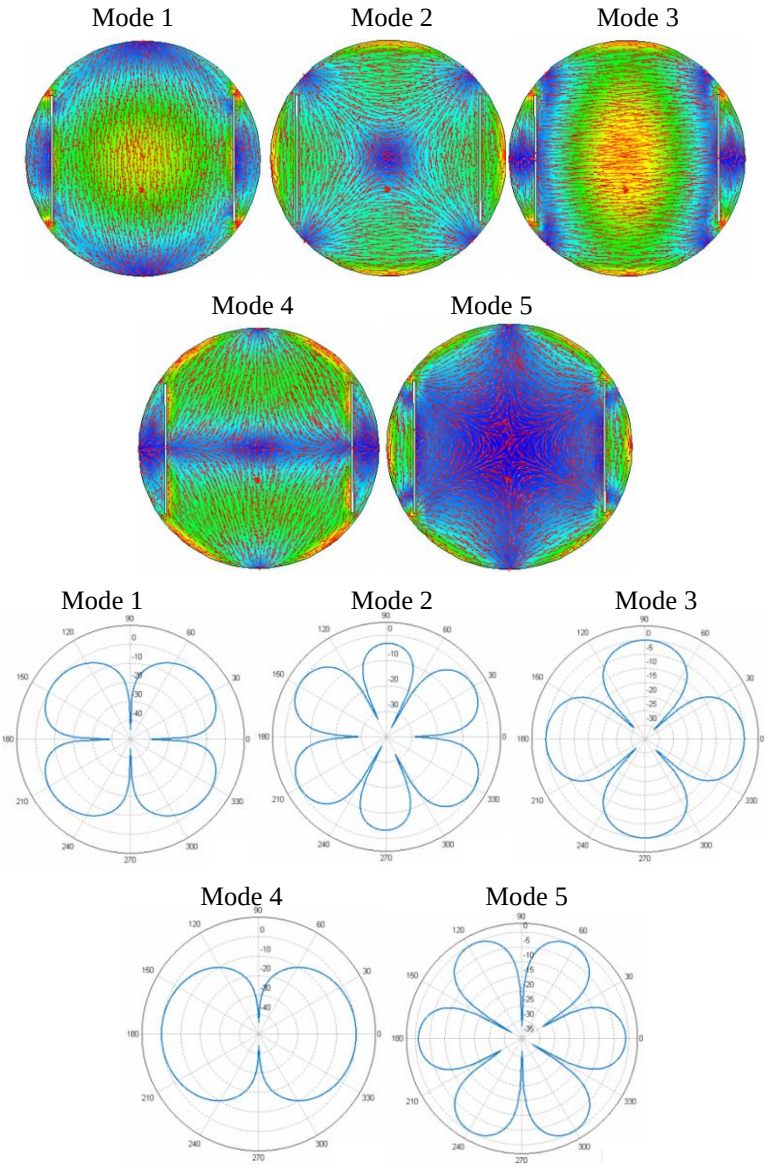

Figure 60. *The first 5 characteristic surface currents and corresponding radiation patterns of a circular patch antenna*

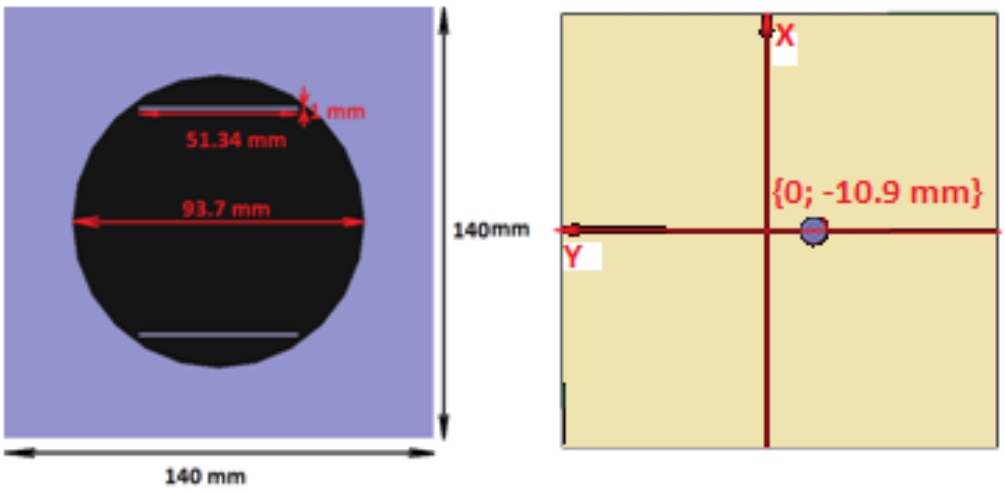

Figure 61. *Final HFSS model of a circular patch antenna for L1 and L2 GPS bands*

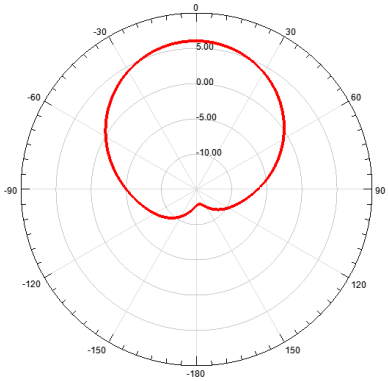

a) E-plane radiation pattern ($\phi = 90^o, \theta = -180^o \dots 180^o$)

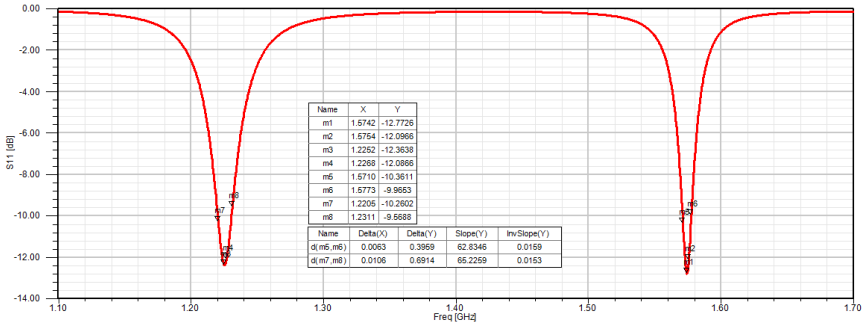

b) S11 parameters within frequency range from 1 GHz to 1.7 GHz

Figure 62. *S11 parameters and E-plane radiation pattern at L2 frequency*

In this example the main aim was to show that it is possible to design the antenna with pre-defined resonant frequencies. Bandwidth effects and precise explanation of radiation fields were out of this master thesis scope. It is possible to observe from

Figure 62 at L2 frequency S11 value is -12.5 dB, whereas at L1 frequency it is -12.8 dB. However, due to reasons, which will be discovered further, only band L2 will radiate. Thus, only its E-plane radiation pattern is shown and it has maximum gain of 6 dB.

In the first ideal model S11 parameters for both L1 and L2 bands were in the region of -20 dB, but the problem was that a gap between slots and radiator's edge was less than 0.4 mm and it would be quite hard to implement physically such model. Due to this fact, it was decided to increase this gap between the edge of a radiator and a slot. This resulted in decreased values of S11 values for both bands L1 and L2.

5.1.3 Design of a single-band rectangular patch antenna using theory of characteristic modes

In this example the design approach given in chapter 5.2.1 is used to design patch antenna with pre-defined resonant frequency and polarization. In addition, it will be shown that overall radiation pattern can be predicted as well.

The aim is to design patch antenna for Wi-Fi application. With resonant frequency of 2.4 GHz, and of linear polarization. By following the procedure described in chapter 5.2.1:

1. Required resonant frequency is 2.4 GHz, as a result for trial model in FEKO it is required to take the value of $\lambda_{2.4GHZ} * 0.3536 = 44.2$ mm for width and length of a rectangular patch radiator. Ground plane's width and length should be chosen at first by 15% larger than for a radiator's plane, thus, it should be 50.83 mm. However, since it was not planned to construct this particular antenna, ground plane's width and length were chosen to be 100 mm to perform less empirical trials in FEKO model. Height between ground plane and a radiator was chosen as 3.175 mm.
2. Since in this particular case rectangular radiator is used, it was decided to excite the first characteristic mode, because in chapter 3 it was described that it has capacitive effects. As a result, it should provide linear polarization. After several trials in FEKO software and using conclusions from chapter 3, it was found that weighting coefficients will be maximized for the first characteristic mode if feed will be placed at the position [-5 mm; 0] and radiator's width and length should be respectively 39.5 mm and 30 mm. In addition, to obtain higher gain, it was decided to tune the ground plane as well. It was found that weighting coefficients increase if ground plane width and length are 100 mm and 90 mm, respectively.
3. Corresponding HFSS model based on FEKO results was made, see Figure 63. As it is possible to see from Figure 64, at 2.4 GHz S11 parameter is -24.38 dB. In addition, radiation pattern and axial ratio at 2.4 GHz shown in Figure 65 prove that this rectangular patch antenna, indeed, is radiating and it should have

linear polarization. Total surface current distribution, which is shown in Figure 66, proves that total surface current distribution is similar to the first characteristic mode.

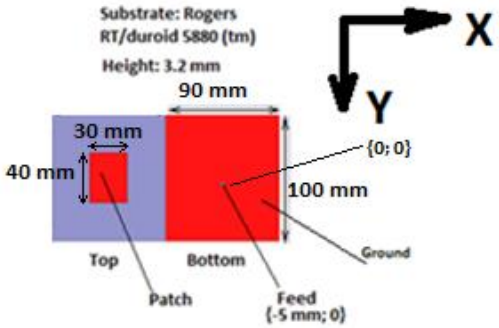

Figure 63. *HFSS final implementation of a rectangular patch antenna for 2.4 GHz*

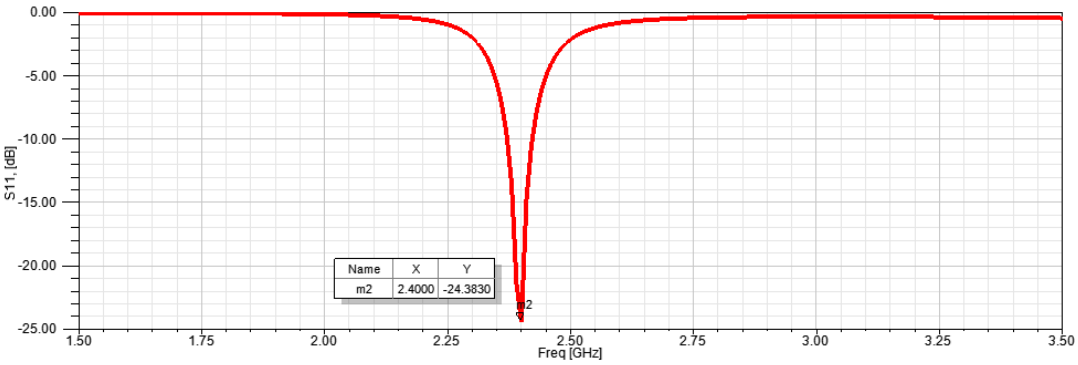

Figure 64. *S11 parameters of a rectangular patch antenna for 2.4 GHz obtained from HFSS software*

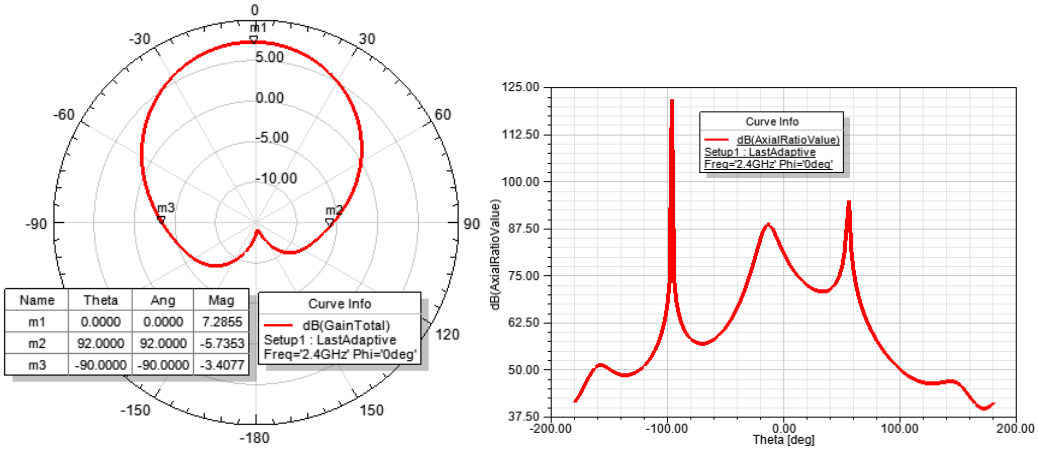

Figure 65. *AR and E-plane radiation pattern of a rectangular patch antenna for 2.4 GHz*

The results of HFSS model prove that it is possible to use efficiently TCM approach for a single-band patch antenna design with linear polarization. It took only 4 trials in FEKO software to obtain the above mentioned values of lengths and widths.

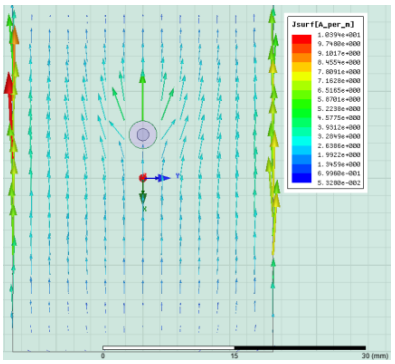

Figure 66. *Total surface current distribution on top of a rectangular patch antenna for Wi-Fi application*

5.2 Measurements of a dual-band circular patch antenna

It was decided to construct only the dual-band circular patch antenna as the most interesting example from characteristic mode point of view, because this example should work in dual-band. As was pointed out during design stage it is much more difficult to design dual-band antennas using TCM than to design a single-band antenna.

Measurements of the antenna were done both using vector network analyzer [VNA] for S11 parameters measurements and Satimo StarLab for near-to-far field measurements. To perform field measurement using Satimo StarLab, it is required to place the antenna correctly and to memorize its default position. In addition, antenna itself during field measurements in Satimo StarLab should be fixed such that it does not shake during rotation procedure.

5.2.1 Measurements using VNA

Measurement set-up is shown in Figure 67. It is possible to observe VNA equipment and a circular patch antenna connected to it. When VNA is properly calibrated for one-port measurements, antenna can be connected. Additional bending of connection cables should be avoided, because it may result in measurement error and even in breakdown of a connection.

Figure 67. *Measurement set-up of the antenna using VNA*

S11 parameter measurements of the antenna can be observed in Figure 68. It shows two curves, one represents results of the constructed antenna and another represents modified version of it. Modified version means that slots were made a bit shorter using sticky copper foil in order to move L1 band to a higher value. Indeed, in the modified version of the antenna, L1 band moved to a higher band and S11 parameters of it improved, see Appendix B for modified version of the antenna. It is possible to observe that for modified version of the antenna S11 parameters for L1 and L2 bands are respectively -5 dB and -15 dB, which is different from designed values in HFSS model.

Obtained results are logical. Already on the design stage of this antenna it has been noticed that dual-band nature is highly affected by even small changes in geometrical parameters and, specially, in feed placement. The last reason is extremely important, it was discovered that even 0.1 mm change in feed placement results in significant decrease of S11 parameters for L1 band. In other words, from TCM point of view, weighting coefficients at L1 band decreased significantly when feed position changed by 0.1 mm. Thus, S11 parameters at L1 band decreased.

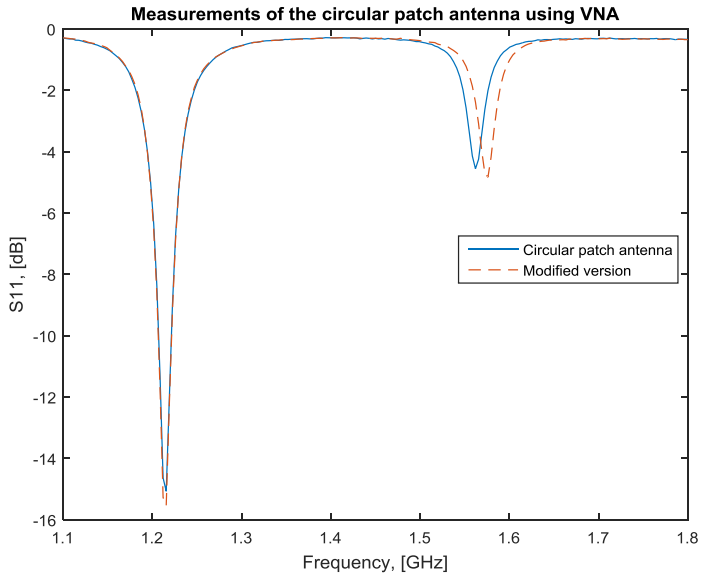

Figure 68. *S11 measurements of the antenna using VNA*

Since the results of modified antenna were better than of the original antenna, it was decided to use modified antenna version during measurement in Satimo StarLab. These results show that characteristic mode excitation is extremely sensitive for correct feed position.

5.2.2 Measurements in Satimo StarLab

Measurements in Satimo StarLab were used mostly for representative reasons, because precise definition of the total far field of the antenna based on TCM was not observed in details in this master thesis. Antenna's position in Satimo StarLab as well as coordinate system of this system both are given in Appendix A.

Efficiency and gain plots of the antenna both are given in Figure 69. It is possible to see that at L1 band efficiency is low – nearly 30%, whereas efficiency at L2 band is much higher – 91%. The same shows also gain plot versus frequency, where it is possible to observe that gain at L2 band is 7.5 dB, whereas at L1 band it is extremely low and equal to -15 dB. Explanation of these results is already given in previous chapter. Obtained results only proves that moved feed position decreased weighting coefficients of the 4^{th} characteristic mode, as a result, instead of radiating at L1 frequency, the antenna is storing reactive energy in near field.

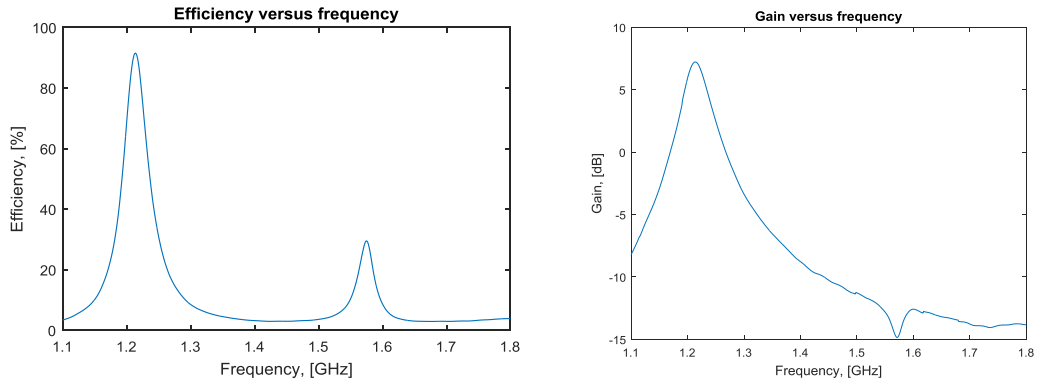

Figure 69. *Efficiency and gain of a circular patch antenna with slots, measured in Satimo StarLab*

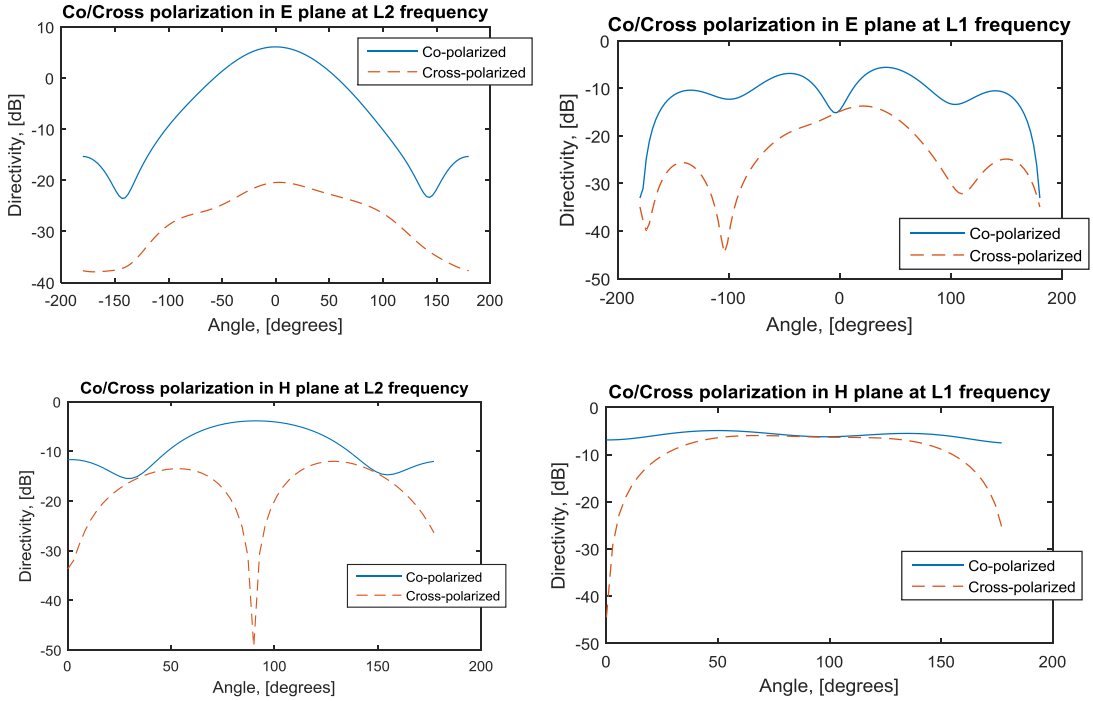

Figure 70. *Co/Cross polarized E and H planes of the antenna at L1 and L2 frequencies.*

Co and Cross polarization situations of E and H fields at L1 and L2 frequencies are given in Figure 70. It is possible to observe that at L2 band both Co/Cross polarized directivity plots of E and H plane are behaving with respect to theory [4], whereas at L1 frequency directivity results are very low. This proves previously mentioned statements once again. In addition, it is possible to observe maximum directivity value of Co-polarized E-plane at L2 frequency is 6 dB, which is in correspondence with HFSS model.

Thus, it is possible to conclude that produced antenna model behaves for L2 band as it was predicted with both FEKO and HFSS programs, but L1 band does not radiate, because 4th characteristic mode is not excited due to moved position of the feed.

5.3 Summary of the design and construction of patch antennas using theory of characteristic modes

It is shown that in general it is possible to use TCM to design patch antennas. A possible approach has been described and two patch antennas were designed using it – single band rectangular patch antenna for Wi-Fi application and dual-band circular patch antenna. Circular patch antenna was also constructed and measured using VNA and Satimo StarLab. As a result, it was discovered that dual-band nature requires additional explorations and experiments in order to achieve more stable and predictable results in the constructed antenna. The main issue of different results for dual-band antennas can be, in particular, moved feed location. Nevertheless, it was proved also that single band patch antennas can be designed using TCM approach quite precisely both in terms of radiation fields, surface currents, polarization and resonant frequencies.

6. CONCLUSIONS AND FUTURE WORK

In this section the most important conclusions from each chapter are provided and future work is detailed. Moreover, more detailed summaries are available separately at the end of each chapter.

6.1 Conclusions from theory of characteristic modes

Matrix operators in theory of characteristic modes as well as eigenvalues and eigencurrents belong to real number set. This simplifies and speeds up the calculation process which need to be repeated for each separate frequency. Excitation and weighting coefficients can be used to describe radiation properties of conductive plates and antennas. Essential interest in TCM is in surface currents. Based on characteristic surface currents it is possible to conclude the following: what kind of polarization will occur if some certain characteristic mode will be excited and what kind of radiation pattern will appear if several characteristic modes will be excited. All characteristic modes are orthogonal to each other. Thus, also the fields radiated by them characteristic fields are orthogonal.

The results of TCM calculations can be given in either surface current form, eigenvalue magnitude form, MS or characteristic angle form. Each one of these representation forms provides different physical aspects from TCM point of view. For example, characteristic mode resonating properties can be observed if its eigenvalue magnitude is 0, or MS is 1, or characteristic angle is 180^o. Bandwidth properties can be studied by observing 0.707 level in MS representation. Based on characterstic angle results and on characteristic surface currents it is possible to predict all radiation parameters of the antenna.

6.2 Conclusions from radiators properties in terms of characteristic modes

Geometrical changes of a conductive plate involve changes in resonant frequencies of characteristic modes. Regular geometrical shapes lead to equal eigenvalue magnitudes over certain frequency range for several characteristic modes.

Ground plane and a substrate both decrease resonant frequency of characteristic modes. Changes of height between radiator and a ground plane are proportional to changes of characteristic mode resonant frequencies. Scaling theory is applicable in terms of TCM. Finally, it was discovered that isospectral geometries can create isospectral radiators

and, in perspective, antennas with different geometrical shapes, but similar radiation properties.

6.3 Conclusions from analysis, design and construction of antennas using theory of characteristic modes

It is described that all radiation parameters of patch antennas, in general, can be described using TCM analysis procedure, which is shown in chapter 4. Cuts or other changes in radiator structure lead to frequency-dependent characteristic surface current distribution. Even small changes in dielectric constant of a substrate lead to directly proportional and significant changes in resonant frequency of characteristic modes. Single radiator can be used for TCM analysis to obtain information about antenna's polarization, normalized total surface current distribution, and normalized total radiation fields. Thus, many analysis steps can be avoided if it is not required to obtain precise and very accurate radiation values.

In addition, it was shown that TCM can be used to design and to construct patch antennas. Possible procedures were described in chapter 5. It was discovered that the recommended approach provides accurate results for single-band patch antennas, whereas for dual-band antennas difference in the final measured results compared to theoretical TCM is appearing due to non-precise placement of a feed. Chapter 5 can be used further for deeper research and studies of patch antenna construction using TCM approach. It provides good basis in terms of detailed explanation of both TCM construction approach usage and detailed explanation of a construction procedure.

6.4 Future work

The future work in TCM field can be divided into 5 parts. The first part is related to enhancement of computational algorithms for patch antenna models in terms of characteristic mode usage. This would provide even more possibilities to use TCM design and analysis approaches for antennas in the future. Studies of this master thesis have shown that it would be even possible to avoid necessity to introduce a ground plane and substrate in the model for TCM calculations.

The second part of the future studies can be related to BW correlation with TCM results in different configurations, such as: stand-alone radiator; stand-alone ground plane; radiator and a ground plane together; radiator, substrate and a ground plane. Also other configurations can be introduced. Different techniques for BW enhancement can be studied from TCM point of view. This part would give possibilities to increase BW of antennas.

The third part would consist of development of the best matching techniques for different feed types of micro-strip antennas, based on characteristic surface current

values for single and dual-band antennas. This can be done, for example, in MATLAB, using characteristic surface current values obtained from commercial software FEKO. As a result, this would decrease amount of trials (and time) required to obtain the best location of the feed for excitation of the required characteristic mode. In ideal case developed code should provide exact coordinates for feed placement, based on geometrical parameters of a radiator, substrate and a ground plane, to excite required characteristic modes.

In the fourth part multi-band analysis and design can be studied based on TCM. Different existing techniques for multi-band creation can be studied in terms of TCM to generalize them. In addition, new techniques fully based on TCM can be found.

In the fifth part isospectral properties of radiators can be studied more in terms of TCM, such as: BW behavior of isospectral antennas, radiation pattern effects of isospectral antennas. As one of the finals results would be to obtain minimization technique of antennas based on TCM and isospectral theory or BW enhancement technique based on TCM and isospectral theory.

REFERENCES

[1] J. A. Ansari, A. Mishra, P. Singh, N. P. Yadav, Dualband, Slot Loaded Circular Disk Patch Antenna for WLAN, International journal of microwave and optical technology, Vol.5, No.3, May 2010.

[2] Ansys, H. F. S. S. Release 15 Ansoft Corporation, Pittsburgh, PA 2014

[3] Ali Araghi, Gholamreza Dadashzadeh, Oriented Design of an antenna for MIMO applications using theory of characteristic modes, IEEE Antennas and Wireless Propagation Letters,Vol.11, 2012.

[4] Balanis C. A., Antenna theory: analysis and design, John Wiley & Sons, 2005.

[5] Cabedo-Fabres, M., Antonio-Daviu, E., Ferrando-Bataller, M., & Valero-Nogueira, A., On the use of characteristic modes to describe patch antenna performance, Antennas and Propagation Society International Symposium, IEEE Vol. 2, June 2003.

[6] Marta Cabedo Fabres, Ph. D. Dissertation Systematic design of antennas using the theory of characteristic modes, Universitat Politècnica de València. Departamento de Comunicaciones - Departament de Comunicacions, 2007.

[7] Miloslav Capek, Pavel Hamouz, Pavel Hazdra, Jan Eichler, "Implementation of the Theory of characteristic modes in matlab", IEEE Antennas and Propagation Magazine, Vol. 55, No. 2, 2013.

[8] S. J. Chapman, Drums That Sound the Same, Mathematical Association of America, Feb 1995.

[9] Chen Y., Wang C. F., Characteristic modes: Theory and Applications in Antenna Engineering, John Wiley & Sons, 2015.

[10] Cockburn, Bernardo. "Discontinuous galerkin methods." ZAMM-Zeitschrift für Angewandte Mathematik und Mechanik 83.11 2003.

[11] Fabry C., Fonda A. Nonlinear equations at resonance and generalized eigenvalue problems. Elsevier, 1992.

[12] FEKO, EM. "Software & Systems." FEKO 7.0 May 2014.

[13] P.Hamouz, P. Hazdra, M. Mazanek, Theory of Characteristic Modes and its Applications for Analysis of Fractal Microstrip Patch Antennas, Czech Technical University in Prague, FEE, Department of Electromagnetic Field, 2007.

[14] R. F. Harrington, Jan L. Harrington, Field Computation by Moment Methods, Oxford University Press, 1996.

[15] R.F Harrington and J.R. Mautz, Theory of characteristic modes for conducting bodies. IEEE Trans. Antennas Propagat., AP-19, 1971.

[16] Hazdra, P., Capek, M., Eichler, J., Korinek, T., Mazanek, M. "On the modal resonant properties of microstrip antennas."Antennas and Propagation (EUCAP), 2012 6th European Conference on. IEEE, 2012.

[17] Hazdra, P., Hamouz, P., On the modal Superposition Lying under the MoM matrix Equations, Dept. of Electromagnetic Field, Czech Technical University, 2008.

[18] J. Kaur, R. Khanna, Co-axial Fed Rectangular Microstrip Patch Antenna for 5.2 GHz WLAN Application, Universal Journal of Electrical and Electronic Engineering, 2013.

[19] John D. Kraus, Antennas, McGraw-Hill, 1950.

[20] M. Levitin, L. Parnovski, I. Polterovich, Isospectral domains with mixed boundary conditions, J. Phys. A: Math. Gen., Mar 2006.

[21] Danie Ludick, Intelligent Design with Characteristic Mode Analysis, FEKO Ltd webinar, 2013, duration 1 h.

[22] Alak Majumder, Rectangular Microstrip Patch Antenna Using Coaxial Probe Feeding Technique to Operate in S-Band, International Journal of Engineering Trends and Technology, Apr 2013.

[23] Sergey N. Makarov, Antenna and EM modeling with MATLAB, Wiley interscience, 2012.

[24] Zachary Miers, Hui Li , Buon Kiong Lau, Design of Bandwidth-Enhanced and Multiband MIMO Antennas Using Characteristic modes, IEEE Antennas and Wireless Propagation Letters,Vol.12, 2013.

[25] A.B. Mutiara, Design of microstrip antenna for wireless communication at 2.4 GHz, Journal of Theoretical and Applied Information Technology, Nov 2011.

APPENDIX A: COORDINATE SYSTEM OF SATIMO STARLAB

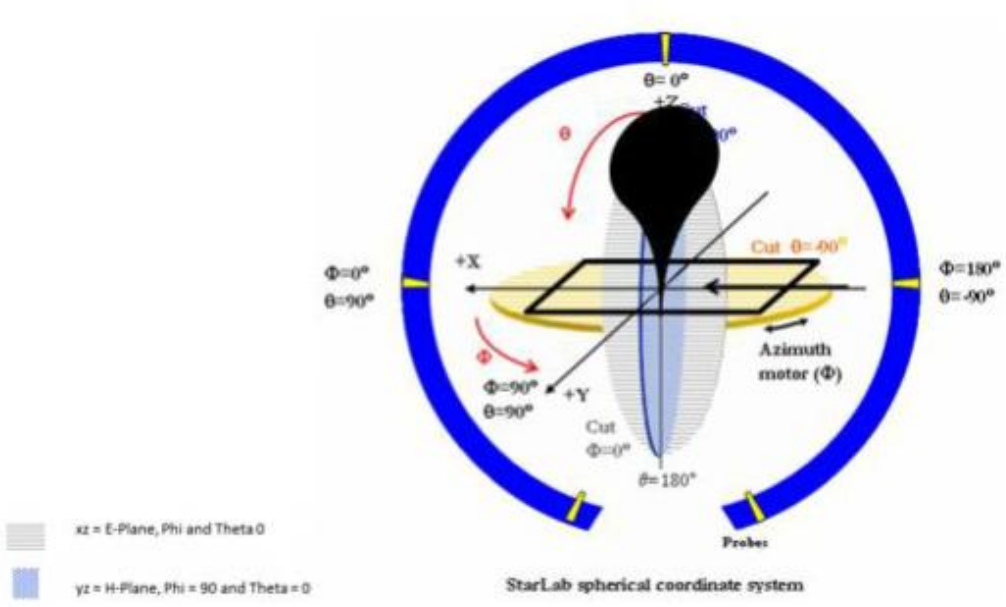

a) *Coordinate system in Satimo StarLab*

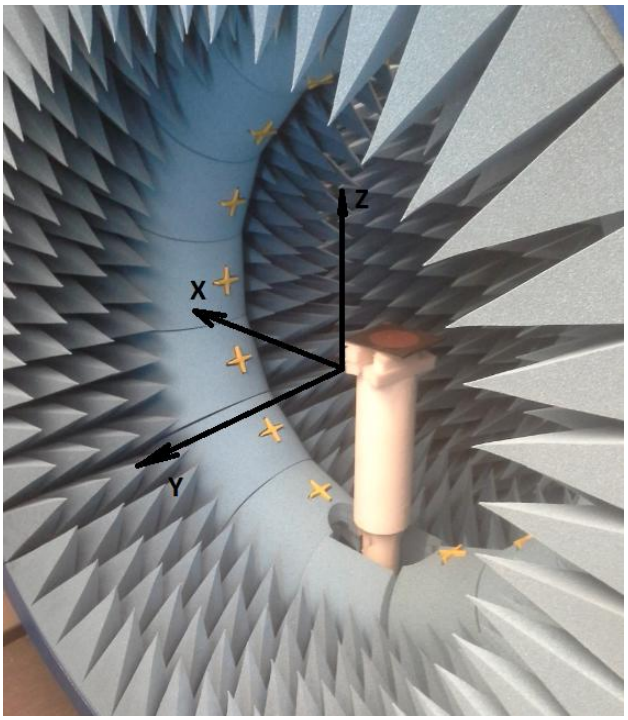

b) Position of the antenna in Satimo StarLab stand with coordinates

APPENDIX B: CONSTRUCTED CIRCULAR PATCH ANTENNA

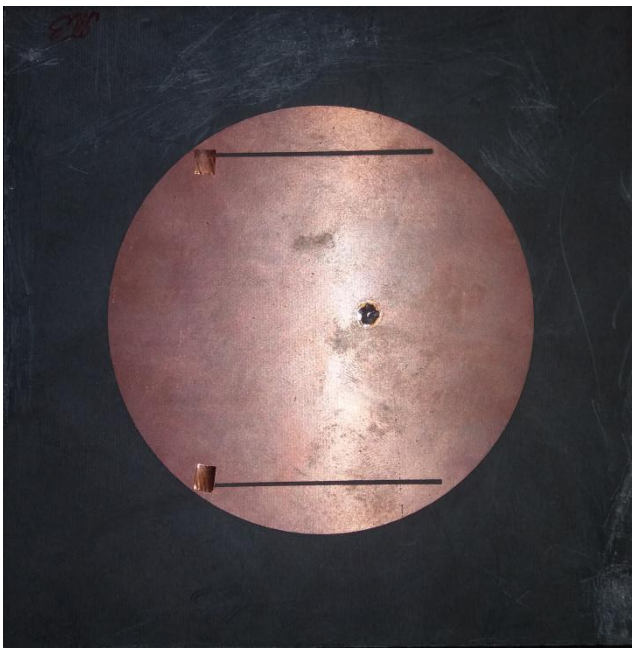

a) Modified version of a circular patch antenna

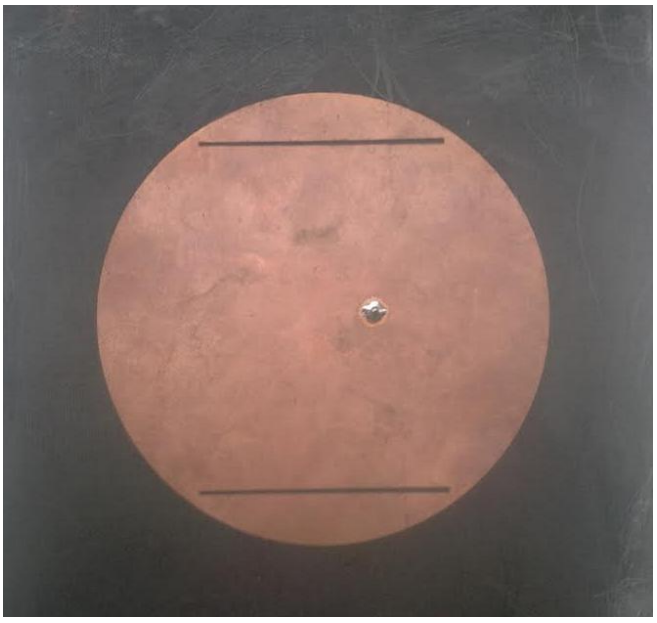

b) Circular patch antenna without modifications